FRED HUTCHINSON CANCER RESEARCH CENTER

Richard G. Gardner, Ph.D.
Postdoctoral Fellow - Division of Basic Sciences

26 September 2005

Yves Brun
Systems Biology/Microbiology Faculty Search
Indiana University
Jordan Hall 142
1001 E 3rd Street
Bloomington, IN 47405-7005

Dear Dr. Brun,

I would like to apply for a position as an Assistant Professor in the Department of Biology. My main interest is how the cell uses protein ubiquitination to control its critical processes. In particular, I've been pursuing a number of studies that focus on how ubiquitin is used in the nucleus to effect or regulate important nuclear functions, such as telomeric silencing and nuclear protein quality control.

From my studies of telomeric silencing, I found that removal of ubiquitin from histone H2B in silent regions is required to prevent the methylation of histone H3, which disrupts the binding of silencing complexes to chromatin. I am continuing my studies of histone H2B deubiquitination to understand its role is in active chromatin as well.

From my studies of nuclear protein quality control, I discovered a new ubiquitination pathway that targets structurally aberrant proteins in the nucleus for proteasomal degradation, thereby preventing their accumulation and aggregation. I'm continuing characterization of this degradation pathway to understand how it initially targets aberrant nuclear proteins, how the nucleus responds transcriptionally to accumulation of aberrant proteins in the absence of this pathway, and how this degradation pathway influences protein aggregation in the nucleus.

Although I have described future plans for only one of my interests in my enclosed research plan, you can see that one area of study alone provides opportunity for multiple graduate students and/or postdocs. Furthermore, I'm committed to developing and utilizing global proteomic and genomic technologies that will take my research into areas that are presently unknown or poorly understood. I'm very excited about the experimental future because I know that it will lead to very interesting biology in a variety of organisms.

I believe the broad scope of my studies complements the variety of cellular processes studied in your department. Some of my current interests, such as regulation of chromatin structure, are shared by a number of your faculty. Other avenues of study, such as nuclear protein quality control, are quite different and would add a new dimension to the biological processes studied in your department. I am very open to collaboration and believe I can significantly contribute to the intellectual environment in your department and at Indiana University.

Enclosed, please find my CV, statements of my research interests and future research plans, representative reprints, and the names and addresses of five people who are sending letters of recommendation. The letters themselves will arrive under separate cover.

Thank you for your consideration.

Sincerely,

Richard Gardner, Ph.D.

1100 Fairview Avenue North, A3-025 P.O. Box 19024 Seattle, WA 98109-1024 Phone: 206 667-6660 Fax: 206 667-5894 email: rgardner@fhcrc.org

AREA OF INTEREST

Ubiquitin was discovered as a covalent modifier of histone H2A nearly 30 years ago, and has since emerged as one of the cell's most broadly utilized protein modifications. From a systems perspective, ubiquitin can be thought of as a universal cellular rheostat, deployed in an array of different configurations that are used in distinct ways to regulate a myriad of activities. And though the full extent of ubiquitin's action in the cell is unknown, it's easy to imagine that every cellular process is controlled in some way by ubiquitination. The large number of genes encoding known or predicted ubiquitination-associated proteins in eukaryote genomes – more than 900 in humans (*1-3*) – hints at ubiquitin's vast regulatory potential. Functions for a considerable number of these ubiquitination-associated proteins have been identified in a variety of organisms. Most, however, remain functionally uncharacterized. Even for those with known functions, only a handful of substrates have been identified for each. To expand our knowledge and approach a complete understanding of ubiquitin's scope within the cell, I am interested in discovering new ubiquitination pathways, especially those that function in the nucleus to regulate chromatin-associated processes or act in novel ways.

POSTDOCTORAL STUDIES

My interest in ubiquitination began as a graduate student in Randy Hampton's lab at UCSD, where I examined the regulation of sterol synthesis in yeast by ubiquitin-mediated degradation of HMG-CoA reductase – the rate-limiting enzyme of the sterol biosynthetic pathway and a main therapeutic target for high cholesterol intervention. As I read about new roles for ubiquitination in many different aspects of cell function, I became intrigued by what the full scope of ubiquitination might be within the cell. In particular, few nuclear ubiquitination pathways had been identified, and I wondered how ubiquitination is employed in the nucleus to regulate its various functions. For my postdoctoral studies in Dan Gottschling's lab at FHCRC, I decided to identify and characterize new ubiquitination pathways that operate in the nucleus.

One of my interests is the role of ubiquitination in regulating chromatin structure. Dan's lab previously identified the ubiquitin protease Ubp10 as a factor important for silencing of telomeric regions (*4*), but a substrate for Ubp10 had not been identified. I focused on histone H2B as a candidate because ubiquitination of H2B is required for specific methylation of histone H3 (*5-7*), which interferes with the formation of silencing complexes on chromatin. As anticipated, I found that ubiquitinated H2B is a substrate of Ubp10. To bring about silencing, Ubp10 is specifically concentrated at silent regions where it prevents H3 methylation by reversing H2B ubiquitination, thus creating a chromatin state permissive for the binding of silencing complexes. Interestingly, Ubp10 is not restricted to silent regions, but also functions in active chromatin to regulate H2B ubiquitination and its dependent H3 methylation. However, the functional role for Ubp10 in active chromatin is not yet known.

While in graduate school, I became fascinated by the idea that the nucleus may contain **P**rotein **Q**uality **C**ontrol (PQC) systems that degrade mutant, misfolded, denatured or damaged proteins to prevent their toxic accumulation and/or aggregation. Although PQC degradation was suspected in the nucleus (*8*), no pathways had been identified. So I initiated studies in Dan's lab to find nuclear ubiquitination systems that function in PQC degradation. I exploited the fact that mutant temperature-sensitive (ts) proteins are often degraded by PQC, even though they may retain normal activity. In these cases, the ts phenotype is the result of reduced protein levels, rather than loss of activity, and can be suppressed by preventing degradation. I speculated that, if PQC degradation systems exist in the nucleus, mutations in a nuclear PQC degradation gene should commonly suppress many disparate nuclear ts phenotypes. Because suppression analysis of ts phenotypes has been a routine strategy for yeast geneticists over the years, I thought evidence of nuclear PQC degradation components might lurk in published suppression studies. Upon searching the literature, I uncovered independent reports where mutations in a single gene, *SAN1*, commonly suppressed two distinct nuclear ts phenotypes (*9, 10*). Upon further analysis, I discovered that San1 is a nuclear-localized ubiquitin-protein ligase that targets unrelated mutant proteins in the nucleus for proteasomal degradation. As expected for *bona fide* PQC degradation, San1 does not target or regulate the wild-type versions of these proteins. Loss of *SAN1* results in a transcriptional upregulation of numerous protein chaperones known or implicated to function in the nucleus, underscoring San1's nuclear PQC role and indicating that the nucleus has a system to sense and respond to nuclear protein stress.

FUTURE RESEARCH PLANS

Although my long-term vision is to understand the regulation of all cellular systems through the lens of ubiquitination, my near-term goals are to continue studying chromatin regulation and nuclear PQC degradation,

while developing technologies to identify novel nuclear ubiquitination pathways. For this research plan, however, I will limit the description of my future research to three salient questions regarding nuclear PQC degradation: (**1**) How do nuclear PQC degradation pathways recognize and target aberrant proteins? (**2**) What is the scope of PQC degradation in the nucleus? (**3**) How do nuclear protein aggregates form and why are they toxic?

How do nuclear PQC degradation pathways recognize and target aberrant proteins?

It is not understood how nuclear PQC degradation systems target aberrant proteins, or even what they recognize as aberrant. This is not a trivial problem for the cell because the nuclear degradation machinery must recognize common hallmarks of aberrancy in a wide variety of nuclear proteins that share little, if any, sequence homology. From recent 2-hybrid studies of San1-substrate interactions, I found that the San1 pathway likely recognizes aberrantly exposed hydrophobic regions. Protein chaperones also bind exposed hydrophobic regions, so it is not clear if the San1 pathway coordinates or competes with nuclear-localized chaperones. How the cell decides if an aberrantly folded protein is to be repaired by chaperones or destroyed by PQC degradation systems is a fundamental unanswered question of general PQC.

As a first step, it must be determined if substrate targeting is intrinsic to San1 itself, or if San1 uses ancillary factors, such as chaperones, for targeting. To identify additional proteins that function with San1, I'm performing a variety of genetic and biochemical analyses. Traditional random mutant hunts and directed null allele screens using the yeast deletion array comprise the genetic approach. Mutants will be isolated by their ability to suppress ts phenotypes that are suppressed by loss of *SAN1*. I expect three classes of mutants: (1) those incapable of initial substrate recognition, (2) those defective in substrate ubiquitination, and (3) those impaired in proteasomal degradation. These classes will be distinguished from each other using assays I've developed that are specific for San1-substrate binding, ubiquitination, or degradation. As a complementary biochemical approach, I'm purifying San1 complexes from lysates and characterizing San1-interacting proteins by mass spectrometry.

San1 could directly target its substrates via a substrate-binding domain. This can be determined by developing an in vitro assay that recapitulates San1 specificity for aberrant proteins – the assay should result in the ubiquitination of San1's mutant substrates, but not the wild-type counterparts. Should San1 alone be required for substrate recognition, the assay will require only San1 and its cognate ubiquitin-conjugating enzymes. If so, mutagenic analysis of San1 will identify regions required for substrate binding. If other substrate-recognition components are identified by genetics or biochemistry, they'll be additionally required in the assay.

What is the scope of PQC degradation in the nucleus?

The full extent of PQC in the nucleus is not known – a few chaperones have been implicated in protein refolding and disaggregation in the nucleus (*11*, *12*), and I've identified the only known nuclear PQC degradation pathway. But I believe nuclear PQC is broader than these few systems. For example, I've discovered mutant nuclear proteins that are degraded in a San1-independent manner, indicating that other nuclear PQC degradation pathways likely exist. Furthermore, I've found that loss of *SAN1* results in a transcriptional stress response that includes the increased expression of six chaperones, implicating the likely subset of chaperones that function in the nucleus. The stress response also reveals that the nucleus possesses a PQC sensing mechanism to detect the accumulation of aberrant proteins, though what is sensed and how the signal is transmitted are unknown. I'm currently conducting directed and random genetic analyses to identify these other nuclear PQC systems.

Knowing the complete cohort of substrates for any individual ubiquitination pathway, including those involved in nuclear PQC, is key to understanding these pathways as complete regulatory systems. For virtually all known ubiquitination pathways, however, a systematic analysis of their substrates has yet to be undertaken, so their functional scope remains unknown. This includes the San1 pathway, for which I've identified only a few mutant nuclear proteins as substrates. I believe San1 acts more globally in the nucleus to target proteins that have become structurally aberrant not only by mutation, but by synthesis defects, stochastic unfolding, or exposure to chemical or physical stresses. Such substrates will likely be random representatives of all nuclear proteins, but San1 may also target specific subclasses of nuclear proteins that are more prone to damage under particular conditions. It's possible that San1 also functions in the regulated degradation of specific nuclear proteins.

To understand the full scope of San1's action, I need a global unbiased way to identify proteins that are ubiquitinated by San1. For this purpose, I've modified a previously developed global ubiquitin proteomics method, which involves affinity purification of ubiquitinated proteins from lysates and subsequent identification of the purified proteins by mass spectrometry (*13*). My modifications include proteasome inhibition prior to lysis

(to allow accumulation of ubiquitinated proteins that are degraded), and additional denaturants during extraction (to reduce background). Proteins that are ubiquitinated specifically by San1 will be identified by incorporating differential metabolic stable isotope labeling (*14*), which will facilitate comparative quantification of protein levels between wild-type *SAN1* and *san1Δ* cells (San1 substrates should be absent or have decreased abundance in the *san1Δ* profile). I've performed initial iterations of the assay using standard growth conditions, but conditions known to damage or denature proteins will also be used to identify San1 substrates that may be sensitive to these conditions. Once established, this global ubiquitin proteomics strategy will be used to identify the cohort of substrates targeted by other ubiquitination pathways, including those involved in nuclear PQC degradation.

How do nuclear protein aggregates form and why are they toxic?

There are 9 neurodegenerative diseases and 8 congenital malformation syndromes caused by the nuclear aggregation of proteins with expanded polyglutamine (polyQ) or polyalanine (polyA) tracts (*15*, *16*). With PQC degradation systems operating in the nucleus, however, it's not clear why these mutant polyQ- or polyA-expansion proteins aren't degraded prior to aggregation. Do these proteins lack the features recognized by nuclear PQC degradation systems? Does aggregation occur at a faster rate than PQC degradation? Or, are aggregates initially formed prior to nuclear import? It's also not understood why aggregates in the nucleus are toxic. Do they sequester other essential proteins, or engage a critical pool of chaperones or the proteasome? Do they damage DNA? Or, do they block important nuclear functions by taking up essential space?

Until metazoan nuclear PQC degradation systems are identified, nuclear aggregation models in yeast will provide the unique and immediate opportunity to examine the interplay between protein aggregation and PQC degradation in the nucleus. As one approach to nuclear aggregation, I've identified 33 native yeast proteins that contain endogenous polyQ or polyA tracts, and I'm currently expanding those tracts to toxic aggregation-prone lengths. The major utility of this strategy is that, for the first time, aggregate progression and toxicity of different polyQ- or polyA-expansion proteins can be directly compared to see if they occur by similar or distinct paths. This is a fundamental issue that could impact treatment of polyQ- or polyA-associated human diseases. In an initial attempt, I've expanded the polyA tract in the polyadenine-binding protein Pab1, which, in humans, appears to by the underlying cause for oculopharyngeal muscular dystrophy (*17*). Expression of the polyA-expanded Pab1 in yeast is toxic, consistent with the human pathology. I'm now examining nuclear aggregation of the polyA-expanded Pab1, and if loss of nuclear PQC degradation influences toxicity.

In another approach to nuclear aggregation, I've recently discovered a mutant version of the DNA damage repair protein Rad16 that forms cytoplasmic aggregates when San1 function is intact, but forms additional nuclear aggregates when San1 function is eliminated. Expression of the Rad16 mutant protein is toxic to the cell only in the absence of San1 function. Thus, it is the presence of this aggregated mutant protein specifically in the nucleus that causes toxicity. This is the first case demonstrating that the absence of nuclear PQC degradation leads to the toxic nuclear aggregation of an abnormal protein, underscoring the importance of a functional PQC degradation system in the nucleus. Because the Rad16 mutant doesn't have polyQ or polyA tracts, it will be interesting to see if aggregate progression and the nature of toxicity are distinct from or similar to those proteins that do.

There are number of means by which I'll determine the mechanism of nuclear aggregation and the nature of toxicity. For example, I'll systematically examine if the ~1000 nuclear-localized GFP-tagged proteins, identified in global GFP localization studies (*18*), colocalize within nuclear aggregates. I'll test if aggregates increase DNA damage sensitivity or activate DNA damage repair pathways. I'll use transcript microarray analyses to determine if nuclear aggregates induce extensive transcriptional changes. Because the aggregation-prone proteins are expressed from a regulated promoter, I can follow the dynamics of aggregate formation, and determine if nuclear aggregates are permanent once formed or if they are cleared from the cell when production ceases. Finally, I'll use the toxicity of these aggregates to discover genes involved in the progression from full-length soluble protein to truncated insoluble aggregate, and to screen libraries of small molecules for those that ameliorate toxicity.

LONG TERM FUTURE PLANS

Nothing is known about nuclear PQC degradation in metazoans. I intend to use the knowledge gained in these yeast studies as a basis for studies of nuclear PQC degradation in flies and mammals.

Yeast ubiquitin proteomics studies will yield insights into many general cellular processes, but I also plan to modify the protocol for use in metazoans to identify ubiquitination events that occur with cell-type specificity or during development.

REFERENCES

1. A. R. Willems, M. Schwab, M. Tyers, *Biochim Biophys Acta* **1695**, 133 (2004).
2. F. F. Assaad, *Curr Opin Plant Biol* **4**, 478 (2001).
3. S. S. Wing, *Int J Biochem Cell Biol* **35**, 590 (2003).
4. A. Kahana, D. E. Gottschling, *Mol Cell Biol* **19**, 6608 (1999).
5. Z. W. Sun, C. D. Allis, *Nature* **418**, 104 (2002).
6. S. D. Briggs *et al.*, *Nature* **418**, 498 (2002).
7. H. H. Ng, R. M. Xu, Y. Zhang, K. Struhl, *J Biol Chem* **277**, 34655 (2002).
8. O. Ullrich *et al.*, *Proc Natl Acad Sci U S A* **96**, 6223 (1999).
9. R. Schnell, L. D'Ari, M. Foss, D. Goodman, J. Rine, *Genetics* **122**, 29 (1989).
10. Q. Xu, G. C. Johnston, R. A. Singer, *Mol Cell Biol* **13**, 7553 (1993).
11. J. M. Rossi, S. Lindquist, *J Cell Biol* **108**, 425 (1989).
12. D. A. Parsell, A. S. Kowal, M. A. Singer, S. Lindquist, *Nature* **372**, 475 (1994).
13. J. Peng *et al.*, *Nat Biotechnol* **21**, 921 (2003).
14. H. Zhu, S. Pan, S. Gu, E. M. Bradbury, X. Chen, *Rapid Commun Mass Spectrom* **16**, 2115 (2002).
15. B. S. Shastry, *Neurochem Int* **43**, 1 (2003).
16. A. Albrecht, S. Mundlos, *Curr Opin Genet Dev* **15**, 285 (2005).
17. B. Brais, *Cytogenet Genome Res* **100**, 252 (2003).
18. W. K. Huh *et al.*, *Nature* **425**, 686 (2003).

I'm very passionate about teaching science. I believe that the student well versed in the scientific method and fascinated by scientific discoveries will impact society no matter what they endeavor after they have graduated. To inspire my students, I strive to bring the excitement of discovery and the joy of learning to my teaching, be it on an individual basis or in a classroom. Because not all students learn in the same way, I'm creative with my teaching methods and I try to connect esoteric topics to everyday interests and exposures.

As an undergraduate, I worked in the tutoring center in the Science Department at Bucks County Community College, helping students with biology, chemistry, and physics problems. At Cornell University, I served as a volunteer tutor for those who needed help in various biology courses.

As a graduate student at UCSD, I was a teaching assistant for three biochemistry courses: a laboratory course (Biochemical Techniques), and two lecture courses (Structural Biochemistry and Physical Biochemistry). In both lecture courses, I was the head TA, and I was involved in creating exam questions, designing section lecture material, and supervising undergraduate TAs. For the lab course, I lectured and supervised the students in my subsection of the course. For my teaching in the lab course, I was awarded an Excellence in Teaching Award as voted by the students. Additionally, I served as a teaching consultant in the Center for Teaching Development, where I critiqued and helped students who were TAing for the first time. As a graduate student, I also supervised a number of undergraduate students in the lab, helping them to develop their own undergraduate research projects.

As a postdoctoral fellow at FHCRC, I haven't had any formal teaching experience. However, I've continued as a volunteer tutor and helped students who attend a local high school and community college. In the lab, I've supervised both graduate students and technicians, and mentored a high school student for the summer.

I look forward to teaching at the level of professor, and I'm very excited about the opportunity to teach courses in Biochemistry, Cell Biology, Molecular Biology, and Genetics, both at the undergraduate and graduate level.

Cell, Vol. 120, 803–815, March 25, 2005, Copyright ©2005 by Elsevier Inc. DOI 10.1016/j.cell.2005.01.016

Degradation-Mediated Protein Quality Control in the Nucleus

Richard G. Gardner, Zara W. Nelson, and Daniel E. Gottschling*
Fred Hutchinson Cancer Research Center
Seattle, Washington 98109

Summary

Protein quality control degradation systems rid the cell of aberrant proteins, preventing detrimental effects on normal cellular function. Although such systems have been identified in most subcellular compartments, none have been found in the nucleus. Here, we report the discovery of such a system in *Saccharomyces cerevisiae*. It is defined by San1p, a ubiquitin-protein ligase that, in conjunction with the ubiquitin-conjugating enzymes Cdc34p and Ubc1p, targets four distinct mutant nuclear proteins for ubiquitination and destruction by the proteasome. San1p has exquisite specificity for aberrant proteins and does not target the wild-type versions of its mutant substrates. San1p is nuclear localized and requires nuclear localization for function. Loss of *SAN1* results in a chronic stress response, underscoring its role of protein quality control in the cell. We propose that San1p-mediated degradation acts as the last line of proteolytic defense against the deleterious accumulation of aberrant proteins in the nucleus and that analogous systems exist in other eukaryotes.

Introduction

Aberrant proteins can be produced in the cell by mutation, transcriptional or translational errors, incorrect folding, imbalanced subunit synthesis, improper trafficking, or damage caused by environmental conditions or metabolic byproducts (Goldberg, 2003). Accumulation or persistence of aberrant proteins within the cell can often have deleterious consequences. For example, aberrant proteins may lose regulation, may form inactive complexes that compete with functional complexes, may assemble into aggregates that eliminate protein function or cause toxicity, or may introduce harmful activities if mislocalized. In humans, accumulation of aberrant proteins may underlie the pathology of diseases such as Alzheimer's, Huntington's, Parkinson's, and prion pathologies like Creutzfeld-Jakob's (Shastry, 2003).

To minimize harmful effects from aberrant proteins, the cell possesses a set of protein quality control (PQC) systems that operate in distinct ways. Some PQC systems function in repair, such as protein chaperones that refold or sequester aberrantly folded proteins (Stirling et al., 2003). Protein chaperones reside in every major cellular compartment and function either by refolding misfolded proteins (e.g., Hsp70 and Hsp90), binding to misfolded proteins and preventing aggregation (e.g., Hsp40), or disrupting protein aggregates (e.g., Hsp104). Not all aberrant proteins can be repaired, however. For these lost causes, the cell has PQC systems that function in disposal, such as proteolytic systems that destroy proteins that are mutant, damaged, or misfolded and recalcitrant to refolding (Goldberg, 2003). PQC degradation systems have been identified in the cytoplasm, the secretory pathway, and mitochondria. In the cytoplasm and endoplasmic reticulum (ER), PQC degradation is primarily brought about by protein-ubiquitination complexes that mark proteins for proteasomal degradation (Hampton, 2002; McDonough and Patterson, 2003; Trombetta and Parodi, 2003). PQC degradation in the cytoplasm and ER can also occur via transport to the lysosome/vacuole (Trombetta and Parodi, 2003). In the mitochondria, localized proteases function in PQC degradation (Arnold and Langer, 2002). Repair and degradation systems may not be mutually exclusive, as various protein chaperones appear to interface with PQC degradation systems (McDonough and Patterson, 2003; Trombetta and Parodi, 2003).

How the cell targets and destroys aberrant proteins depends upon how and when aberrant proteins are produced. Aberrant proteins may be evident immediately upon production due to errors in synthesis or folding. It is estimated that nearly a third of all newly synthesized proteins are defective and destroyed during or shortly after synthesis (Schubert et al., 2000), indicating that PQC degradation systems may be intimately linked with the production process. Properly synthesized proteins can become aberrant even after they are performing their normal functions. Postproduction damage can be caused by physical or chemical means including heat, irradiation, free radicals, and changes in hydration or osmolarity (Goldberg, 2003). It is not clear if particular PQC degradation systems are dedicated exclusively to production-level defects or postproduction damage or if they target both classes of aberrant proteins.

In contrast to the cytoplasm, ER, and mitochondria, very little is known about PQC in the nucleus. A number of chaperones have been implicated in protein refolding and disaggregation in the nucleus (Parsell et al., 1994; Rossi and Lindquist, 1989), but no nuclear PQC degradation systems have been identified. Because there is no functional protein synthesis in the nucleus, the cell would not have to contend with production defects in the nucleus unless they eluded cytoplasmic PQC systems. Nuclear proteins can be damaged by the same stresses that damage proteins in other cellular compartments; thus, the cell must contend with aberrant proteins that arise within the nucleus. It is not clear if PQC degradation systems exist in the nucleus and, if so, whether they would be similar to those in other cellular compartments where protein synthesis occurs. Yet, similar to the protein synthetic compartments, accumulation of aberrant proteins in the nucleus can have deleterious effects. For example, aberrant protein accumulation in the nucleus likely underlies the pathology

*Correspondence: dgottsch@fhcrc.org

of Huntington's disease (HD) and oculopharyngeal muscular dystrophy (OPMD) (Brais, 2003; Jana and Nukina, 2003). With a significant amount of regulated degradation occurring in the nucleus via ubiquitination and nuclear-localized proteasomes (Wojcik and DeMartino, 2003), the nucleus certainly has the potential machinery for PQC degradation. In fact, nuclear aggregates of mutant polyglutamine- and polyalanine-expanded proteins in HD and OPMD, respectively, are ubiquitinated and associated with proteasome subunits (Abu-Baker et al., 2003; Calado et al., 2000; Davies et al., 1997; Waelter et al., 2001), providing some evidence that PQC degradation systems may be operating in the nucleus.

Given the potential importance of PQC degradation in the nucleus, we asked if such a system existed in the budding yeast, *Saccharomyces cerevisiae*.

Results

Mutant Nuclear Proteins Are Degraded in a *SAN1*-Dependent Manner

We searched for nuclear PQC degradation pathways in yeast working under the assumption that temperature-sensitive mutant nuclear proteins might be substrates for such a pathway. This idea was based on the observation that some temperature-sensitive proteins in other cellular compartments are recognized as aberrant and destroyed by PQC machinery, despite the fact that the mutant proteins often possess normal or near-normal activity (Betting and Seufert, 1996; Bordallo et al., 1998). In these cases, the temperature-sensitive phenotype results from reduced steady-state levels of the protein and can be suppressed by inhibiting the protein's degradation, thus allowing the mutant protein to accumulate to functional levels (Bordallo et al., 1998).

We speculated that if a general nuclear-localized PQC degradation system exists, then the temperature-sensitive phenotypes of different mutant nuclear proteins with disparate normal functions would be suppressed by a common extragenic mutation. We focused on temperature-sensitive alleles of nuclear protein genes that had been previously identified, particularly those for which suppressor analyses had been reported. From our search, we found two independently conducted genetic analyses: one targeting the *sir4-9* allele (Schnell et al., 1989) and the other targeting the *cdc68-1* allele (Xu et al., 1993). Both analyses identified mutations in the gene *SAN1* that suppressed the respective temperature-sensitive phenotypes. *SAN1* made an excellent candidate gene for a nuclear PQC degradation factor given the different nuclear functions of Sir4p, which is a structural component of silent chromatin at the silent mating-type loci and telomeres (Aparicio et al., 1991; Rine and Herskowitz, 1987), and Cdc68p, which facilitates DNA replication, transcriptional initiation, and elongation (Belotserkovskaya et al., 2003; Brewster et al., 2001; Formosa et al., 2001). In fact, the mutant Cdc68-1 protein was previously shown to be unstable compared to wild-type Cdc68p (Xu et al., 1995), and *SAN1* was required for the mutant protein's degradation (Evans et al., 1998).

To assess San1p's role in the QC degradation of mutant nuclear proteins, we first confirmed the *SAN1* requirement for Cdc68-1p degradation (Figure 1A). Next, we examined the stability of the mutant Sir4-9 protein and found that it too was degraded in a *SAN1*-dependent manner, whereas the wild-type version of Sir4p was stable in the presence of *SAN1* (Figure 1B). Thus, mutations in both the Sir4 and Cdc68 proteins caused them to be rapidly degraded in the presence of *SAN1*, while their wild-type counterparts were stable.

To facilitate additional genetic and biochemical assays, single Myc-tagged versions of wild-type Sir4p and the mutant Sir4-9p were created. While we found that N- or C-terminal addition of epitope sequences to Sir4p abrogated its silencing function and, in the case of N-terminal tags, resulted in aberrant degradation (data not shown), we found that conversion of the internal native sequence of Sir4p, ^{372}EQKMKEDADL, to the highly similar c-Myc epitope sequence, EQKLIS EEDL, had no effect on *SIR4* silencing function (data not shown). Furthermore, overexpression of each internal Myc-tagged protein from the constitutive *TDH3* promoter did not alter the stability of wild-type Sir4p or the *SAN1*-dependent degradation of mutant Sir4-9p (Figure 1C).

We next determined if San1p's degradative function was limited to the mutant Sir4-9 and Cdc68-1 proteins or if San1p acted more generally in aberrant nuclear protein degradation. To do so, we examined the stability of two other temperature-sensitive mutant nuclear proteins, Cdc13-1p and Sir3-8p. Detection of Cdc13 proteins was facilitated by the addition of a 9× Myc epitope sequence to the C terminus, which does not alter wild-type Cdc13p function (Qi and Zakian, 2000). Detection of Sir3 proteins was facilitated by replacement of the wild-type Sir3p sequence, ^{426}ETDNEMNG NGK, with the VSV epitope sequence, ^{426}YTDIEMNR LGK, which had no effect on *SIR3* silencing function (data not shown). Similar to the mutant Cdc68-1 and Sir4-9 proteins, the mutant Cdc13-1 and Sir3-8 proteins were rapidly degraded, and each was stabilized in the absence of *SAN1* (Figures 1D and 1E, respectively). Cdc13-1p stabilization in *san1*Δ cells was complete, whereas Sir3-8p stabilization was partial. Both wild-type Cdc13p and Sir3p were stable in the presence of *SAN1* (Figures 1D and 1E, respectively).

Although the absence of *SAN1* stabilized both Cdc13-1p and Sir3-8p, neither the *cdc13-1* nor the *sir3-8* temperature-sensitive phenotype was suppressed by the *san1*⊿ allele (data not shown; Schnell et al., 1989). This lack of phenotypic suppression contrasted with the *san1*⊿ effect on the *sir4-9* and *cdc68-1* phenotypes (Schnell et al., 1989; Xu et al., 1993), indicating that the stabilized Cdc13-1 and Sir3-8 proteins are likely to be nonfunctional at the restrictive temperatures. Nevertheless, the fact that all four mutant proteins were aberrantly degraded in a *SAN1*-dependent manner is consistent with San1p functioning in nuclear PQC degradation.

San1p Is a RING-Domain Ubiquitin-Protein Ligase

Analysis of its sequence revealed that San1p contained a variant version of the canonical RING domain (from residues 165–279; Figure 2A), which is common among

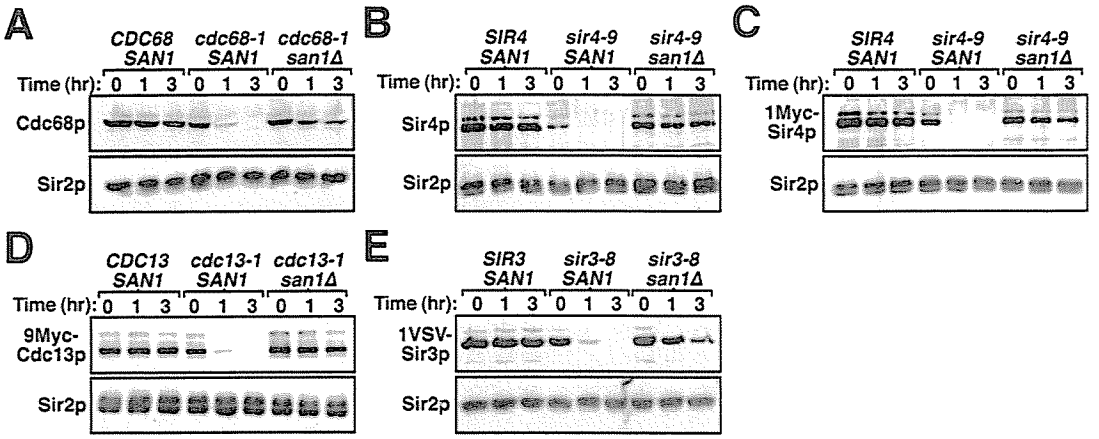

Figure 1. Degradation of Mutant Nuclear Proteins Requires *SAN1*

Cycloheximide-chase assays of cells expressing the indicated wild-type or mutant protein were performed to assess stability in the presence or absence of *SAN1*. Time after addition of cycloheximide is indicated above each lane. Images are of the same blot, first probed with either anti-Cdc68p, anti-Sir4p, anti-Myc, or anti-VSV antibodies to detect the appropriate protein and subsequently probed with anti-Sir2p antibodies to assess Sir2p levels as a loading control.

(A) Cdc68-1p degradation, (B) Sir4-9p degradation, (C) 1Myc-Sir4-9p degradation, with expression from the *TDH3* promoter, (D) 9Myc-Cdc13-1p degradation, and (E) 1VSV-Sir3-8p degradation, with expression from the *TDH3* promoter.

a subset of ubiquitin-protein ligases (Jackson et al., 2000). In San1p's RING domain, the fifth canonical zinc binding His/Cys residue is replaced by Gly (Figure 2A). Because mutation of any of the conserved zinc binding Cys or His residues results in loss of activity in other ubiquitin-protein ligases tested (Bays et al., 2001; Joazeiro et al., 1999; Lorick et al., 1999), the presence of a Gly residue in this position might be expected to disrupt RING domain structure and impair or prevent potential ubiquitin-protein ligase activity. To test San1p for ubiquitin-protein ligase activity, we used a standard in vitro autoubiquitination assay (Joazeiro et al., 1999; Lorick et al., 1999). The addition of a purified GST fusion of San1p to purified ubiquitin-activating enzyme, ubiquitin-conjugating enzyme, ubiquitin, and ATP resulted in autoubiquitination of GST-San1p (Figure 2B). This effect was not observed with GST alone or when any critical component of the reaction was excluded (Figure 2B). The activity was also RING domain dependent, as replacement of either Cys257 or Cys279 with Ser abolished the ubiquitin-protein ligase activity of the GST-San1p fusion (Figure 2C). Thus, San1p possessed

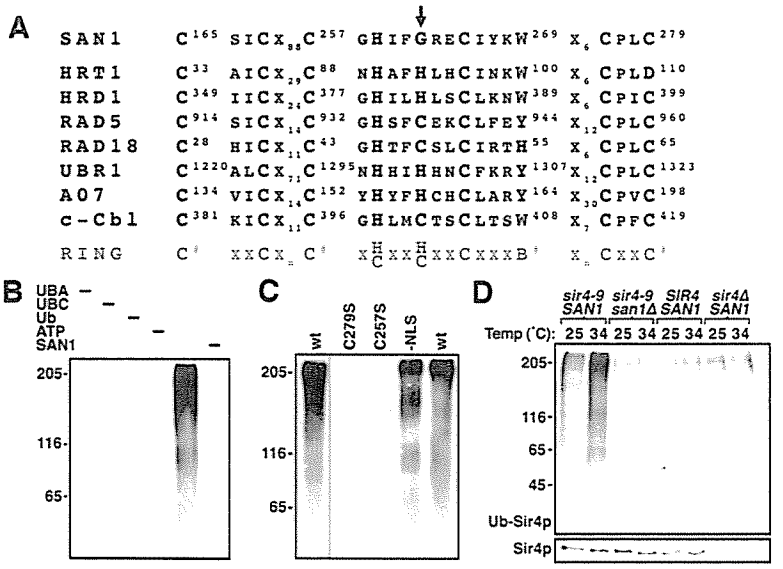

Figure 2. San1p Is a Ubiquitin-Protein Ligase

(A) The RING domain of San1p is compared to the RING domain of five yeast and two mammalian ubiquitin-protein ligases. Consensus RING domain is in gray on the bottom. Zinc binding cysteine and histidine residues are in large typeface. The "B" represents a bulky, hydrophobic residue common among ubiquitin-protein ligases. The arrow points to the noncanonical glycine in San1p's RING domain.

(B) Purified GST-San1p was added to a reaction containing ubiquitin-activating enzyme (UBA), ubiquitin-conjugating enzyme (UBC), ubiquitin (Ub), and ATP. Dashes above gel lanes indicate which reagent was excluded from final reaction mixture. Blot was probed with a monoclonal anti-ubiquitin antibody. Numbers on left indicate positions of protein molecular weight markers.

(C) San1p ubiquitin-protein ligase activity requires the RING domain. Purified GST-San1p containing the indicated mutations was used in an in vitro ubiquitin-ligase assay described in (B).

(D) San1p is required for Sir4-9p ubiquitination in vivo. Sir4 protein was immunoprecipitated from lysates of cells expressing either 1Myc-Sir4-9p, 1Myc-Sir4p, or no Sir4p, and the indicated *SAN1* allele. Blots of the immunoprecipitates were probed with anti-HA antibodies to detect ubiquitin (top panel) or anti-Myc antibodies to assess Sir4p levels (bottom panel).

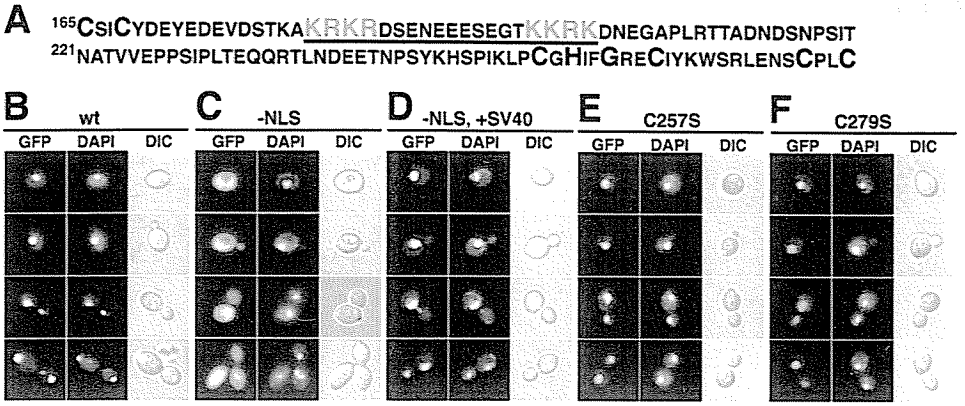

Figure 3. San1p Is Nuclear Localized

(A) The San1p RING domain. Zinc binding cysteine and histidine residues are in large black typeface. Residues comprising the bipartite nuclear localization sequence are in large gray typeface, with the entire sequence underlined.

(B–F) Cells expressing the indicated San1p-3HSV-GFP fusion were fixed with 4% paraformaldehyde, stained with DAPI, and examined by fluorescence microscopy as previously described (Biggins et al., 1999). Single cell images were taken showing different stages of the cell cycle. Left panels show GFP fluorescence, middle panels show DAPI-stained DNA, and right panels show bright field images. Cells expressing (B) *SAN1-3HSV-GFP*, (C) *SAN1(-NLS)-3HSV-GFP*, (D) *SAN1(-NLS)-3HSV-SV40NLS-GFP*, (E) *SAN1(C257S)-3HSV-GFP*, or (F) *SAN1(C279S)-3HSV-GFP* are shown.

in vitro RING-dependent ubiquitin-protein ligase activity, which is in agreement with recent findings (Dasgupta et al., 2004).

Next, we assessed San1p activity in vivo by determining if one of its cellular substrates, Sir4-9p, was ubiquitinated in a San1p-dependent manner. Immunoprecipitates of Sir4-9p contained high molecular weight ubiquitin conjugates that increased dramatically after incubation at the nonpermissive temperature (Figure 2D), consistent with the temperature-sensitive degradation of Sir4-9p. Importantly, the ubiquitination of Sir4-9p required the presence of *SAN1*. Furthermore, *SAN1*-dependent ubiquitination was specific for only the mutant Sir4-9p, as the stable wild-type Sir4p showed no ubiquitination. Together, our in vivo and in vitro observations indicate that San1p is a ubiquitin-protein ligase that acts in the ubiquitination and degradation of aberrant nuclear proteins.

Nuclear Localization of San1p Is Required for Its Function

It was evident that San1p was involved in the QC degradation of mutant nuclear proteins, but it was not clear if San1p carried out its function in the nucleus per se. Indeed, San1p resides in the nucleus, as evidenced by colocalization of GFP-tagged San1p with DAPI-stained nuclear DNA (Figure 3B). By analyzing San1p's sequence with PROSITE (http://au.expasy.org/prosite/), we found that San1p has a putative bipartite nuclear-localization sequence (NLS) from residues 182–199 (Figure 3A). In fact, the NLS was bona fide, as mutagenesis of the San1p NLS (Lys182Cys, Arg183Ser, Lys184Ala, Arg185Thr, Lys197Ser, Lys198Gln, Arg199Ser) resulted in predominantly cytoplasmic localization (Figure 3C). Although the NLS resides within a loop of the RING domain, RING domain structure was not critical for nuclear localization, as substitution of Cys257 or Cys279 with Ser had no effect on San1p-GFP nuclear localization (Figures 3E and 3F).

Importantly, mislocalization of San1p by the NLS mutations abrogated the degradation of Sir4-9p and Cdc68-1p and suppressed the temperature sensitivity of *cdc68-1* cells in a manner similar to that observed when *SAN1* was deleted or the RING domain was mutated (Figure 4). However, the NLS-deficient San1p still retained normal ubiquitin-protein ligase activity in vitro (Figure 2C), indicating that mutation of the NLS did not adversely affect RING-domain activity. Curiously, the NLS mutations resulted in a slower mobility of San1p in SDS-PAGE gels (Figures 4A and 4B). It is not clear why this change occurred; perhaps the NLS-deficient San1 protein was subject to additional or new modifications that also interfered with San1p function. To rule out this possibility, we added the SV40 NLS onto the C terminus of the NLS-deficient San1p. This addition restored nuclear localization (Figure 3D) and in vivo degradation function (Figure 4), indicating that disruption of San1p nuclear localization by mutations to the endogenous NLS simply prevented San1p from gaining access to its nuclear substrates and did not alter another function of San1p.

Ubc1p and Ubc3p/Cdc34p Function in San1p-Mediated Degradation

In addition to a ubiquitin-protein ligase (E3), the covalent attachment of ubiquitin to substrates requires the action of two other enzymes: a ubiquitin-activating enzyme (UBA or E1), which forms a high-energy, thiol-ester bond with ubiquitin in a reaction that requires ATP, and a ubiquitin-conjugating enzyme (UBC or E2), which accepts the charged ubiquitin from the activating enzyme by forming an identical, high-energy, thiol-ester

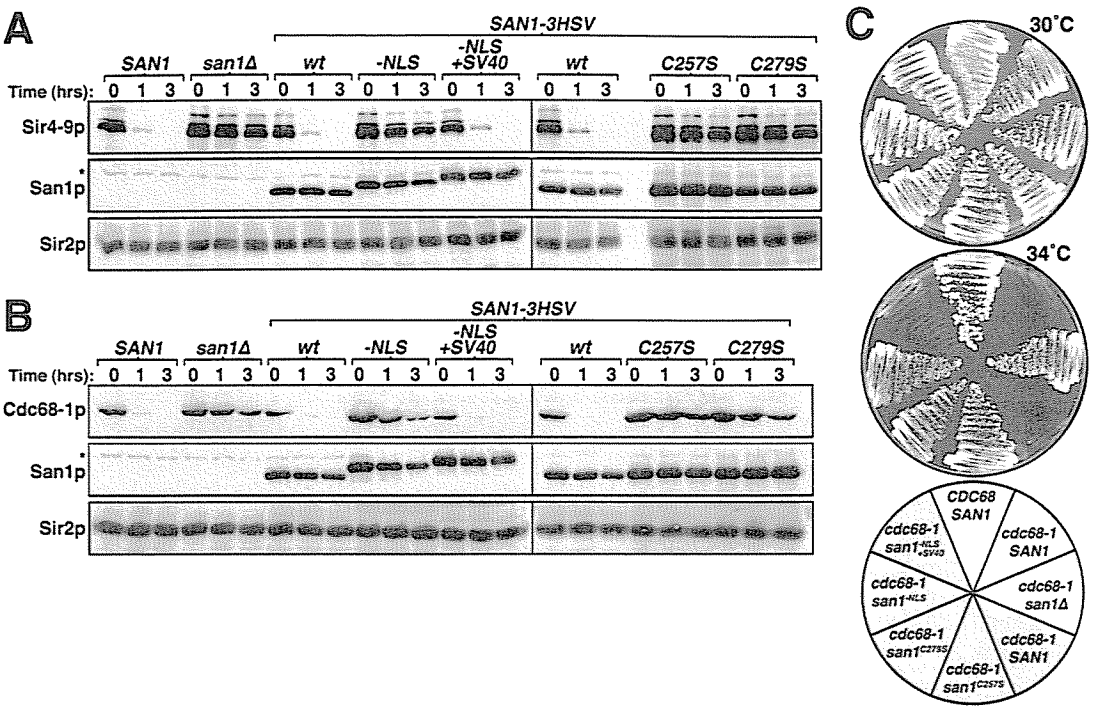

Figure 4. Nuclear Localization of San1p Is Required for Function

(A and B) Cycloheximide-chase assays of cells expressing the indicated San1p substrates were performed to assess stability in the presence of various *san1* alleles. Images are of the same blot, probed sequentially with anti-Myc or anti-Cdc68p antibodies, anti-HSV antibodies, and anti-Sir2p antibodies. The degradation of (A) 1Myc-Sir4-9p and (B) Cdc68-1p was analyzed.

(C) Strains containing the indicated *SAN1* and *CDC68* alleles were streaked onto YC Trp plates and incubated at the indicated temperatures for 3 days. Gray triangles in the plate map indicate strains in which the indicated *SAN1-3HSV* allele covered the *san1Δ* allele.

bond with ubiquitin (Jackson et al., 2000). *S. cerevisiae* has a single essential UBA, Uba1p, and eleven UBCs, ten of which are not essential for viability (Jackson et al., 2000).

To identify the UBC(s) participating in *SAN1*-mediated degradation, Sir4-9p degradation was examined in the absence of each nonessential *UBC* gene. *ubc1Δ* was the only single null allele that had a detectable effect on Sir4-9p degradation (Figure 5A). However, loss of *UBC1* resulted in partial stabilization of Sir4-9p, unlike the *san1Δ* allele, indicating that Ubc1p likely acts in concert with another UBC and San1p to ubiquitinate target proteins. Accumulation of Sir4-9p proteolytic fragments in *ubc1Δ* cells (Figure 5A, arrows) might indicate that Ubc1p activity is important in a processive aspect of *SAN1*-mediated degradation.

The remaining untested UBC was *CDC34/UBC3,* which is a member of the SCF complex and is essential for yeast cells to progress through the cell cycle (Deshaies, 1999). To assess a possible role of *CDC34* in San1p-mediated degradation, we analyzed Sir4-9p degradation in a strain carrying the *cdc34-2* allele (Liu et al., 1995). When compared to a wild-type *CDC34* strain, Sir4-9p was stable in the *cdc34-2* strain (Figure 5B). Degradation was restored when the *cdc34-2* allele was complemented by introduction of the wild-type *CDC34* gene (Figure 5B), indicating that the *cdc34-2* allele itself was responsible for Sir4-9p stability.

We further tested the involvement of *UBC1* and *CDC34* in *SAN1*-mediated degradation by examining the effect of overexpressing catalytically inactive versions of each UBC on Sir4-9p degradation. Mutation of the active-site Cys residue in UBCs destroys their function, and overexpression of the mutant can dominantly interfere with the function of the wild-type cognate (Banerjee et al., 1995; Madura et al., 1993). We created catalytically inactive mutants by substituting a Ser at Cys88 for Ubc1p and at Cys95 for Cdc34p. Overexpression of either mutant *UBC* from the galactose-inducible *GAL1,10* promoter significantly stabilized Sir4-9p (Figure 5C).

Given the nuclear-restricted activity of *SAN1* and nuclear localization of Sir4p (Palladino et al., 1993), it was possible that overexpression of any nuclear-localized catalytically inactive UBC might affect Sir4-9p degradation. To address this, we made a catalytically inactive variant of Rad6/Ubc2p, which is located in the nucleus (Ulrich and Jentsch, 2000). In contrast to $CDC34^{C95S}$ or $UBC1^{C88S}$, $RAD6^{C88S}$ overexpression had little effect on Sir4-9p degradation (Figure 5C).

Ubc1p also functions with Ubc7p in degradation of proteins at the ER (Bays et al., 2001; Friedlander et al., 2000). However, loss of *UBC7* or overexpression of the $UBC7^{C89S}$ allele did not stabilize Sir4-9p (Figures 5A and 5C), indicating that Ubc1p function in Sir4-9p degradation is distinct from its ER function. The lack of

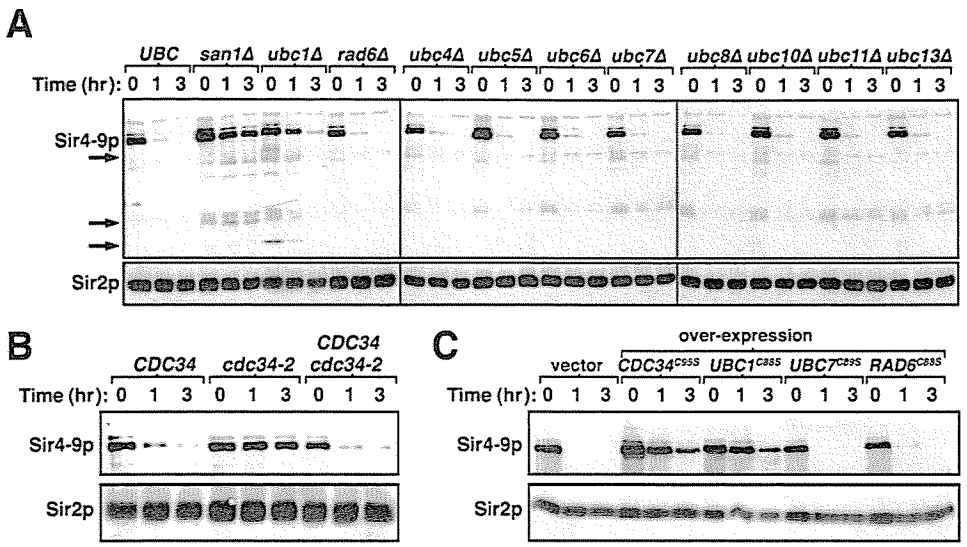

Figure 5. Ubc1p and Cdc34p Are Required for Optimal Degradation of San1p Substrates

(A) Cycloheximide-chase assays of cells expressing 1Myc-Sir4-9p were performed to assess stability in the absence of the individual *UBC* genes. Images are of the same blot, probed sequentially with anti-Sir4p antibodies and anti-Sir2p antibodies.

(B) Cycloheximide-chase assays of cells expressing 1Myc-Sir4-9p were performed to assess stability in the presence of the *cdc34-2* allele. Images are of the same blot, sequentially probed with anti-Myc antibodies and anti-Sir2p antibodies.

(C) Cycloheximide-chase assays of cells expressing 1Myc-Sir4-9p were performed to assess stability in the presence of the individual catalytically inactive $CDC34^{C95S}$, $UBC1^{C88S}$, $UBC7^{C89S}$, and $RAD6^{C88S}$ alleles. Images are of the same blot, which was probed as in (B).

effect seen with the $UBC7^{C89S}$ and $RAD6^{C88S}$ alleles indicates that Sir4-9p stabilization due to overexpression of the $CDC34^{C95S}$ or $UBC1^{C88S}$ alleles is not a general feature of overexpressing dominant-negative versions of UBCs. Similar stabilizing effects on Cdc68-1p degradation were observed after overexpression of the $UBC1^{C88S}$ or $CDC34^{C95S}$ alleles but not the $UBC7^{C89S}$ or $RAD6^{C88S}$ alleles (data not shown).

The Proteasome Is the Primary Protease Involved in San1p-Mediated Degradation

Because *SAN1*-mediated degradation is ubiquitin dependent, the proteasome is the likely protease involved. In fact, the previously described *cdc68-1* suppressor analysis identified mutations in the proteasomal 19S regulatory particle subunit *RPT6/SUG1/CIM3* that suppressed *cdc68-1* temperature sensitivity (Xu et al., 1993; Xu et al., 1995). To test this idea more thoroughly, we examined the degradation of the Sir4-9 protein in a strain containing the *cim3-1* allele and found that Sir4-9p was stable (Figure 6A). Sir4-9p was also very stable in the presence of *cim5-1*, a mutant allele of another proteasomal 19S subunit (Figure 6A). Finally, to test whether the proteasome's 20S catalytic activity was required for *SAN1*-mediated degradation, we added the proteasome inhibitor MG-132 to cells and assayed for protein stability. Addition of MG-132 stabilized Sir4-9p, Cdc13-1p, and Cdc68-1p (Figure 6B). Thus, *SAN1*-dependent QC degradation requires a functional 26S proteasome.

San1p Does Not Regulate Wild-Type Versions of Its Mutant Substrates

Our observations support a model in which San1p is part of a nuclear-localized PQC degradation machinery. However, San1p could also be a regulator of the wild-type proteins whose mutant versions were its degradation substrates. To see if this were the case, we determined if loss of *SAN1* affected any functions normally associated with the wild-type proteins. Cdc13p is a single-stranded DNA binding protein that regulates telomere length (Smogorzewska and de Lange, 2004). When we examined telomere length in *san1Δ* cells, we saw no significant difference in global telomere length compared to wild-type *SAN1* cells (see Figure S1A in the Supplemental Data available with this article online). Sir4p and Sir3p function together in silent chromatin formation at the silent mating-type loci and telomeres (Aparicio et al., 1991; Rine and Herskowitz, 1987). When we assayed effects on silencing using telomeric reporter genes (Gottschling et al., 1990), we found telomeric silencing was unaffected by loss of *SAN1* (Figure S1B). Cdc68p functions as part of the FACT complex in transcriptional initiation and elongation (Belotserkovskaya et al., 2003; Brewster et al., 2001; Formosa et al., 2001). When comparing gene expression profiles from wild-type or *san1Δ* cells grown in complete synthetic media (YC) or rich media (YEPD; Table 1), we found no difference in expression for genes affected by mutations in *CDC68/SPT16* (Kaplan et al., 2003; Rowley et al., 1991). We also found no significant difference in expression for genes regulated by *SIR4*-mediated silent chromatin at telomeres, the silent mating loci, or for genes regulated by the mating loci (Wyrick et al., 1999). Altogether, we found no evidence that *SAN1* normally regulates any of the processes in which the wild-type Cdc13, Sir4, Sir3, and Cdc68 proteins normally function.

In contrast to our results, it was recently claimed that wild-type Sir4p is degraded in a *SAN1*-dependent man-

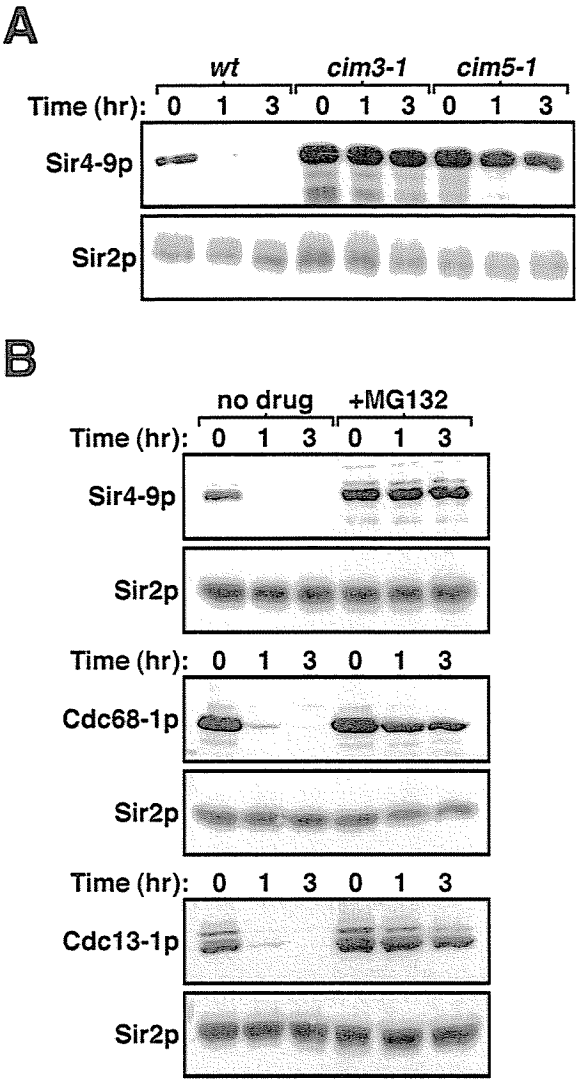

Figure 6. The Proteasome Is Required for Degradation of Mutant Nuclear Proteins

(A) Cycloheximide-chase assays of cells expressing 1Myc-Sir4-9p were performed to assess stability in the presence of either the *cim3-1* or *cim5-1* alleles. Images are of the same blot, probed sequentially with anti-Myc antibodies and anti-Sir2p antibodies.

(B) Cycloheximide-chase assays of cells expressing either wild-type or mutant protein were performed to assess stability in the presence or absence of the proteasome inhibitor MG-132. Assays were performed in *pdr5*Δ cells to increase sensitivity of cells to MG-132 (Chernova et al., 2003). Images are of the same blot, sequentially probed with anti-Myc or anti-Cdc68p antibodies and anti-Sir2p antibodies.

ner (Dasgupta et al., 2004). To resolve this difference, we examined the degradation of wild-type Sir4p in five different strain backgrounds, including the ones reported in the recent study. We found that wild-type Sir4p was stable in every strain background tested. In our hands, mutant Sir4-9p was the only version of Sir4p that was degraded (Figures 1 and S1C). Although we cannot explain these differences, we are confident from our reproducible observations that San1p acts specifically upon mutant versions of Sir4p, Sir3p, Cdc68p, and Cdc13p and not as a regulator of the wild-type proteins.

A Cellular Stress Response Is Induced in the Absence of *SAN1*

Given San1p's role in degrading aberrant nuclear proteins, we speculated that its activity would be important for cellular viability under growth conditions that create aberrant proteins. Consequently, *san1Δ* and wild-type cells were compared for their ability to grow at elevated temperatures or in the presence of $CdCl_2$, in the presence of canavanine, or after exposure to UV, MMS, EMS, or hydrogen peroxide. In no instance did we observe a growth difference between *SAN1* and *san1Δ* cells (data not shown). In fact, *san1* mutant alleles have never been identified in any screen looking for mutations that cause sensitivity to cell stress. A possible explanation for the lack of a cell-stress phenotype is the compensatory upregulation or activation of other pathways in the absence of *SAN1*.

To explore this possibility further, we carefully compared the transcript-microarray profiles of wild-type and *san1Δ* cells. When we placed the genes affected differentially in *san1Δ* cells in order of increased expression, the top thirty upregulated genes for cells grown in YC media were highly represented by those that are induced under cellular stress (Causton et al., 2001; Jelinsky et al., 2000). Using the *Saccharomyces* Genome Database Gene Ontology (GO) Term Finder tool (http://db.yeastgenome.org/cgi-bin/GO/goTermFinder), 12 of the 30 genes belonged to the class of proteins involved in cellular stress ($p = 1.2 \times 10^{-8}$), including seven protein chaperones: *HSP26*, *HSP12*, *HSP42*, *HSP104*, *HSP82*, *HSC82*, and *SSA4* (Table 1). Furthermore, transcript-microarray profiles from the literature revealed that 29 of the 30 genes are induced 2-fold or greater under defined cellular stress conditions (Causton et al., 2001; Jelinsky et al., 2000) and 18 contain a stress response element (STRE) in their promoters (Burchett et al., 2002; Cameroni et al., 2004; DeRisi et al., 1997; Grant et al., 2000; Lagorce et al., 2003; Moskvina et al., 1998) or are regulated by *MSN2/MSN4* (Causton et al., 2001). Although the induction of these genes in our transcript-microarray analysis was modest, ranging from 1.3- to 2.1-fold increases, independent verification by quantitative Northern analyses indicated that some had increased expression by as much as 6-fold (data not shown).

In contrast, when cells were grown in YEPD media, there was no similar transcriptional signature for *san1Δ* cells. Fewer genes were upregulated in *san1Δ* cells under these conditions, and only three of the top thirty genes upregulated during growth in synthetic medium were also upregulated during growth in YEPD (Table 1). The numerous differences between these growth media make it difficult to assess the source of the cell stress resulting from growth in synthetic media. Nevertheless, our data indicate that *san1Δ* cells grown in synthetic media are under a cellular stress that induces the expression of numerous protein chaperones that operate in the nucleus.

Table 1. Genes Upregulated in *san1Δ* Cells

YC Media					
ORF	Gene	Fold Change	p Value	STRE	Stress Induced
YFL014W	HSP12	2.1	3.1×10^{-8}	Yes[1,3,8]	Yes[3,6]
YBR072W	HSP26	1.9	5.0×10^{-8}	Yes[1,3,8]	Yes[3,6]
YNL111C	CYB5	1.7	5.8×10^{-7}		Yes[3,6]
YGR234W	YHB1	1.6	5.7×10^{-8}		Yes[6]
YJR048W	CYC1	1.6	5.1×10^{-8}		Yes[6]
YHR087W		1.5	1.6×10^{-4}	Yes[1,3]	Yes[3,6]
YML128C	MSC1	1.5	5.3×10^{-6}	Yes[1,3]	Yes[3,6]
YER103W	SSA4	1.4	1.1×10^{-6}	Yes[1,3,8]	Yes[3,6]
YER044C	ERG28	1.4	4.6×10^{-6}		Yes[6]
YGR248W	SOL4	1.4	1.9×10^{-3}	Yes[3,4]	Yes[3, 6]
YGR008C	STF2	1.4	1.0×10^{-5}	Yes[1,3]	Yes[3,6]
YLL026W	HSP104	1.4	4.4×10^{-4}	Yes[8]	Yes[3,6]
YDL130W-A	STF1	1.4	7.1×10^{-5}		
YDR070C		1.4	1.0×10^{-4}	Yes[1,3]	Yes[3,6]
YIL111W	COX5B	1.4	2.7×10^{-5}	Yes[3,8]	Yes[3,6]
YMR251W-A	HOR7	1.4	2.9×10^{-4}		Yes[6]
YAR015W	ADE1	1.3	3.7×10^{-6}		Yes[6]
YPR160W	GPH1	1.3	2.6×10^{-3}	Yes[1,3,8]	Yes[3,6]
YMR105C	PGM2	1.3	2.5×10^{-3}	Yes[1,3,8]	Yes[3,6]
YKR080W	MTD1	1.3	4.4×10^{-5}		Yes[6]
YMR186W	HSC82	1.3	2.5×10^{-5}		Yes[6]
YNL015W	PBI2	1.3	1.2×10^{-5}	Yes[3,7]	Yes[3,6]
YMR196W		1.3	1.0×10^{-5}	MSN2/MSN4[3]	Yes[3]
YLR205C	HMX1	1.3	4.4×10^{-5}		Yes[3,6]
YLR217W		1.3	3.6×10^{-5}		Yes[3]
YPL240C	HSP82	1.3	7.3×10^{-5}	Yes[6]	
YDR171W	HSP42	1.3	1.7×10^{-3}	Yes[3,8]	Yes[3,6]
YMR250W	GAD1	1.3	1.5×10^{-3}	Yes[2,3]	Yes[3,6]
YCL035C	GRX1	1.3	1.4×10^{-5}	Yes[3,5]	Yes[3,6]
YFR053C	HXK1	1.3	2.4×10^{-3}	Yes[1,3,8]	Yes[3,6]
YEPD Media					
ORF	Gene	Fold Change	p Value	STRE	Stress Induced
YOL152W	FRE7	2.0	3.3×10^{-10}		
YPR123C		1.6	4.4×10^{-9}		
YPR124W	CTR1	1.5	3.3×10^{-9}		Yes[6]
YGR164W		1.5	2.1×10^{-8}		
YNL111C	CYB5	1.4	1.8×10^{-8}		Yes[3,6]
YLR214W	FRE1	1.4	2.6×10^{-8}		
YJR048W	CYC1	1.4	1.8×10^{-5}		Yes[6]
YER044C	ERG28	1.4	7.3×10^{-8}		Yes[6]
YML075C	HMG1	1.3	4.8×10^{-7}		
YGR234W	YHB1	1.3	5.5×10^{-7}		Yes[6]
YPR200C	ARR2	1.3	1.8×10^{-5}		
YLR158C	ASP3-3	1.3	1.6×10^{-7}		Yes[6]
YOL106W		1.3	9.1×10^{-5}		

Genes whose expression is increased by greater than 1.3-fold in *san1Δ* cells compared to wild-type *SAN1* cells are listed above. For complete data set, including genes that are downregulated, see Table S3. Genes that possess a STRE in their promoter are listed. Genes that are regulated by various stress conditions are annotated with the appropriate references below.

[1] Burchett et al., 2002
[2] Cameroni et al., 2004
[3] Causton et al., 2001
[4] DeRisi et al., 1997
[5] Grant et al., 2000
[6] Jelinsky et al., 2000
[7] Lagorce et al., 2003
[8] Moskvina et al., 1998

Discussion

SAN1 Defines a Nuclear PQC Degradation System within the Nucleus

In this study, we provide evidence for a PQC system that resides within the nucleus and degrades aberrant proteins. The defining member of this degradation system is San1p, a ubiquitin-protein ligase that requires nuclear localization for its proper function. San1p mediates the ubiquitination of aberrant nuclear proteins, which ultimately leads to their degradation by the proteasome. The critical evidence that San1p is part of a PQC degradation system comes from its specific destruction of mutant nuclear proteins, while it leaves the

wild-type counterparts of these proteins unscathed. Yet San1p is not a global degradation factor; loss of *SAN1* does not stabilize PQC substrates of the endoplasmic reticulum (Dasgupta et al., 2004).

Because San1p is a ubiquitin-protein ligase, it must act in concert with ubiquitin-conjugating enzymes. Of the eleven UBCs in *S. cerevisiae*, only mutant alleles of *CDC34* and *UBC1* stabilized San1p substrates. Formally, it is possible that other UBCs are involved in San1p-mediated degradation, given that some UBCs appear to be redundant in other degradation pathways (Betting and Seufert, 1996; Chen et al., 1993; Seufert and Jentsch, 1990). Nevertheless, both Ubc1p and Cdc34p are found in the nucleus (Blondel et al., 2000; Huh et al., 2003), which is consistent with their role in the degradation of San1p substrates. Previously, the only function assigned to Cdc34p was as part of the SCF complex, where it mediates the regulated ubiquitination of numerous substrates, including those required for cell-cycle progression (Deshaies, 1999). Thus, Cdc34p involvement in nuclear PQC degradation defines a new role for the UBC. Ubc1p has already been shown to function in PQC degradation at the ER as part of the HRD complex (Bays et al., 2001; Friedlander et al., 2000), so involvement in nuclear PQC degradation is an extension of Ubc1p function.

The involvement of Cdc34p and Ubc1p in the degradation of San1p substrates and the nature of San1p itself opens up intriguing parallels with PQC degradation in the ER, mediated by the RING-domain ubiquitin-protein ligase Hrd1p (Bays et al., 2001; Deak and Wolf, 2001). The closest homolog to San1p in the *S. cerevisiae* genome is Hrd1p, with 24% identity and 40% similarity shared between them in a 174 residue stretch comprising the RING domain and an adjacent C-terminal region (https://proteome.incyte.com/proteome/YPD/SAN1.html). Ubc1p is required for both the normal degradation of Hrd1p-dependent substrates (Bays et al., 2001; Friedlander et al., 2000) and San1p-dependent substrates (Figure 5). Cdc34p shares the greatest homology with Ubc7p (Ptak et al., 2001), which interacts with Hrd1p and is the primary UBC required for Hrd1p-mediated degradation (Bays et al., 2001; Deak and Wolf, 2001). Given the homology between Hrd1p and San1p and the involvement of identical and highly similar UBCs, we speculate that the two PQC degradation systems may have evolved from a common pathway, with Hrd1p anchored to the ER and San1p targeted to the nucleus.

Although we have identified four mutant protein substrates of the *SAN1* system, we cannot yet explain what hallmarks of the mutant proteins are recognized as "aberrant" by this system (e.g., exposed hydrophobic patches, atypical posttranslational modifications, aggregation, etc.). Clearly, whatever is recognized as aberrant does not necessarily coincide with complete loss of protein activity. Otherwise, the *sir4-9* and *cdc68-1* phenotypes would not have been suppressed by deleting *SAN1*.

We also do not yet know what properties of San1p allow it to recognize aberrant proteins. Is aberrant protein targeting an autonomous feature of San1p, or does San1p engage ancillary factors, such as protein chaperones, to target aberrant proteins for ubiquitination? It also is not clear if San1p targets aberrant proteins from all regions of the nucleus or if San1p action is restricted to aberrant chromatin-associated proteins such as the ones examined in this study.

SAN1 Reduces Cellular Stress

In support of San1p's role in nuclear PQC, *san1Δ* cells grown in synthetic media had a transcript-microarray signature indicative of a cellular stress response. Of the 30 upregulated genes, 29 are induced under cellular stress conditions, 18 have STRE in their promoters, and 7 are protein chaperones. Of the chaperones, *HSP26* and *HSP104* are implicated in nuclear protein homeostasis (Parsell et al., 1994; Rossi and Lindquist, 1989); overexpression of *HSP82* or *HSC82* partially suppresses the temperature sensitivity of the *cdc13-1* allele (Grandin and Charbonneau, 2001), which encodes one of the San1p substrates we identified, and Hsp12p, Hsp26p, Hsp104p, and Ssa4p are localized to the nucleus (Chughtai et al., 2001; Huh et al., 2003; Kawai et al., 1999; Rossi and Lindquist, 1989). The increased expression of these genes in *san1Δ* cells is consistent with the idea that loss of *SAN1* results in the accumulation of aberrant proteins in the nucleus, which in turn triggers a cellular response that attempts to refold or otherwise sequester the aberrant nuclear proteins. By extension, we propose that San1p normally rids the nucleus of aberrant proteins, and its presence alleviates the need for such a response.

The increased expression of protein chaperones may buffer the cell from dramatic phenotypic effects when *SAN1* is absent. In fact, the low level of chronic stress that *san1Δ* cells are under may precondition them for additional challenges, similar to what occurs in thermotolerance (Kregel, 2002). This may explain why a significant growth difference between *san1Δ* and wild-type cells was not observed under standard lab conditions or after exposure to physical and chemical challenges. The use of alternate mechanisms to handle aberrant proteins when degradation is alleviated appears to be typical for PQC, as evidenced by what occurs in ER PQC (Friedlander et al., 2000; Travers et al., 2000).

The induction of the stress response in *san1Δ* cells might also be explained if *SAN1* facilitates the rapid and continuous degradation of a positive regulator of stress response genes. In the absence of *SAN1*, the positive regulator would rise above a critical threshold required for activation of the stress response. However, we find this explanation unlikely, since a similar stress response was not detected when cells were grown in YEPD media. Instead, the differential response implies that the metabolism of cells grown in synthetic media generated more aberrant nuclear proteins than when cells were grown in rich media.

San1p as a Last Line of Proteolytic Defense against Aberrant Nuclear Proteins

One implication of our findings is that the *SAN1* system functions downstream of protein production, recognizing determinants in aberrant proteins that were not detected by earlier cytoplasmic PQC checkpoints, which in principle should act on aberrant proteins before they become nuclear localized. If San1p substrates were de-

stroyed by cytoplasmic PQC, the degradation and, consequently, the temperature-sensitive phenotypes of both the Sir4-9 and Cdc68-1 proteins would not be suppressed by loss of *SAN1* function (Schnell et al., 1989; Xu et al., 1993). Why are cytoplasmic PQC degradation pathways unable to target the mutant San1p substrates for destruction? Perhaps there are environmental differences between the cytoplasm and nucleus, such that the determinants of aberrancy are only revealed upon import into the nucleus. Alternatively, such determinants may be hidden from cytoplasmic PQC by proteins that function as escorts prior to nuclear import, or the determinants may be uncovered during nuclear import itself. Given the failure of earlier PQC checkpoints to recognize these aberrant proteins, it may be that the cell uses San1p as a last line of proteolytic defense against accumulation of aberrant proteins in the nucleus, initiating degradation when other PQC pathways upstream in the hierarchy of PQC fail.

As noted above, a lack of *SAN1*-mediated nuclear PQC degradation manifests a stress response in *S. cerevisiae*. This may be indicative of a cellular pathology that can occur in any eukaryotic cell, including those associated with some neurodegenerative diseases in which there is accumulation and aggregation of mutant proteins in the nucleus. From our sequence-based searches, we have identified homologs of San1p in a number of fungi (data not shown). Using those in subsequent iterative searches, we found proteins with regions of similarity, including the noncanonical RING domain, in metazoa and plants, indicating that an analogous pathway may exist in other species. In metazoans, nuclear PQC may be most critical in cell types that remain in a nondividing state for long periods of time, such as neural and muscle cells. We speculate that the severity in onset of nuclear protein aggregation diseases may be influenced by the activity of this or a similar pathway.

Experimental Procedures

Materials and Reagents

Reagents were from New England Biolabs (Beverley, Massachusetts), Sigma (St. Louis, Missouri), and Fisher (Pittsburgh, Pennsylvania). Nitrocellulose (Protran, pore size 0.2 μM) was from Schleicher and Schuell (Keene, New Hampshire). Mouse anti-Myc, anti-VSV, and anti-HA antibodies were from Sigma (St. Louis, Missouri) and used at 1:10,000 dilutions. Mouse anti-HSV antibody was from Novagen (Madison, Wisconsin) and used at a 1:10,000 dilution. Goat anti-Sir2p polyclonal antibodies and donkey anti-goat HRP-conjugated antisera were from Santa Cruz Biotechnology (Santa Cruz, California) and used at a 1:2000 dilutions. Rabbit anti-Cdc68p antisera was kindly provided by Tim Formosa (University of Utah) and used at a 1:1000 dilution. Affinity-purified rabbit anti-Sir4p antibodies were kindly provided by Danesh Moazed (Harvard University) and used at a 1:2000 dilution. Rabbit anti-Sir4p antisera were from Covance (Princeton, New Jersey), after providing them with GST-Sir4p (C1) purified as previously described (Moazed et al., 1997), and used at a 1:500 dilution. ECL chemiluminescence reagents, sheep anti-mouse, and donkey anti-rabbit HRP-conjugated antisera were from Amersham Biosciences (Piscataway, New Jersey) and used at 1:2000 dilutions. FastFlow rProtein G-agarose was from Repligen (Waltham, Massachusetts). Purified yeast E1 enzyme, human UbcH5a, ubiquitin, Mg-ATP, and MG-132 were from Boston Biochem (Boston, Massachusetts). GST-Bind resin was from Novagen. Talon resin was from BD Biosciences Clontech (Palo Alto, California).

Plasmids and Yeast Strains

Standard molecular biology techniques were used. All plasmids used in this study and brief descriptions of their construction are listed in Table S1.

Standard yeast methods were used. Recipes for YEPD media and YC media can be found at http://www.fhcrc.org/labs/gottschling. All yeast strains used in this study are listed in Table S2.

Degradation Assays

Protein degradation was assessed by cycloheximide-chase assays similar to previously described (Gardner and Hampton, 1999), with some changes. Cells were usually grown in YEPD media to an approximate cell density of 2×10^7 cells/ml at the permissive temperature of 20°C or 25°C before addition of cycloheximide (50 μg/ml final concentration), and further incubated at the restrictive temperatures of 30°C, 34°C, or 37°C for 0–3 hr after addition of cycloheximide. In some cases, cells were grown first in YC + 3% raffinose, with galactose added to a final concentration of 3% and cultures incubated for 4 hr prior to addition of cycloheximide. In other cases, the proteasome inhibitor MG-132 was added to a final concentration of 25 μg/ml, and cultures were further incubated at 25°C for 30 min prior to addition of cycloheximide. Cells were lysed in 200 μl SUMEB (8 M urea, 1% SDS, 10 mM MOPS [pH6.8], 10 mM EDTA, 0.01% bromophenol blue) + 10 mM PMSF. Fifteen to thirty microliter samples of the cellular lysates were resolved on 8% SDS-PAGE gels, the proteins transferred to nitrocellulose, and immunoblotted with the appropriate antibody.

Ubiquitination Assays

GST fusions of San1p were purified per manufacturer's instructions (Novagen GST-Bind kit) from 100 ml LB + amp cultures, which were initially grown at 37°C to an optical density (OD_{600}) of 0.3. IPTG was added to a final concentration of 0.8 mM and the cultures were incubated for 6 hr at 37°C. Cells were harvested by centrifugation and then frozen at −80°C overnight. Frozen cells were lysed in 20 ml lysis buffer (20 mM Tris-HCl [pH8.0], 200 mM NaCl, 1 mM EDTA, 1 mM EGTA) + 10 mM PMSF + 10 mM benzamide + 200 μg/ml lysozyme. Clarified lysates were loaded onto 1.5 ml glutathione columns prewashed with 5 ml lysis buffer. Columns were washed with 20 ml lysis buffer then 20 ml wash buffer (20 mM HEPES-KOH [pH7.6], 350 mM NaCl, 1 mM DTT). Bound proteins were eluted with 10 ml wash buffer + 10 mM glutathione. Samples containing purified GST-San1 protein were combined and concentrated using a Centricon10 (Millipore, Bedford, Massachusetts).

In vitro ubiquitination assays were performed similar to previously described (Lorick et al., 1999), with some changes. Fifteen microliter reactions containing 0.08 μg ubiquitin activating enzyme (yeast Uba1p), 0.1 μg ubiquitin conjugating enzyme (human UbcH5a), 1.75 μg purified GST-San1p (or its mutant variants or GST alone), 2.5 μg ubiquitin, 2 mM Mg-ATP, 50 mM Tris-HCl (pH7.5), 2.5 mM $MgCl_2$, and 0.5 mM DTT were incubated at 25°C for 90 min. Fifteen microliters SUMEB was added to each sample and incubated at 65°C for 10 min. The entire reaction was resolved on 8% SDS-PAGE gels, the proteins transferred to nitrocellulose, and immunoblotted with anti-ubiquitin monoclonal antibody (Kahana and Gottschling, 1999).

In vivo ubiquitination assays were performed similar to previously described (Gardner and Hampton, 1999), with modifications. Strains expressing either 1Myc-Sir4p or 1Myc-Sir4-9p and a triple HA-epitope-tagged ubiquitin expressed from the constitutive *TDH3* promoter were grown in 20 ml YC Ura$^-$ media to an approximate cell density of 2×10^7 cells/ml. Cultures were divided into 2–5 ml aliquots, with one aliquot incubated at 25°C and the other incubated at 34°C for 20 min. Cellular lysates were prepared in 200 μl SUME + 10 mM PMSF + 5 mM N-ethylmaleimide (NEM). 1Myc-Sir4 proteins were immunoprecipitated in 1 ml IP buffer (15 mM Na_2PO_4, 150 mM NaCl, 2% Triton-X100, 0.1% SDS, 0.5% deoxycholate, 10 mM EDTA [pH7.5]) + 10 mM PMSF + 5 mM NEM + 20 μl anti-Sir4p antibodies. 100 μl FastFlow rProtein G-agarose was used to capture the immunocomplexes. Proteins were eluted from beads using 60 μl SUMEB + 5% β-mercaptoethanol and incubation at 65°C for 10 min. Ten microliter or forty microliter samples were resolved on 8%

SDS-PAGE gels, proteins transferred to nitrocellulose, and immunoblotted with either an anti-Myc antibody or an anti-HA antibody.

Transcript DNA Microarrays

Transcript DNA microarrays were performed similar to previously described (Fazzio et al., 2001). Three independent *san1Δ* cultures and three independent wild-type cultures were grown to midlog phase at 30°C in 50 ml YEPD or YC media. Dye-reversal experiments were performed to identify sequence-specific dye biases. Statistical analysis of microarray data was performed as previously described (Cullen et al., 2004). The entire normalized data set is in Table S3.

Supplemental Data

Supplemental Data include one figure, three tables, and Supplemental Experimental Procedures and can be found with this article online at http://www.cell.com/cgi/content/full/120/6/803/DC1/.

Acknowledgments

We thank C. Boone, T. Formosa, R. Hampton, L. Hartwell, M. Hochstrasser, S. Jentsch, D. Moazed, L. Pillus, M. Rosbash, R.A. Singer, V. Lundblad, and V. Zakian for plasmids, strains, and/or antibodies, R. Hampton for experimental advice, R. Lipford and R. Deshaies for advice on proteasome inhibitors, S. Biggins and members of the Biggins lab for advice with microscopy, J. Delrow for assistance with microarray data analysis, and H. Eisen and members of the Gottschling lab for insightful discussions and critical reading of this manuscript. R.G.G. is a Bristol Myers Squibb fellow of the Life Sciences Research Foundation. This work was supported by National Institutes of Health grant GM43893 to D.E.G.

Received: December 6, 2004
Revised: January 11, 2005
Accepted: January 18, 2005
Published: March 24, 2005

References

Abu-Baker, A., Messaed, C., Laganiere, J., Gaspar, C., Brais, B., and Rouleau, G.A. (2003). Involvement of the ubiquitin-proteasome pathway and molecular chaperones in oculopharyngeal muscular dystrophy. Hum. Mol. Genet. *12*, 2609–2623.

Aparicio, O.M., Billington, B.L., and Gottschling, D.E. (1991). Modifiers of position effect are shared between telomeric and silent mating-type loci in S. cerevisiae. Cell *66*, 1279–1287.

Arnold, I., and Langer, T. (2002). Membrane protein degradation by AAA proteases in mitochondria. Biochim. Biophys. Acta *1592*, 89–96.

Banerjee, A., Deshaies, R.J., and Chau, V. (1995). Characterization of a dominant negative mutant of the cell cycle ubiquitin-conjugating enzyme Cdc34. J. Biol. Chem. *270*, 26209–26215.

Bays, N.W., Gardner, R.G., Seelig, L.P., Joazeiro, C.A., and Hampton, R.Y. (2001). Hrd1p/Der3p is a membrane-anchored ubiquitin ligase required for ER-associated degradation. Nat. Cell Biol. *3*, 24–29.

Belotserkovskaya, R., Oh, S., Bondarenko, V.A., Orphanides, G., Studitsky, V.M., and Reinberg, D. (2003). FACT facilitates transcription-dependent nucleosome alteration. Science *301*, 1090–1093.

Betting, J., and Seufert, W. (1996). A yeast Ubc9 mutant protein with temperature-sensitive in vivo function is subject to conditional proteolysis by a ubiquitin- and proteasome-dependent pathway. J. Biol. Chem. *271*, 25790–25796.

Biggins, S., Severin, F.F., Bhalla, N., Sassoon, I., Hyman, A.A., and Murray, A.W. (1999). The conserved protein kinase Ipl1 regulates microtubule binding to kinetochores in budding yeast. Genes Dev. *13*, 532–544.

Blondel, M., Galan, J.M., Chi, Y., Lafourcade, C., Longaretti, C., Deshaies, R.J., and Peter, M. (2000). Nuclear-specific degradation of Far1 is controlled by the localization of the F-box protein Cdc4. EMBO J. *19*, 6085–6097.

Bordallo, J., Plemper, R.K., Finger, A., and Wolf, D.H. (1998). Der3p/Hrd1p is required for endoplasmic reticulum-associated degradation of misfolded lumenal and integral membrane proteins. Mol. Biol. Cell *9*, 209–222.

Brais, B. (2003). Oculopharyngeal muscular dystrophy: a late-onset polyalanine disease. Cytogenet. Genome Res. *100*, 252–260.

Brewster, N.K., Johnston, G.C., and Singer, R.A. (2001). A bipartite yeast SSRP1 analog comprised of Pob3 and Nhp6 proteins modulates transcription. Mol. Cell. Biol. *21*, 3491–3502.

Burchett, S.A., Flanary, P., Aston, C., Jiang, L., Young, K.H., Uetz, P., Fields, S., and Dohlman, H.G. (2002). Regulation of stress response signaling by the N-terminal dishevelled/EGL-10/pleckstrin domain of Sst2, a regulator of G protein signaling in Saccharomyces cerevisiae. J. Biol. Chem. *277*, 22156–22167.

Calado, A., Tome, F.M., Brais, B., Rouleau, G.A., Kuhn, U., Wahle, E., and Carmo-Fonseca, M. (2000). Nuclear inclusions in oculopharyngeal muscular dystrophy consist of poly(A) binding protein 2 aggregates which sequester poly(A) RNA. Hum. Mol. Genet. *9*, 2321–2328.

Cameroni, E., Hulo, N., Roosen, J., Winderickx, J., and De Virgilio, C. (2004). The novel yeast PAS kinase Rim 15 orchestrates G0-associated antioxidant defense mechanisms. Cell Cycle *3*, 462–468.

Causton, H.C., Ren, B., Koh, S.S., Harbison, C.T., Kanin, E., Jennings, E.G., Lee, T.I., True, H.L., Lander, E.S., and Young, R.A. (2001). Remodeling of yeast genome expression in response to environmental changes. Mol. Biol. Cell *12*, 323–337.

Chen, P., Johnson, P., Sommer, T., Jentsch, S., and Hochstrasser, M. (1993). Multiple ubiquitin-conjugating enzymes participate in the in vivo degradation of the yeast MAT alpha 2 repressor. Cell *74*, 357–369.

Chernova, T.A., Allen, K.D., Wesoloski, L.M., Shanks, J.R., Chernoff, Y.O., and Wilkinson, K.D. (2003). Pleiotropic effects of Ubp6 loss on drug sensitivities and yeast prion are due to depletion of the free ubiquitin pool. J. Biol. Chem. *278*, 52102–52115.

Chughtai, Z.S., Rassadi, R., Matusiewicz, N., and Stochaj, U. (2001). Starvation promotes nuclear accumulation of the hsp70 Ssa4p in yeast cells. J. Biol. Chem. *276*, 20261–20266.

Cullen, P.J., Sabbagh, W., Jr., Graham, E., Irick, M.M., van Olden, E.K., Neal, C., Delrow, J., Bardwell, L., and Sprague, G.F., Jr. (2004). A signaling mucin at the head of the Cdc42- and MAPK-dependent filamentous growth pathway in yeast. Genes Dev. *18*, 1695–1708.

Dasgupta, A., Ramsey, K.L., Smith, J.S., and Auble, D.T. (2004). Sir antagonist 1 (San1) is a ubiquitin ligase. J. Biol. Chem. *279*, 26830–26838.

Davies, S.W., Turmaine, M., Cozens, B.A., DiFiglia, M., Sharp, A.H., Ross, C.A., Scherzinger, E., Wanker, E.E., Mangiarini, L., and Bates, G.P. (1997). Formation of neuronal intranuclear inclusions underlies the neurological dysfunction in mice transgenic for the HD mutation. Cell *90*, 537–548.

Deak, P.M., and Wolf, D.H. (2001). Membrane topology and function of Der3/Hrd1p as a ubiquitin-protein ligase (E3) involved in endoplasmic reticulum degradation. J. Biol. Chem. *276*, 10663–10669.

DeRisi, J.L., Iyer, V.R., and Brown, P.O. (1997). Exploring the metabolic and genetic control of gene expression on a genomic scale. Science *278*, 680–686.

Deshaies, R.J. (1999). SCF and Cullin/Ring H2-based ubiquitin ligases. Annu. Rev. Cell Dev. Biol. *15*, 435–467.

Evans, D.R., Brewster, N.K., Xu, Q., Rowley, A., Altheim, B.A., Johnston, G.C., and Singer, R.A. (1998). The yeast protein complex containing cdc68 and pob3 mediates core-promoter repression through the cdc68 N-terminal domain. Genetics *150*, 1393–1405.

Fazzio, T.G., Kooperberg, C., Goldmark, J.P., Neal, C., Basom, R., Delrow, J., and Tsukiyama, T. (2001). Widespread collaboration of Isw2 and Sin3-Rpd3 chromatin remodeling complexes in transcriptional repression. Mol. Cell. Biol. *21*, 6450–6460.

Formosa, T., Eriksson, P., Wittmeyer, J., Ginn, J., Yu, Y., and Still-

man, D.J. (2001). Spt16-Pob3 and the HMG protein Nhp6 combine to form the nucleosome-binding factor SPN. EMBO J. *20*, 3506–3517.

Friedlander, R., Jarosch, E., Urban, J., Volkwein, C., and Sommer, T. (2000). A regulatory link between ER-associated protein degradation and the unfolded-protein response. Nat. Cell Biol. *2*, 379–384.

Gardner, R.G., and Hampton, R.Y. (1999). A 'distributed degron' allows regulated entry into the ER degradation pathway. EMBO J. *18*, 5994–6004.

Goldberg, A.L. (2003). Protein degradation and protection against misfolded or damaged proteins. Nature *426*, 895–899.

Gottschling, D.E., Aparicio, O.M., Billington, B.L., and Zakian, V.A. (1990). Position effect at S. cerevisiae telomeres: Reversible repression of Pol II transcription. Cell *63*, 751–762.

Grandin, N., and Charbonneau, M. (2001). Hsp90 levels affect telomere length in yeast. Mol. Genet. Genomics *265*, 126–134.

Grant, C.M., Luikenhuis, S., Beckhouse, A., Soderbergh, M., and Dawes, I.W. (2000). Differential regulation of glutaredoxin gene expression in response to stress conditions in the yeast Saccharomyces cerevisiae. Biochim. Biophys. Acta *1490*, 33–42.

Hampton, R.Y. (2002). ER-associated degradation in protein quality control and cellular regulation. Curr. Opin. Cell Biol. *14*, 476–482.

Huh, W.K., Falvo, J.V., Gerke, L.C., Carroll, A.S., Howson, R.W., Weissman, J.S., and O'Shea, E.K. (2003). Global analysis of protein localization in budding yeast. Nature *425*, 686–691.

Jackson, P.K., Eldridge, A.G., Freed, E., Furstenthal, L., Hsu, J.Y., Kaiser, B.K., and Reimann, J.D. (2000). The lore of the RINGs: substrate recognition and catalysis by ubiquitin ligases. Trends Cell Biol. *10*, 429–439.

Jana, N.R., and Nukina, N. (2003). Recent advances in understanding the pathogenesis of polyglutamine diseases: involvement of molecular chaperones and ubiquitin-proteasome pathway. J. Chem. Neuroanat. *26*, 95–101.

Jelinsky, S.A., Estep, P., Church, G.M., and Samson, L.D. (2000). Regulatory networks revealed by transcriptional profiling of damaged Saccharomyces cerevisiae cells: Rpn4 links base excision repair with proteasomes. Mol. Cell. Biol. *20*, 8157–8167.

Joazeiro, C.A., Wing, S.S., Huang, H., Leverson, J.D., Hunter, T., and Liu, Y.C. (1999). The tyrosine kinase negative regulator c-Cbl as a RING-type, E2-dependent ubiquitin-protein ligase. Science *286*, 309–312.

Kahana, A., and Gottschling, D.E. (1999). DOT4 links silencing and cell growth in Saccharomyces cerevisiae. Mol. Cell. Biol. *19*, 6608–6620.

Kaplan, C.D., Laprade, L., and Winston, F. (2003). Transcription elongation factors repress transcription initiation from cryptic sites. Science *301*, 1096–1099.

Kawai, R., Fujita, K., Iwahashi, H., and Komatsu, Y. (1999). Direct evidence for the intracellular localization of Hsp104 in Saccharomyces cerevisiae by immunoelectron microscopy. Cell Stress Chaperones *4*, 46–53.

Kregel, K.C. (2002). Heat shock proteins: modifying factors in physiological stress responses and acquired thermotolerance. J. Appl. Physiol. *92*, 2177–2186.

Lagorce, A., Hauser, N.C., Labourdette, D., Rodriguez, C., Martin-Yken, H., Arroyo, J., Hoheisel, J.D., and Francois, J. (2003). Genome-wide analysis of the response to cell wall mutations in the yeast Saccharomyces cerevisiae. J. Biol. Chem. *278*, 20345–20357.

Liu, Y., Mathias, N., Steussy, C.N., and Goebl, M.G. (1995). Intragenic suppression among CDC34 (UBC3) mutations defines a class of ubiquitin-conjugating catalytic domains. Mol. Cell. Biol. *15*, 5635–5644.

Lorick, K.L., Jensen, J.P., Fang, S., Ong, A.M., Hatakeyama, S., and Weissman, A.M. (1999). RING fingers mediate ubiquitin-conjugating enzyme (E2)-dependent ubiquitination. Proc. Natl. Acad. Sci. USA *96*, 11364–11369.

Madura, K., Dohmen, R.J., and Varshavsky, A. (1993). N-recognin/Ubc2 interactions in the N-end rule pathway. J. Biol. Chem. *268*, 12046–12054.

McDonough, H., and Patterson, C. (2003). CHIP: a link between the chaperone and proteasome systems. Cell Stress Chaperones *8*, 303–308.

Moazed, D., Kistler, A., Axelrod, A., Rine, J., and Johnson, A.D. (1997). Silent information regulator protein complexes in Saccharomyces cerevisiae: a SIR2/SIR4 complex and evidence for a regulatory domain in SIR4 that inhibits its interaction with SIR3. Proc. Natl. Acad. Sci. USA *94*, 2186–2191.

Moskvina, E., Schuller, C., Maurer, C.T., Mager, W.H., and Ruis, H. (1998). A search in the genome of Saccharomyces cerevisiae for genes regulated via stress response elements. Yeast *14*, 1041–1050.

Palladino, F., Laroche, T., Gilson, E., Axelrod, A., Pillus, L., and Gasser, S.M. (1993). SIR3 and SIR4 proteins are required for the positioning and integrity of yeast telomeres. Cell *75*, 543–555.

Parsell, D.A., Kowal, A.S., Singer, M.A., and Lindquist, S. (1994). Protein disaggregation mediated by heat-shock protein Hsp104. Nature *372*, 475–478.

Ptak, C., Gwozd, C., Huzil, J.T., Gwozd, T.J., Garen, G., and Ellison, M.J. (2001). Creation of a pluripotent ubiquitin-conjugating enzyme. Mol. Cell. Biol. *21*, 6537–6548.

Qi, H., and Zakian, V.A. (2000). The Saccharomyces telomere-binding protein Cdc13p interacts with both the catalytic subunit of DNA polymerase alpha and the telomerase-associated est1 protein. Genes Dev. *14*, 1777–1788.

Rine, J., and Herskowitz, I. (1987). Four genes responsible for a position effect on expression from HML and HMR in Saccharomyces cerevisiae. Genetics *116*, 9–22.

Rossi, J.M., and Lindquist, S. (1989). The intracellular location of yeast heat-shock protein 26 varies with metabolism. J. Cell Biol. *108*, 425–439.

Rowley, A., Singer, R.A., and Johnston, G.C. (1991). CDC68, a yeast gene that affects regulation of cell proliferation and transcription, encodes a protein with a highly acidic carboxyl terminus. Mol. Cell. Biol. *11*, 5718–5726.

Schnell, R., D'Ari, L., Foss, M., Goodman, D., and Rine, J. (1989). Genetic and molecular characterization of suppressors of SIR4 mutations in Saccharomyces cerevisiae. Genetics *122*, 29–46.

Schubert, U., Antón, L.C., Gibbs, J., Norbury, C.C., Yewdell, J.W., and Bennink, J.R. (2000). Rapid degradation of a large fraction of newly synthesized proteins by proteasomes. Nature *404*, 770–774.

Seufert, W., and Jentsch, S. (1990). Ubiquitin-conjugating enzymes UBC4 and UBC5 mediate selective degradation of short-lived and abnormal proteins. EMBO J. *9*, 543–550.

Shastry, B.S. (2003). Neurodegenerative disorders of protein aggregation. Neurochem. Int. *43*, 1–7.

Smogorzewska, A., and de Lange, T. (2004). Regulation of telomerase by telomeric proteins. Annu. Rev. Biochem. *73*, 177–208.

Stirling, P.C., Lundin, V.F., and Leroux, M.R. (2003). Getting a grip on non-native proteins. EMBO Rep. *4*, 565–570.

Travers, K.J., Patil, C.K., Wodicka, L., Lockhart, D.J., Weissman, J.S., and Walter, P. (2000). Functional and genomic analyses reveal an essential coordination between the unfolded protein response and ER-associated degradation. Cell *101*, 249–258.

Trombetta, E.S., and Parodi, A.J. (2003). Quality control and protein folding in the secretory pathway. Annu. Rev. Cell Dev. Biol. *19*, 649–676.

Ulrich, H.D., and Jentsch, S. (2000). Two RING finger proteins mediate cooperation between ubiquitin-conjugating enzymes in DNA repair. EMBO J. *19*, 3388–3397.

Waelter, S., Boeddrich, A., Lurz, R., Scherzinger, E., Lueder, G., Lehrach, H., and Wanker, E.E. (2001). Accumulation of mutant huntingtin fragments in aggresome-like inclusion bodies as a result of insufficient protein degradation. Mol. Biol. Cell *12*, 1393–1407.

Wojcik, C., and DeMartino, G.N. (2003). Intracellular localization of proteasomes. Int. J. Biochem. Cell Biol. *35*, 579–589.

Wyrick, J.J., Holstege, F.C., Jennings, E.G., Causton, H.C., Shore, D., Grunstein, M., Lander, E.S., and Young, R.A. (1999). Chromosomal landscape of nucleosome-dependent gene expression and silencing in yeast. Nature *402*, 418–421.

Xu, Q., Johnston, G.C., and Singer, R.A. (1993). The Saccharomyces cerevisiae Cdc68 transcription activator is antagonized by San1, a protein implicated in transcriptional silencing. Mol. Cell. Biol. *13*, 7553–7565.

Xu, Q., Singer, R.A., and Johnston, G.C. (1995). Sug1 modulates yeast transcription activation by Cdc68. Mol. Cell. Biol. *15*, 6025–6035.

Accession Numbers

The GEO accession number for the series of transcript array datasets is GSE2159.

MOLECULAR AND CELLULAR BIOLOGY, July 2005, p. 6123–6139 Vol. 25, No. 14
0270-7306/05/$08.00+0 doi:10.1128/MCB.25.14.6123–6139.2005

Ubp10/Dot4p Regulates the Persistence of Ubiquitinated Histone H2B: Distinct Roles in Telomeric Silencing and General Chromatin†

Richard G. Gardner, Zara W. Nelson, and Daniel E. Gottschling*

Fred Hutchinson Cancer Research Center, Seattle, Washington 98109

Received 16 February 2005/Returned for modification 23 March 2005/Accepted 8 April 2005

We previously discovered that the ubiquitin protease Ubp10/Dot4p is important for telomeric silencing through its interaction with Sir4p. However, the mechanism of Ubp10p action was unknown. We now provide evidence that Ubp10p removes ubiquitin from histone H2B; cells with *UBP10* deleted have increased steady-state levels of H2B ubiquitination. As a consequence, *ubp10*Δ cells also have increased steady-state levels of histone H3 Lys4 and Lys79 methylation. Consistent with its role in silencing, Ubp10p is preferentially localized to silent chromatin where its ubiquitin protease activity maintains low levels of H3 Lys4 and Lys79 methylation to allow optimal Sir protein binding to telomeres and global telomeric silencing. The ubiquitin protease Ubp8p has also been shown to remove ubiquitin from H2B, and *ubp8*Δ cells have increased steady-state levels of H2B ubiquitination similar to those in *ubp10*Δ cells. Unlike *ubp10*Δ cells, however, *ubp8*Δ cells do not have increased steady-state levels of H3 Lys4 and Lys79 methylation, nor is telomeric silencing affected. Despite their separate functions in silencing and SAGA-mediated transcription, respectively, deletion of both *UBP10* and *UBP8* results in a synergistic increase in the steady-state levels of H2B ubiquitination and in the number of genes with altered expression, indicating that Ubp10p and Ubp8p likely overlap in some of their target chromatin regions. We propose that Ubp10p and Ubp8p are the only ubiquitin proteases that normally remove monoubiquitin from histone H2B and, while there are regions of the genome to which each is specifically targeted, both combine to regulate the global balance of H2B ubiquitination.

Posttranslational modifications of nucleosomal histones play pivotal regulatory roles in all aspects of eukaryotic chromosome dynamics: replication, recombination, repair, segregation, and gene expression. These modifications include acetylation, methylation, phosphorylation, ubiquitination, sumoylation, and ADP-ribosylation (71). Many of these modifications often occur together within the same histone or nucleosome or within neighboring nucleosomes, creating distinct chromatin domains (71). Particular combinations of residue-specific modifications typically correlate with specific functional consequences for the modified chromatin domains (71).

In *Saccharomyces cerevisiae*, chromatin-mediated silencing at telomeres and the *HM* loci is particularly sensitive to histone acetylation and methylation, which appear to disrupt the ability of the silencing proteins Sir3p and Sir4p to bind to, or assemble along, the nucleosome fiber. For example, tethering of histone acetylases to silent domains increases histone acetylation within these domains and blocks the propagation of silencing (16). Similarly, overexpression of a histone methylase greatly increases global histone methylation and disrupts silencing (85, 92). In vitro, fragments of Sir3p bind unacetylated and unmethylated histone peptides better than those that are acetylated or methylated (13, 81), demonstrating the preference of Sir3p for unmodified histones. Because of this preference, histone acetylation and methylation appear to be excluded from silent chromatin (5–7, 63, 79, 88, 90).

In genetic screens looking for factors that compromise telomeric silencing, we previously identified a number of genes that encode protein modification enzymes, such as *DOT1*, *DOT4*, and *RAD6* (37, 85). Dot1p is a histone methyltransferase that methylates Lys79 of histone H3 in the context of the nucleosome (24, 49, 65, 92). H3 Lys79 methylation is primarily associated with active chromatin—approximately 90% of histone H3 in yeast is methylated at this site (92)—and the modification is absent from silent chromatin loci (63). Loss of *DOT1* completely abrogates Lys79 methylation, which results in a reduction of Sir protein binding to the telomeres and a concomitant loss of telomeric silencing (92). However, loss of *DOT1* also results in increased Sir protein binding to subtelomeric regions (92). We have hypothesized that this reflects a promiscuous binding of Sir3p to nucleosomes outside of silent regions due to the absence of H3 Lys79 methylation (92). Because Sir3p is limiting in the cell (11, 87, 89), such promiscuous binding reduces the effective amount of Sir3p available for the normally silenced loci (93).

Methylation also occurs on Lys4 of histone H3 by action of the Set1 protein (8, 45, 62, 69, 77). Lys4 methylation is similar to Lys79 methylation: it is normally associated with active chromatin (5, 82), and Sir protein binding is reduced in silent regions when Lys4 methylation is abolished (81). Simultaneous loss of H3 Lys79 and Lys4 methylation by deletion of *DOT1* and *SET1* synergistically reduces Sir protein binding to the telomeres (64), indicating that these two modifications function together to prevent the promiscuous binding of Sir proteins to active chromatin.

* Corresponding author. Mailing address: Fred Hutchinson Cancer Research Center, Mail stop A3-025, P.O. Box 19024, Seattle, WA 98109-1024. Phone: (206) 667-4494. Fax: (206) 667-5894. E-mail: dgottsch@fhcrc.org.

† Supplemental material for this article may be found at http://mcb.asm.org/.

The ubiquitin-conjugating enzyme Rad6p is also required for telomeric silencing (37). Rad6p functions with Bre1p, its cognate ubiquitin-protein ligase (39, 95), to attach ubiquitin to Lys123 of histone H2B (76). Over 25 years ago it was found that ubiquitinated H2B and H2A are associated with transcriptionally active chromatin in higher eukaryotes (54, 68). Consistent with this, components of the Paf1 transcriptional elongation complex are required for H2B ubiquitination in *S. cerevisiae* (46, 64, 96). Although its precise role in transcription is unclear, H2B ubiquitination is required in vivo for H3 Lys4 and Lys79 methylation (9, 20, 67, 91). It is proposed that the ubiquitin moiety on H2B may recruit proteasomal ATPases to prepare the chromatin for Set1p and Dot1p activity (22). Because loss of H3 Lys4 and Lys79 methylation disrupts silencing (81, 92), the requirement of Rad6p function for telomeric silencing is likely to be indirect and due to its role in ubiquitinating H2B as a precursor to establishing both H3 Lys4 and Lys79 methylation in active chromatin.

Taking all of this together, it is clear that silencing requires both the addition of histone acetylation and methylation in active chromatin and the removal or prevention of these histone modifications in silent regions. Removal of histone acetylation in silent regions is carried out by the silencing protein and histone deacetylase Sir2p (40, 50, 86). Although a demethylase that targets H3 Lys4 mono- and dimethylation has been identified in mammals (83), no homologous lysine demethylases are known in *S. cerevisiae*. Thus, it is not known if H3 Lys4 and Lys79 methylation can be directly removed from silent regions if established. Instead, removal of ubiquitin from H2B by ubiquitin proteases prior to the establishment of H3 Lys4 and Lys79 methylation may be one mechanism for limiting these H3 modifications in silent regions. Of the 17 known and putative ubiquitin proteases in *S. cerevisiae* (2), Ubp8p has been shown to regulate the levels of ubiquitinated H2B as part of the transcriptional activator complex SAGA (18, 33, 80), indicating that removal of ubiquitin from H2B does occur. However, Ubp8p is not known to function in silencing.

We previously discovered that the ubiquitin protease Dot4p (now known as Ubp10p) is important for silencing in vivo (43). The absence of Dot4p ubiquitin protease activity, either by deletion of *DOT4* or mutation of the catalytic residue, results in reduced silencing, especially at telomeres (43, 85). By two-hybrid analysis, we found that Dot4p interacts with the silencing protein Sir4p (43), and we proposed that Dot4p acts at, or is part of, silent chromatin. However, we had not identified any in vivo substrates of Dot4p. Given the association of Dot4p with silent chromatin and the role of H2B ubiquitination in H3 Lys4 and Lys79 methylation, we investigated whether Dot4p's ubiquitin protease activity regulates the levels of H2B ubiquitination to limit H3 Lys4 and Lys79 methylation in silent regions, as has been previously proposed (78).

MATERIALS AND METHODS

Reagents. General chemical and enzymatic reagents were obtained from New England Biolabs (Beverley, MA), Sigma (St. Louis, MO), Fisher (Pittsburgh, PA) and Pierce (Rockford, IL). Nitrocellulose (Protran; pore size of 0.2 μM) was obtained from Schleicher and Schuell (Keene, NH). The anti-Myc and anti-FLAG antibodies were obtained from Sigma and used at 1:10,000 dilutions for Western blotting or 1:500 dilutions for chromatin immunoprecipitations (ChIP). Anti-monomethyl, -dimethyl, and -trimethyl Lys4 histone H3 antibodies were obtained from Upstate (Waltham, MA) and used at 1:5,000 dilutions for Western blotting and 1:500 dilutions for ChIP. Anti-dimethyl Lys79 histone H3 antibody was made as previously described (92) and used at 1:2,000 dilutions for Western blotting and at 1:100 dilutions for ChIP. Purified anti-Sir2p polyclonal antibodies against the N-terminal 19 residues of Sir2p were obtained from Santa Cruz Biotechnology (Santa Cruz, CA), and used at a 1:500 dilution for ChIP. Mouse anti-Sir3p monoclonal antibodies were made as previously described (92), and used at 1:3 dilutions for ChIP. Vistra Green, ECL chemiluminescence immunodetection reagents, sheep anti-mouse horseradish peroxidase-conjugated antiserum, and donkey anti-rabbit horseradish peroxidase-conjugated antiserum were obtained from Amersham Biosciences (Piscataway, NJ); the antisera were used at 1:2,000 dilutions. IRDye800-conjugated goat anti-mouse and anti-rabbit antibodies were obtained from Rockland Immunochemicals (Gilbertsville, PA). Protein G Dynabeads were obtained from Dynal (Brown Deer, WI).

Recombinant DNA, molecular cloning, and yeast strains. Standard molecular biology techniques were used. Plasmids and yeast strains used in this study are described in Table 1. Yeast deletion alleles were made by PCR amplification of the appropriate knockout construct, followed by transformation into yeast cells using standard yeast transformation techniques (http://www.fhcrc.org/labs/gottschling).

ChIP assays. ChIP assays were performed similar to those previously described (92), with some changes. Yeast extract-peptone-dextrose (YEPD; 200 ml) cultures were grown to a cell density of 2×10^7 cells/ml and subjected to cross-linking with 1% formaldehyde. Cell lysates were prepared, and lysates were sonicated eight times for 30 s using a Fisher Scientific sonic dismembrator model 60. Sonication resulted in an average fragment size of 500 to 800 bp (data not shown). Clarified lysates were stored at −80°C until required.

For the Ubp10p-Myc ChIPs, cross-linking was performed differently. Cells were first harvested by centrifugation, washed twice in phosphate-buffered saline, and resuspended in 50 ml of phosphate-buffered saline. Dimethyl adipimidate was added to a final concentration of 10 mM to improve cross-linking (48), and the cells were incubated at room temperature for 45 min. Formaldehyde was added to a final concentration of 1%, and the cultures were incubated at room temperature for an additional 15 min. Samples were prepared as described above.

Initial multiplex PCR amplifications were performed on various concentrations of immunoprecipitates and total lysates to determine the concentration required for amplification in the linear range. Final multiplex PCR amplifications were performed using a single concentration previously determined to be in the linear amplification range. PCR products were resolved on 2% agarose (1× Tris-acetate-EDTA) gels. Gels were stained with Vistra Green and analyzed using a PhosphorImager (Molecular Dynamics) and ImageJ software. Oligonucleotide sequences for PCR amplifications are listed in Table 1.

Western analyses. Whole-cell lysates were prepared as previously described (26), with some changes. Cultures were grown in YEPD or yeast complete (YC) medium at 30°C to the desired optical density (2×10^7 cells/ml for logarithmically growing cells, overnight saturation for diauxic cells, and 7-day saturation for stationary cells), and equal numbers of cells (1.6×10^8) were harvested by centrifugation. Cells were lysed in 300 μl of SUME (8 M urea, 1% sodium dodecyl sulfate, 10 mM morpholinepropanesulfonic acid, pH 6.8, 10 mM EDTA) containing 0.01% bromophenol blue and 10 mM phenylmethylsulfonyl fluoride by mechanical shearing using acid-washed glass beads. For immunoblotting, 5- to 20-μl samples of the cellular lysates were resolved on 16% sodium dodecyl sulfate-polyacrylamide gel electrophoresis gels, and the proteins were transferred to nitrocellulose and immunoblotted with the appropriate antibody.

Transcript DNA microarrays. Transcript DNA microarrays similar to those previously described (23) were performed in triplicate. Dye-reversal experiments were performed to identify sequence-specific dye biases. Statistical analysis of microarray data was performed as previously described (17), using a Bayesian *t* statistic derived for microarray analyses (3) and a false discovery rate methodology (4) to account for multiple testing. The entire normalized data set is in Table S1 in the supplemental material; the National Center for Biotechnology Information Gene Expression Omnibus accession numbers for the series of individual data sets are GSE2329 (*ubp10*Δ and *ubp8*Δ series) and GSE2330 ($ubp10^{C371S}$ and $ubp10^{\Delta 94\text{-}250}$ series).

RESULTS

In our earlier work, we found that loss of *DOT4* results in reduced steady-state levels of HA epitope-tagged Sir4p, and we speculated that Dot4p might control Sir4p stability, perhaps by regulating its ubiquitin-dependent degradation (43). How-

TABLE 1. Plasmids, yeast strains, and oligonucleotides used in this study

Plasmid, strain, or oligonucleotide	Genotype or description	Source or reference
Plasmids		
pJH23	*HIS3 CEN HTA1-HTB1*	35
pRS314-FLAG/HTB1	*TRP1 CEN FLAG-HTB1*	76
pRG422	1.4-kb BamHI-SacI *FLAG-HTB1* fragment from pRS314-FLAG/HTB1 used to replace the corresponding region in pJH23	This study
pRS406	*URA3 INT*	84
pRG490	2.7-kb SacII-XhoI *HTA1-FLAG-HTB1* fragment from pRG422 inserted between SacII-XhoI sites in pRS406	This study
pRS306	*URA3 INT*	84
pdot4-1-MT6	pBluescript KS+ *ubp10^{C371S}-MT6*	43
pRS306-str4-1-MT6	3.8-kb BamHI-SfuI *ubp10^{C371S}-MT6* fragment from pdot4-1-MT6 inserted between the BamHI-HindIII (blunted) sites in pRS306	This study
pdot4-5-MT6	pBluescript KS+ *ubp10$^{\Delta 94\text{-}250}$-MT6*	43
pRS306-str4-5-MT6	3.3-kb BamHI-SfuI *ubp10$^{\Delta 94\text{-}250}$-MT6* fragment from pdot4-1-MT6 inserted between the BamHI-HindIII (blunted) sites in pRS306	This study
pDot4-MT6	pBluescript KS+ *UBP10-MT6*	43
pRG637	850-bp HindIII-BsrGI wild-type fragment from pDOT4-MT6 used to replace the mutant region in pRS306-str4-1-MT6	This study
pRS404	*TRP1 INT*	84
pRG716	3.9-kb XhoI-SacII *ubp10^{C371S}-MT6* fragment from pRS306-str4-1-MT6 inserted between XhoI-SacII sites in pRS404	This study
pRG717	3.5-kb XhoI-SacII *ubp10$^{\Delta 94\text{-}250}$-MT6* fragment from pRS306-str4-5-MT6 inserted between XhoI-SacII sites in pRS404	This study
pRG718	3.9-kb XhoI-SacII *UBP10-MT6* fragment from pRG637 inserted between XhoI-SacII sites in pRS404	This study
pRS414	*TRP1 CEN*	84
Yeast strains		
AR120	*HMLa MAT***a** *HMR***a** *cdc7-1 bar1 trp1-289 ura3-52 leu2-3,112 his6*	Walt Fangman
UCC4861	*AR120 CDC7*	This study
UCC6195	UCC4861 *CDC7 HTA1-FLAG-HTB1*	This study
UCC6196	UCC6195 *sir2Δ::LEU2*	This study
UCC6197	UCC6195 *sir3Δ::LEU2*	This study
UCC6198	UCC6195 *sir4Δ::LEU2*	This study
UCC6199	UCC6195 *ubp10Δ::KanMX*	This study
UCC6184	UCC6199 *ubp10Δ::KanMX::ubp10^{C371S}-MT6::URA3*	This study
UCC6185	UCC6199 *ubp10Δ::KanMX::ubp10$^{\Delta 94\text{-}250}$-MT6::URA3*	This study
UCC6186	UCC6199 *ubp10Δ::KanMX::UBP10-MT6::URA3*	This study
UCC4825	*MAT***a** *ade2Δ::hisG ura3Δ0 ADE2-TEL-VR*	43
UCC4857	UCC4825 *ubp10Δ::KanMX*	43
UCC4870	UCC4825 *ubp10^{C371S}-MT6*	43
UCC4896	UCC4825 *ubp10$^{\Delta 94\text{-}250}$-MT6*	43
UCC4836	UCC4825 *sir4Δ::KanMX*	This study
UCC7315	*MAT***a** *lys2Δ0 trp1Δ63 his3Δ200 ade2Δ::hisG ura3Δ0 leu2Δ0 met15Δ0 hta1-htb1::MET15 hta2-htb2::LEU2 ADE2-TEL-VR URA3-TEL-VIIL pCS1*	This study
UCC6286	UCC7315 *sir4Δ::KanMX*	This study
UCC6288	UCC7315 *ubp8Δ::KanMX*	This study
UCC6357	UCC7315 *ubp10Δ::NatMX ubp8Δ::KanMX*	This study
UCC6361	UCC7315 *ubp10Δ::NatMX*	This study
UCC6389	*MAT***a** *lys2Δ0 trp1D63 his3Δ200 ade2Δ::hisG ura3Δ0 leu2Δ0 met15Δ0 hta1-htb1::MET15 hta2-htb2::LEU2 ADE2-TEL-VR URA3-TEL-VIIL pRG422*	This study
UCC6390	UCC6389 *ubp10Δ::NatMX*	This study
UCC6391	UCC6389 *sir4Δ::KanMX*	This study
UCC6392	UCC6389 *ubp8Δ::KanMX*	This study
UCC6393	UCC6389 *ubp10Δ::NatMX ubp8Δ::KanMX*	This study
UCC6163	UCC6389 *rad6Δ::KanMX*	This study
UCC6394	*MATα lys2Δ0 trp1Δ63 his3Δ200 ade2Δ::hisG ura3Δ0 leu2Δ0 met15Δ0 hta1-htb1::MET15 hta2-htb2::LEU2 ADE2-TEL-VR URA3-TEL-VIIL pRG422*	This study
UCC6395	UCC6394 *ubp10Δ::NatMX*	This study
UCC6396	UCC6394 *sir4Δ::KanMX*	This study
UCC6397	UCC6394 *ubp8Δ::KanMX*	This study
UCC6398	UCC6394 *ubp10Δ::NatMX ubp8Δ::KanMX*	This study
UCC6406	UCC6390 *ubp10Δ::NatMX::ubp10^{C371S}-MT6::TRP1*	This study
UCC6407	UCC6390 *ubp10Δ::NatMX::ubp10$^{\Delta 94\text{-}250}$-MT6::TRP1*	This study
UCC6408	UCC6390 *ubp10Δ::NatMX::UBP10-MT6::TRP1*	This study
UCC6475	UCC6408 *sir2Δ::HygMX*	This study

Continued on following page

TABLE 1—*Continued*

Plasmid, strain, or oligonucleotide	Genotype or description	Source or reference
UCC6477	UCC6408 *sir3*Δ::*HygMX*	This study
UCC6479	UCC6408 *sir4*Δ::*HygMX*	This study
UCC6422	UCC6389 *ppr1*Δ::*LYS2*	This study
UCC6423	UCC6390 *ppr1*Δ::*LYS2*	This study
UCC6424	UCC6391 *ppr1*Δ::*LYS2*	This study
UCC6425	UCC6392 *ppr1*Δ::*LYS2*	This study
UCC6426	UCC6393 *ppr1*Δ::*LYS2*	This study
UCC6432	UCC6389 *TRP1*	This study
UCC6435	UCC6390 *TRP1*	This study
Oligonucleotides		
STR4RS+ (ubp10Δ 5′)	AAT CCG TCC TAT TGT CAT ATC ACA ATC ACA GAC TGA TTG TAC TGA GAG TGC ACC	43
STR4RS− (ubp10Δ 3′)	TCC AGG AAT ATC GAG TTT TTT CAT TTG GTG AAC CTG TGC GGT ATT TCA CAC CG	43
oRG255 (ubp8Δ 5′)	CTT CGG TCC TCG TCG TCC TAC TTG AAA CCC TGC TTT TTT TAT TTG TTA TTA ATA ATT CTG TGC GGT ATT TCA CAC CGC	This study
oRG256 (ubp8Δ 3′)	TAG CTT TTT CTT CTT TTT TGT TTT ATT ATT ATT GTT GAA TGC TAT TTG CTG AAT CAC AGA TTG TAC TGA GAG TGC ACC	This study
SIR4KO1 (sir4Δ 5′)	CAA CCC ACA ATA CCA AAA AAG CGA AGA AAA CAG CCA GAT TGT ACT GAG AGT GCA CC	This study
SIR4KO2 (sir4Δ 3′)	CAC TTC GTT ACT GGT CTT TTG TAG AAT GAT AAA AAG CTG TGC GGT ATT TCA CAC CG	This study
GAL1-1	GAA GAA GTG ATT GTA CCT GAG	92
GAL1-2	ACC TTT CCG GTG CAA GTT TC	92
ACT1-1	CCA ATT GCT CGA GAG ATT TC	92
ACT1-2	CAT GAT ACC TTG GTG TCT TG	92
oRG58 (SAN1 5′)	GCC CCT ACG CAC AAC CGC	This study
oRG59 (SAN1 3′)	GGA CGT GTT TTC GGA TGG G	This study
5HMR	GAG AAT AAG CGC AGG TAC TCC	92
5HMR-2	TCT TGA GCG GTG AGC CTC TG	92
VIR-1	CAG GCA GTC CTT TCT ATT TC	92
VIR-2	GCT TGT TAA CTC TCC GAC AG	92

ever, in subsequent testing we found that the HA epitope tag (or the T7- or Myc-epitope tag) added to the N terminus of Sir4p results in aberrant degradation of Sir4p (data not shown). Using new antibodies, we found that untagged Sir4p is normally stable and not subject to ubiquitination (27). We also found that the steady-state levels of untagged wild-type Sir4p are unchanged in *dot4*Δ cells (data not shown). Thus, the alteration of Sir4p stability by loss of *DOT4* is an artifact of epitope tagging the protein and not a normal mode of regulation. As a result, we turned our attention to other potential substrates of Dot4p.

(Concurrent with our initial discovery (85), *DOT4* was also found by homology searches for ubiquitin proteases and named *UBP10* (36). Because *UBP10* is now the standard name for the gene in the *Saccharomyces* Genome Database (http ://db.yeastgenome.org/cgi-bin/locus.pl?locus = ubp10), we will henceforth use *UBP10* rather than *DOT4*. By doing so, we have renamed the previously constructed *dot4* alleles, *dot4-1* and *dot4-5* (43), with the more descriptive *ubp10* nomenclature, $ubp10^{C371S}$ and $ubp10^{\Delta 94\text{-}250}$, respectively.)

Ubp10/Dot4p negatively regulates histone H2B ubiquitination in vivo. With Sir4p eliminated as a substrate of Ubp10p, we turned our attention to histone H2B due to the fact that H2B ubiquitination is required for histone H3 Lys4 and Lys79 methylation (9, 20, 67, 91), both of which antagonize Sir protein binding to chromatin (64, 81, 92). To determine if Ubp10p targets ubiquitinated H2B, we examined the steady-state levels of H2B ubiquitination in *ubp10*Δ cells. Compared to wild-type cells, *ubp10*Δ cells have approximately threefold higher steady-state levels of H2B ubiquitination (Fig. 1), supporting the idea that ubiquitinated H2B is a bona fide substrate of Ubp10p. In fact, the increased steady-state levels of H2B ubiquitination in *ubp10*Δ cells are similar to the approximately fivefold higher levels observed in *ubp8*Δ cells (Fig. 1); Ubp8p is a ubiquitin protease recently shown to regulate H2B ubiquitination (18, 33). Deletion of both *UBP10* and *UBP8* results in a further increase in the steady-state levels of H2B ubiquitination that is greater than that seen in either *ubp10*Δ or *ubp8*Δ cells (Fig. 1). These results indicate that Ubp10p and Ubp8p act upon separate populations of ubiquitinated H2B in part, which is consistent with their distinct roles in silencing and SAGA-mediated transcription, respectively (33, 43).

Ubp10/Dot4p negatively regulates global histone H3 Lys4 and Lys79 methylation. The previously documented dependence of histone H3 Lys4 and Lys79 methylation on H2B ubiquitination led us to examine if loss of *UBP10* or *UBP8* altered H3 methylation. Using specific antibodies, we examined steady-state levels of H3 Lys4 mono-, di- or trimethylation or H3 Lys79 dimethylation. Although the changes were often modest, *ubp10*Δ cells did have reproducibly higher steady-state levels of all forms of H3 Lys4 methylation and of H3 Lys79 methylation compared to wild-type cells (Fig. 1, and see Fig. 6 and 7). In contrast, we observed no detectable increase in H3 Lys4 or Lys79 methylation in *ubp8*Δ cells (Fig. 1), indicating

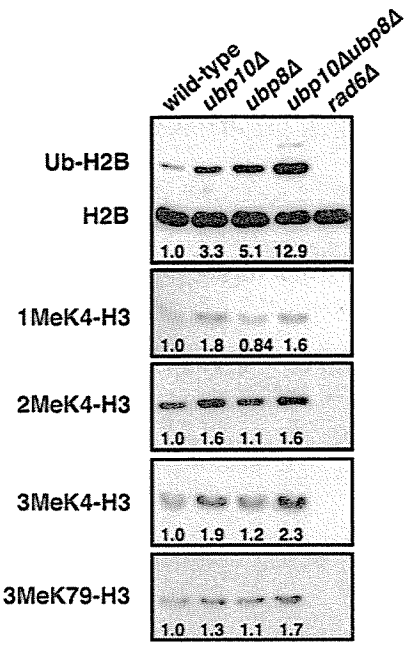

FIG. 1. Ubp10p negatively regulates histone H2B ubiquitination and H3 Lys4 and Lys79 methylation levels. Global steady-state H2B ubiquitination levels from whole-cell lysates were assayed using anti-FLAG antibodies that recognize the FLAG epitope placed on the N terminus of H2B (76). Global steady-state H3 Lys4 and Lys79 methylation levels were also assayed using antibodies specific for mono-, di-, and trimethylated Lys4 forms of H3 as well as an antibody generated against the dimethylated Lys79 form of H3 (92). Whole-cell lysates were derived from strains UCC6369 (wild type), UCC6390 (*ubp10*Δ), UCC6392 (*ubp8*Δ), UCC6393 (*ubp10*Δ *ubp8*Δ), and UCC6163 (*rad6*Δ) that were harvested during log-phase growth. *rad6*Δ cells served as a negative control for H2B lacking ubiquitin. Changes in levels (*n*-fold) of H2B ubiquitination and H3 Lys4 and Lys79 methylation for each mutant strain relative to the wild-type strain are shown below each corresponding lane and are the average of three independent experiments. Quantitation was performed using National Institutes of Health ImageJ software.

that increased H2B ubiquitination alone is not sufficient for increased H3 methylation. In *ubp10*Δ *ubp8*Δ cells, H3 Lys4 and Lys79 methylation are also increased similar to *ubp10*Δ cells (Fig. 1B). Altogether, the higher steady-state levels of H2B ubiquitination in *ubp10*Δ cells likely present an increased opportunity for H3 Lys4 and Lys79 methylation.

A recent study found modest decreases in the steady-state levels of H3 Lys4 di- and trimethylation but a 10-fold increase in the steady-state levels H3 Lys4 monomethylation in *ubp8*Δ cells (18). However, we do not see much change in the levels of any form of H3 Lys4 methylation in *ubp8*Δ cells (Fig. 1). One possibility for the difference is that H3 Lys4 methylation was analyzed in acid-extracted histones in the previous study (18), whereas we examined H3 Lys4 methylation in whole yeast cell extracts (see Materials and Methods). Perhaps there exists a soluble, nonnucleosomal pool of Lys4-methylated histone H3 that is detected by the whole-cell extract but not by the differential extraction method. If so, the extraction method would reveal information about the state of H3 Lys4 methylation exclusively in the nucleosome. Alternatively, the various forms of Lys4-methylated histone H3 could have different solubilities that affect recovery during the extraction procedure. Whatever the reason, our results in whole-cell extracts are reproducible and show little change in global H3 Lys4 methylation in the absence of *UBP8* (Fig. 1; see Fig. 7), which is consistent with very little role for Ubp8p in global transcription (see Fig. 8).

Ubp10/Dot4p is enriched at silenced loci. Negative regulation of H2B ubiquitination would explain the role of Ubp10p in silencing, given that H2B ubiquitination is required for histone H3 Lys4 and Lys79 methylation (9, 20, 67, 91), both of which antagonize Sir protein binding to chromatin (64, 81, 92). Because Ubp10p is involved in silencing telomeric gene expression through a direct interaction with Sir4p (43, 85), it seemed likely that Ubp10p is localized specifically to silent chromatin to reverse H2B ubiquitination. By chromatin immunoprecipitation, we found that Ubp10p is preferentially localized to the silent telomere VIR and the silent mating locus *HMR*a compared to active chromatin regions such as *GAL1* and *SAN1* (Fig. 2).

Previously, we made a number of *ubp10/dot4* mutant alleles that are compromised for telomeric silencing (43). In particular, we constructed two alleles: $ubp10^{C371S}$ (originally named *dot4-1*), which renders Ubp10p nonfunctional by substitution of the active site Cys371 with Ser, and $ubp10^{\Delta 94\text{-}250}$ (originally named *dot4-5*), which is catalytically active but can no longer bind Sir4p due to deletion of the Sir4p-binding region spanned by residues 94 to 250. We found that the $Ubp10^{C371S}$ protein is preferentially localized to the silent regions at telomere VIR and *HMR*a, similar to wild-type Ubp10p (Fig. 2), whereas the $Ubp10^{\Delta 94\text{-}250}$ protein has no preference for silent loci (Fig. 2). Loss of Ubp10p preferential localization to silent regions was also observed when the silencing genes *SIR2*, *SIR3*, or *SIR4* were deleted. Thus, Ubp10p is enriched at silent chromatin via its interaction with Sir4p, and Ubp10p localization is independent of its ubiquitin protease activity.

Loss of Ubp10/Dot4p function and targeting disrupts global silencing of telomeric genes. We next determined if Ubp10p's function in gene repression is similarly biased toward silent regions by examining global gene expression in *ubp10* mutant cells using DNA microarrays. To avoid secondary effects due to the slow-growth phenotype of *ubp10*Δ and $ubp10^{C371S}$ cells in synthetic (YC) medium (43), we grew cells used for the expression analysis in rich (YEPD) medium. After applying rigorous statistical criteria (see Materials and Methods), we found that 90 genes have increased expression by 1.5-fold or greater in *ubp10*Δ cells, and 50 of these genes are located within 20 kbp of the telomeres (Fig. 3A and see Table S1 in the supplemental material). Because less than 5% of all genes are located within 20 kbp of the telomere, the enrichment of telomeric genes in the *ubp10*Δ expression profile indicates that the role of Ubp10p in gene expression is biased toward regulation of telomeric silencing. We also found that 40 genes have decreased expression by at least 1.5-fold in *ubp10*Δ cells; 7 of these genes are located within 20 kbp of the telomeres (Fig. 3A; see Table S1 in the supplemental material). As expected, the gene expression profile of $ubp10^{C371S}$ cells significantly overlaps that of *ubp10*Δ cells (Fig. 3B and see Table S1 in the supplemental material), indicating that Ubp10p's ubiquitin protease activity is largely responsible for its role in gene regulation near telomeres and elsewhere in the genome.

The gene-expression profile of $ubp10^{\Delta 94\text{-}250}$ cells contrasts

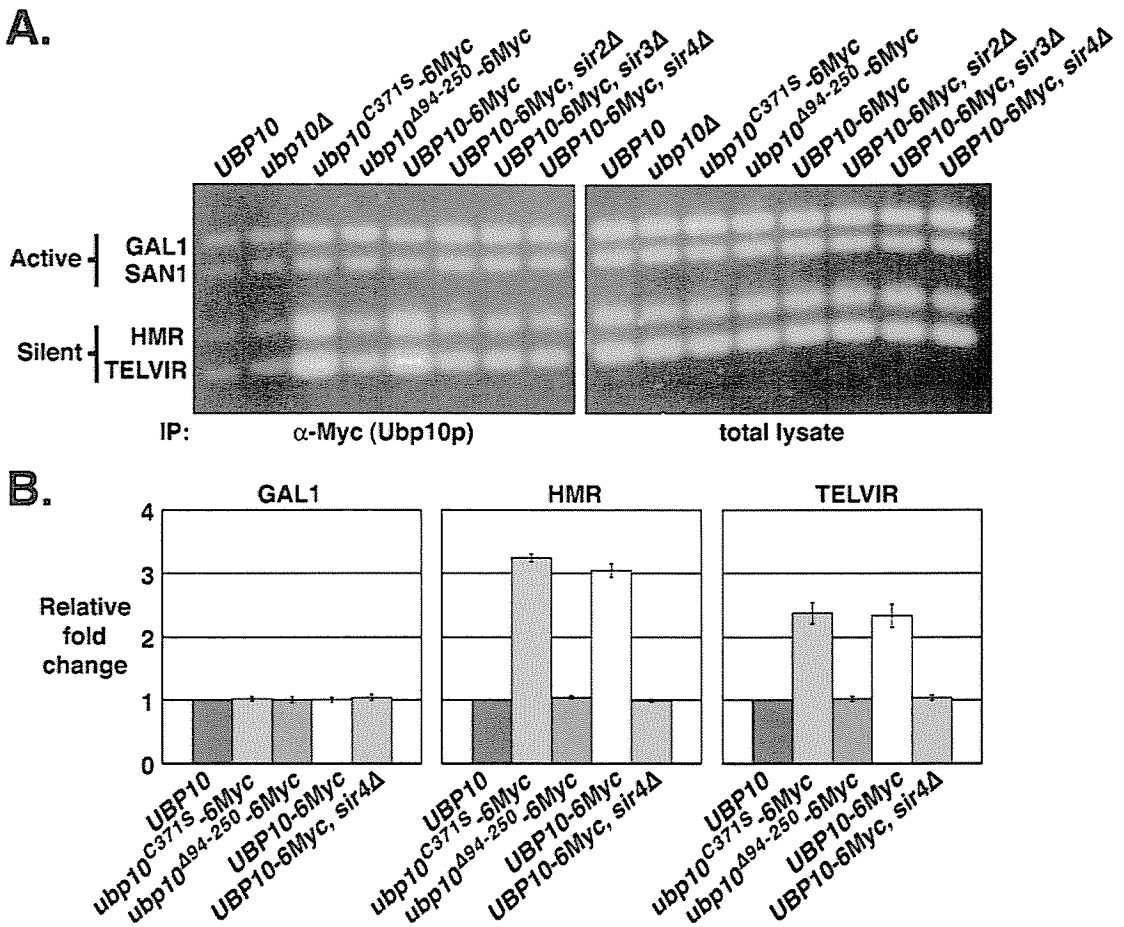

FIG. 2. Ubp10p is preferentially localized to silent chromatin. In vivo cross-linking analysis was performed using strains UCC6389 (untagged *UBP10*), UCC6390 (*ubp10*Δ), UCC6408 (*UBP10-6Myc*), UCC6406 (*ubp10^{C371S}-6Myc*), UCC6407 (*ubp10$^{\Delta 94-250}$-6Myc*), UCC6475 (*UBP10-6Myc*, *sir2*Δ), UCC6477 (*UBP10-6Myc*, *sir3*Δ), and UCC6479 (*UBP10-6Myc*, *sir4*Δ). A ChIP assay of Ubp10 proteins was performed using anti-Myc antibodies specific for the six-Myc tag fused to the C termini of the wild-type Ubp10, mutant Ubp10^{C371S}, and mutant Ubp10$^{\Delta 94-255}$ proteins. ChIP was also performed using untagged wild-type Ubp10p as a control. Multiplex PCR amplifications were performed to assess Ubp10p binding at the silent domains of telomere VIR and *HMR*a, the active *SAN1* gene, and the repressed *GAL1* gene. DNA of the total lysate was amplified as a control. (A) Representative example of Vistra Green-stained PCR amplifications. (B) Quantitative analysis of data in shown in panel A. Values represent the ratio of immunoprecipitate to total lysate for the query gene normalized to the ratio of immunoprecipitate to total lysate for *SAN1*. All values are the averages of at least two independent experiments. Error bars represent the standard deviation.

with that from *ubp10*Δ and *ubp10^{C371S}* cells in one notable way. Only telomeric genes have increased expression in *ubp10$^{\Delta 94-250}$* cells; none of the other nontelomeric genes with altered expression in *ubp10*Δ or *ubp10^{C371S}* cells is affected in *ubp10$^{\Delta 94-250}$* cells (Fig. 3B and see Table S1 in the supplemental material), indicating that the Ubp10$^{\Delta 94-250}$ protein, which has the Sir4p-binding region deleted, is specifically defective in telomeric silencing. These results also indicate that the nontelomeric gene expression changes in *ubp10*Δ and *ubp10^{C371S}* cells are not an indirect result of losing telomeric gene silencing.

Ubp10/Dot4p reduces histone H3 Lys4 and Lys79 methylation at telomeric loci. Ubp10p is preferentially localized to silent chromatin, important for repression of telomere-proximal genes, and negatively regulates H2B ubiquitination levels. It is therefore likely that the increased expression of telomere-proximal genes in the absence of Ubp10p function is the result of increased H2B ubiquitination within silent loci. To determine directly if this is the case, we required reagents (i.e., antibodies) that specifically recognize ubiquitinated H2B and can be used in chromatin immunoprecipitation experiments. Despite multiple efforts, we were unable to generate such reagents, and none are available elsewhere. Instead, we chose to use H3 Lys4 and Lys79 methylation as indirect markers of H2B ubiquitination because these modifications both require H2B ubiquitination and because antibodies specific for these modifications are readily available (9, 20, 67, 91).

For the ChIP assay, we used several loci indicative of different chromatin states including the repressed *GAL1* locus, the actively transcribed *SAN1* locus, the silent *HMR*a locus, and a silent region adjacent to telomere VIR. Under the growth conditions that we used for the assay, neither the repression of *GAL1* nor the expression of *SAN1* is altered by deletion or mutation of *UBP10* (see Table S1 in the supplemental material). Thus, the *GAL1* and *SAN1* loci served as independent internal controls to judge the relative changes in H3 Lys4 and

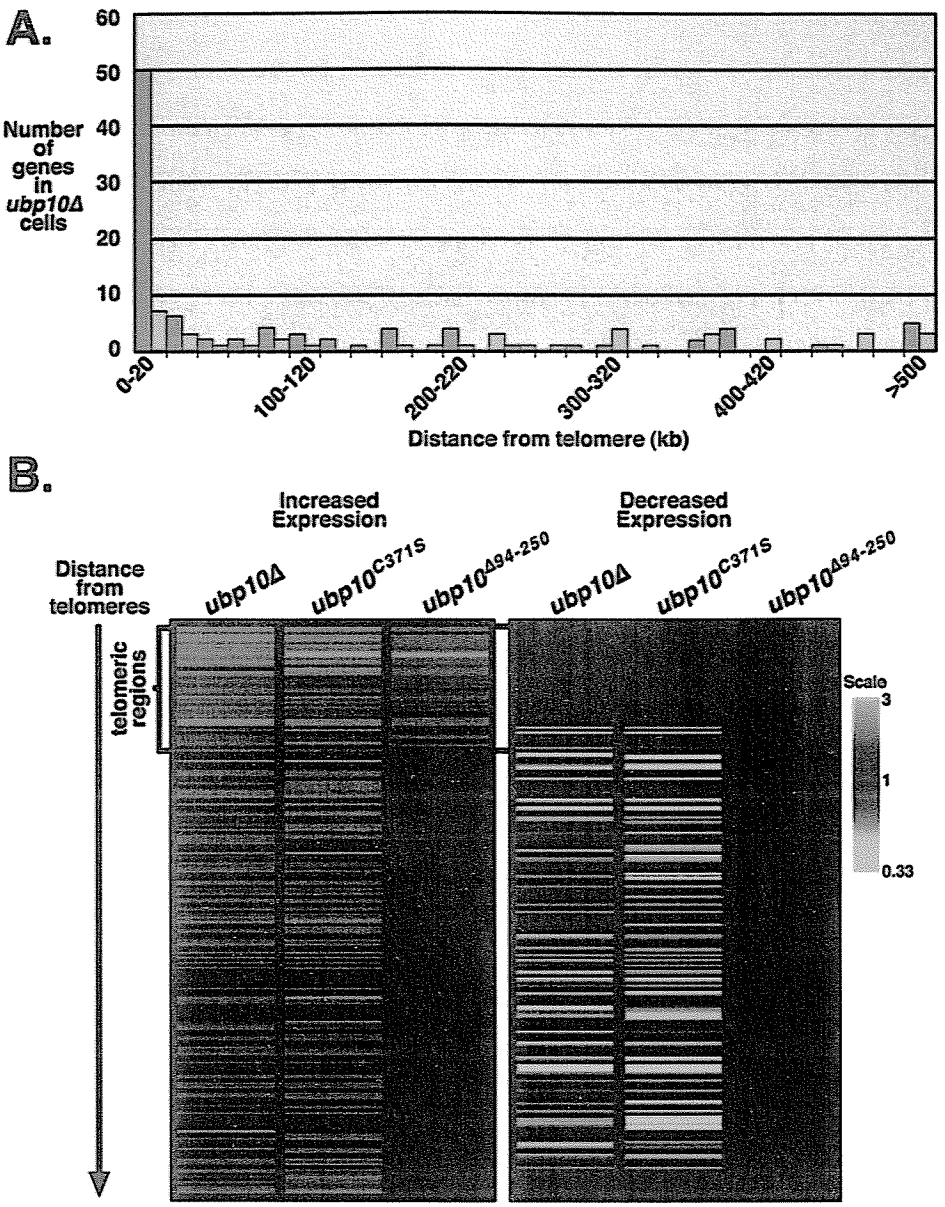

FIG. 3. Loss of *UBP10* primarily affects the expression of telomeric regions. Transcript array analysis was performed using strains UCC6389 (wild type) and UCC6390 (*ubp10*Δ) for panel A and strains UCC6432 (wild type), UCC6435 (*ubp10*Δ), UCC6406 ($ubp10^{C371S}$), and UCC6407 ($ubp10^{\Delta 94\text{-}250}$) for panel B. Cells were grown to log phase in rich medium (YEPD), and transcripts were isolated and analyzed. (A) Increased expression in *ubp10*Δ cells shows a telomeric bias. Number of genes increased in *ubp10*Δ cells plotted by position from the telomere. Histograms represent 20-kb increments from the telomeres. Red histograms represent genes with increased expression; green histograms represent genes with decreased expression. (B) $ubp10^{\Delta 94\text{-}250}$ cells are specifically defective in telomeric silencing. Positional cluster analysis shows expression changes of genes based on distance from telomeres. Only genes expressed greater than or less than 1.5-fold in at least one of the strains are shown (total number of genes shown is 222). Genes located within 20 kbp of their respective telomeres are marked on the left as "telomeric regions." See Table S1 in the supplemental material for the entire normalized data set.

Lys79 methylation at the silent regions in *HMR*a and near telomere VIR.

Using antibodies that recognize H3 Lys4 trimethylation or Lys79 dimethylation, we found that both modifications are increased at the telomere-proximal position on telomere VIR in *ubp10*Δ cells (Fig. 4). We also found similar increases at a telomere-proximal position on telomere VIIL (data not shown). We could not detect an increase in Lys4 methylation at the silent mating-type loci *HMR*a in *ubp10*Δ cells but did detect a small increase in Lys79 methylation (Fig. 4). The lack of a significant increase in H3 Lys4 or Lys79 methylation at *HMR*a is consistent with the absence of transcription at the silent mating loci in *ubp10*Δ cells (see Table S1 in the supplemental material).

We also performed the ChIP analysis with either $ubp10^{C371S}$ or $ubp10^{\Delta 94\text{-}250}$ cells. Interestingly, in $ubp10^{C371S}$ cells we saw a greater increase in H3 Lys4 and Lys79 methylation in the silent regions at telomeres VIR and *HMR*a, even though both

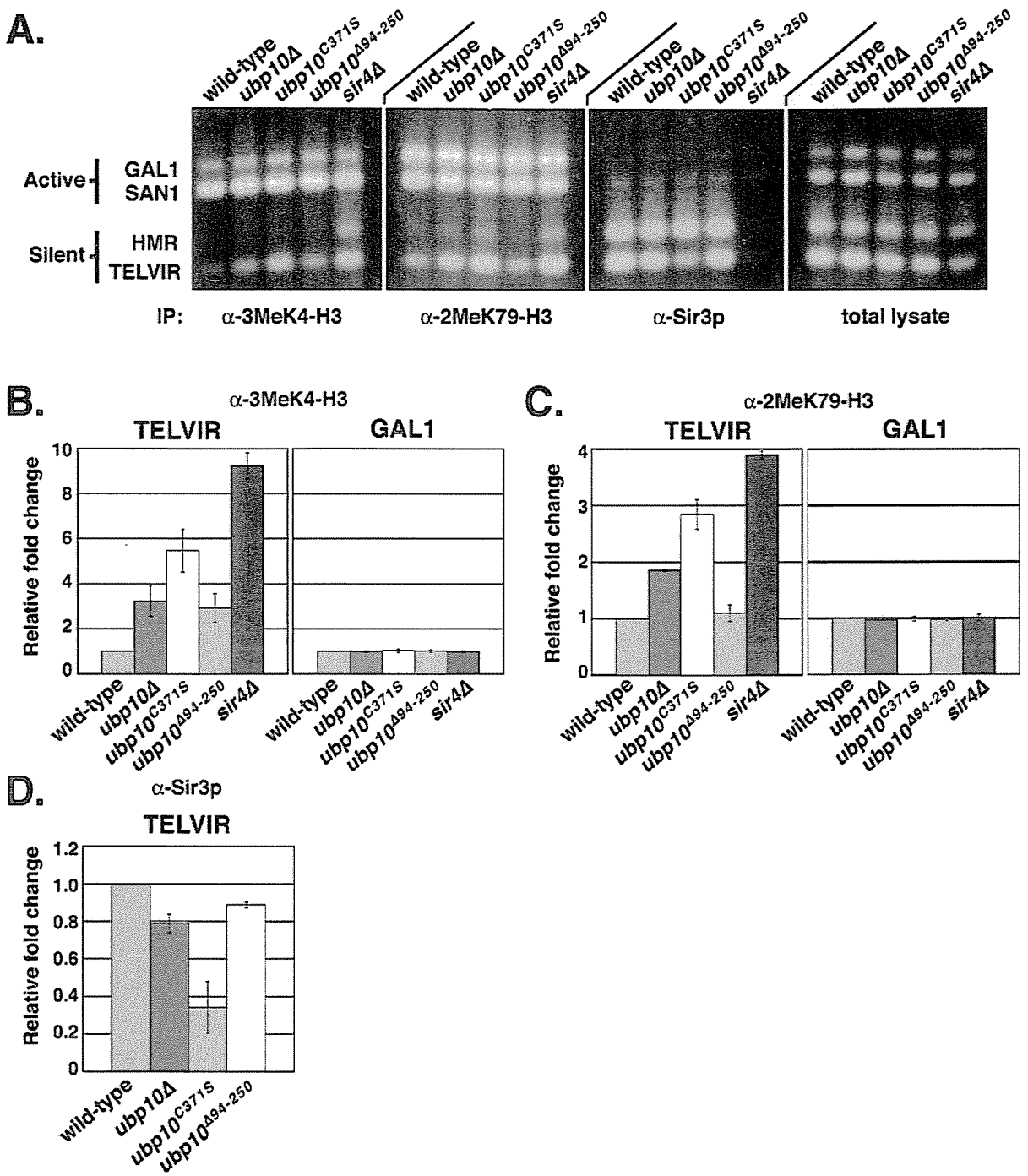

FIG. 4. Loss of Ubp10p activity results in increased histone H3 Lys4 and Lys79 methylation and decreased Sir3p binding at telomeres. In vivo cross-linking analysis was performed using strains UCC4825 (wild type), UCC4857 (*ubp10*Δ), UCC4870 ($ubp10^{C3715}$), UCC4836 ($ubp10^{\Delta 94\text{-}250}$), and UCC4836 (*sir4*Δ). ChIP assays of H3 Lys4 and Lys79 methylation and Sir3p binding were performed using antibodies specific for H3 Lys4 trimethylation, H3 Lys79 dimethylation, or Sir3p. Multiplex PCR amplifications were performed to assess the degree of H3 Lys4 methylation, H3 Lys79 methylation, and Sir3p binding at the silent domains of telomeres VIR and *HMR*a, the active *SAN1* gene, and the repressed *GAL1* gene. DNA of the total lysate was amplified as a control. (A) Representative example of Vistra Green-stained PCR amplifications. (B to D) Quantitative analysis of data in panel A. Values for H3 Lys4 and Lys79 methylation represent the ratio of immunoprecipitate to total lysate for the query gene normalized to the ratio of immunoprecipitate to total lysate for *SAN1*. Values for Sir3p binding represent the ratio of immunoprecipitate to total lysate for telomere VIR normalized to the ratio of immunoprecipitate to total lysate for *HMR*a. All values are the averages of at least two independent experiments. Error bars represent the standard deviation. (B) Relative fold change of H3 Lys4 tri-methylation at telomere VIR and *GAL1*. (C) Relative increase in H3 Lys79 methylation at telomere VIR and *GAL1*. (D) Relative decrease in Sir3p binding at telomere VIR.

*ubp10*Δ and *ubp10*^{C371S} cells are equivalently deficient in Ubp10p catalytic activity (Fig. 4). Although *ubp10*$^{\Delta 94\text{-}250}$ cells also have increased H3 Lys4 methylation at telomere VIR, the increases are less than in *ubp10*Δ cells (Fig. 4), which is consistent with a weaker silencing defect in *ubp10*$^{\Delta 94\text{-}250}$ cells (see Table S1 in the supplemental material). We did not observe statistically significant increases in H3 Lys79 methylation at telomere VIR in *ubp10*$^{\Delta 94\text{-}250}$ cells. However, is possible that the normally high levels of H3 Lys79 methylation in the genome (>90% of all nucleosomes) result in a higher background that masks small increases. Accordingly, increases in H3 K79 methylation at silent regions were consistently two- to threefold lower than increases in H3 Lys4 methylation (Fig. 4 and 5).

As expected, the greatest increases in H3 Lys4 and Lys79 methylation at telomeres VIR and *HMR*a occur in *sir4*Δ cells (Fig. 4), in which silencing is completely disrupted (Fig. 5E). Although loss of Ubp10p function at telomeres does not have as great an effect as loss of Sir4p function, all *ubp10* mutations result in increased histone H3 modifications at silenced loci.

Increased H3 Lys4 and Lys79 methylation at telomere VIR in *ubp10* mutant cells would be expected to result in reduced Sir protein binding. In *ubp10*Δ cells, we observed modest decreases in Sir3p binding to telomere VIR (Fig. 4) and telomere VIIL (data not shown), but there is no effect on Sir3p localization to *HMR*a (Fig. 4), which is consistent with the fact that *ubp10*Δ cells show little change in silencing at *HMR* (or *HML*) and are still able to mate with high efficiency (43, 85). As with the above H3 Lys4 and Lys79 methylation increases, the decreases in Sir3p localization at telomere VIR are far greater in *ubp10*^{C371S} cells than in *ubp10*Δ cells (Fig. 4). One possible explanation for this difference is that the full-length, but catalytically inactive, Ubp10^{C371S} protein has a longer association with Sir4p than wild-type Ubp10p, and this interferes with the binding of the other Sir proteins. Like *ubp10*Δ cells, *ubp10*$^{\Delta 94\text{-}250}$ cells have modest reductions in Sir3p binding to telomeres. In all mutant *ubp10* cells, changes in Sir2p binding to telomeres were similar to those observed for Sir3p, with no detectable change at the silent mating loci (data not shown).

While Sir2p and Sir3p binding in all *ubp10* mutant cells can still be detected, Sir2p and Sir3p binding is eliminated in *sir4*Δ cells (Fig. 4 and data not shown), which is consistent with loss of *SIR4* having a far greater effect on silencing than loss of *UBP10* (85). Thus, it appears that Ubp10p activity is not required for Sir protein binding at silent loci but optimizes Sir protein association instead.

Ubp8p does not regulate Lys4 and Lys79 methylation within silent regions. Loss of *UBP10* results in increased H2B ubiquitination (Fig. 1), which is the likely cause for the increases in H3 Lys4 and Lys79 methylation in silent regions. Loss of *UBP8* also results in increased H2B ubiquitination (Fig. 1), so we tested if similar increases in H3 Lys4 and Lys79 methylation occur at silent regions in *ubp8*Δ cells as they do in *ubp10*Δ cells. By ChIP analysis, we found no effect of losing *UBP8* on H3 Lys4 or Lys79 methylation in silent regions, nor did we find a detectable change in Sir2p or Sir3p binding to the telomeres (Fig. 5A to D). Loss of *UBP8* also has no effect on telomeric silencing (Fig. 5E; see Fig. 8). Ubp8p's lack of involvement in any aspect of silencing indicates that it is specifically Ubp10p's regulation of H2B ubiquitination that is required for silencing.

Loss of *UBP8* has been previously reported to result in an increase in H3 Lys4 trimethylation at *GAL1* under repressing conditions of growth in glucose (33). This is curious because H3 Lys4 trimethylation has been shown to occur specifically in the 5′ coding portion of active genes and is absent from inactive and repressed genes (66, 82). Consistent with *GAL1* repression in glucose-grown cells, we find no noticeable change in H3 Lys4 trimethylation at *GAL1* in the absence of *UBP8* (Fig. 5A to C). The difference between our results and those from the earlier study might be explained by differences in the strains used in each study: Henry and colleagues used yeast strains derived from W303 (33), whereas we used yeast strains derived from S288c. In general, glucose repression appears to be less stringent in W303-derived strains than in S288c-derived strains (10). For *GAL1* gene repression in particular, it has been shown that short-term *GAL1* repression in W303-derived strains occurs more slowly and is less stringent than in S288c-derived strains (25). A low level of *GAL1* expression in glucose-grown W303-derived strains, but not in S288c-derived strains, might explain the difference in the results.

Function of Ubp10/Dot4p is not restricted to silent loci. The gene expression profiles of *dot4* mutant cells (Fig. 3) indicated that Ubp10p activity is not restricted to the regulation of telomeric loci since the majority of total genes with altered expression in *ubp10*Δ cells (73 out of 130) are nontelomeric. The transcriptional effects at these loci are not the indirect result of derepression at telomeres because none of these genes shows altered expression in *ubp10*$^{\Delta 94\text{-}250}$ cells, which are specifically defective in telomeric silencing (Fig. 3). Thus, Ubp10p likely has a direct effect on gene expression at these nontelomeric loci. However, it was not clear whether the expression of these nontelomeric loci is also regulated via modulation of H2B ubiquitination levels by Ubp10p. To address this issue, we examined total H2B ubiquitination and H3 Lys4 dimethylation levels in the various *ubp10* alleles described above. Steady-state levels of both H2B ubiquitination and H3 Lys4 dimethylation are increased to the same level in *ubp10*Δ and *ubp10*^{C371S} cells (Fig. 6A). Surprisingly, H2B ubiquitination and H3 Lys4 dimethylation levels in *ubp10*$^{\Delta 94\text{-}250}$ cells are identical to wild-type *UBP10* cells (Fig. 6A), even though silencing at telomeric loci is compromised in *ubp10*$^{\Delta 94\text{-}250}$ cells. Because silent regions comprise approximately 10% of total chromatin (52, 55, 92), any increases in the steady-state levels of H2B ubiquitination that occur solely as a result of loss of silencing might not be detected by Western analysis. Supporting this idea, deletion of any individual *SIR* gene has no effect on the steady-state levels of H2B ubiquitination or H3 Lys4 dimethylation (Fig. 6B). Thus, the *ubp10*$^{\Delta 94\text{-}250}$ allele reveals that Ubp10p activity is not restricted to silent regions and that Ubp10p also acts on nontelomeric regions to regulate H2B ubiquitination levels.

Ubp10/Dot4p and Ubp8p act on the same chromatin regions. As shown above, *ubp10*Δ cells have higher steady-state levels of H2B ubiquitination than wild-type cells, and the levels are comparable to those in *ubp8*Δ cells (Fig. 1 and 7). Interestingly, deletion of both *UBP10* and *UBP8* results in a synergistic increase in H2B ubiquitination (Fig. 1 and 7). We estimate from dilution blotting and densitometric analyses of blots that 2 to 3% of total H2B is ubiquitinated in wild-type cells, 7 to 10% in *ubp10*Δ cells, 12 to 16% in *ubp8*Δ, and 35 to 40% in

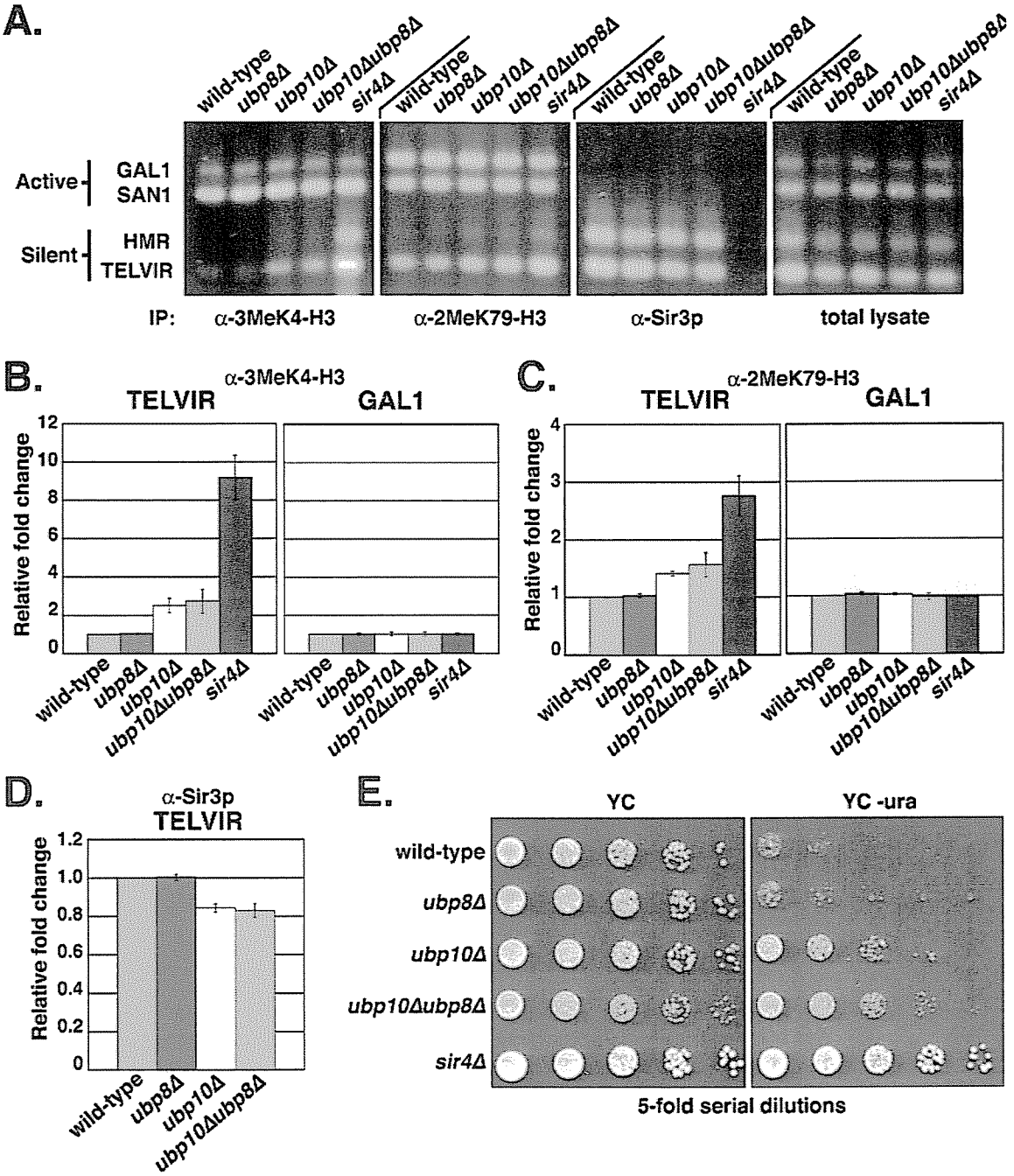

FIG. 5. Loss of *UBP8* does not result in increased histone H3 Lys4 and Lys79 methylation and decreased Sir3p binding at telomeres. In vivo cross-linking analysis was performed as described in the legend of Fig. 4 using stains UCC6389 (wild type), UCC6392 (*ubp8*Δ), UCC6390 (*ubp10*Δ), UCC6393 (*ubp10*Δ *ubp8*Δ), and UCC6391 (*sir4*Δ). (A) Representative example of Vistra Green-stained PCR amplifications. (B to D) Quantitative analysis of data in shown in panel A was performed identically as described in the legend of Fig. 4B to D. (B) Relative increase in H3 Lys4 trimethylation at telomere VIR and *GAL1*. (C) Relative increase in H3 Lys79 methylation at telomere VIR and *GAL1*. (D) Relative decrease in Sir3p binding at telomere VIR. (E) Ubp8p does not function in telomeric silencing. Overnight, saturated cultures of yeast strains UCC6422 (wild type), UCC6423 (*ubp10*Δ), UCC6424 (*sir4*Δ), UCC6425 (*ubp8*Δ), and UCC6426 (*ubp10*Δ *ubp8*Δ), which all carry the *URA3* gene located near telomere VIIL (85), were serially diluted and spotted onto YC plates, with or without uracil. Cells were grown at 30°C for 3 days.

*ubp10*Δ *ubp8*Δ cells. An additive increase in the steady-state levels of H2B ubiquitination in *ubp10*Δ *ubp8*Δ cells would indicate that Ubp10p and Ubp8p exclusively act on separate regions of chromatin. However, the synergistic increase in H2B ubiquitination levels in *ubp10*Δ *ubp8*Δ cells indicates that Ubp10p and Ubp8p also act on overlapping regions of chromatin.

It was recently shown that as yeast cells enter diauxie or when glucose is depleted, H2B ubiquitination is no longer detectable (19). We examined wild-type cells in diauxie and

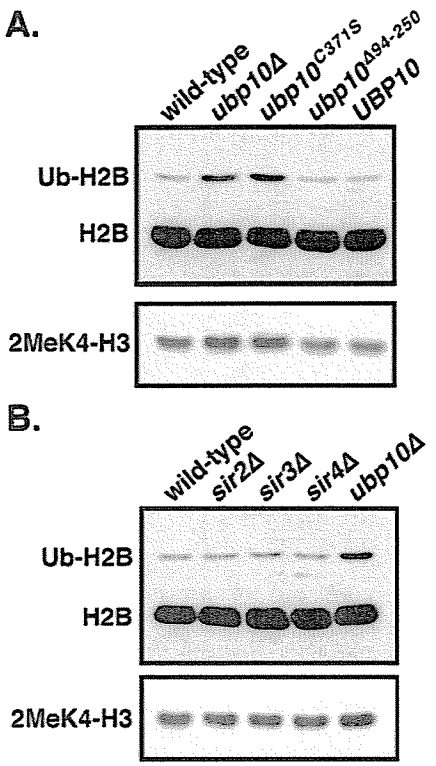

FIG. 6. Loss of silencing does not affect global H2B ubiquitination levels. (A) Loss of Ubp10p catalytic activity but not loss of Sir4p binding affects H2B ubiquitination and H3 Lys4 methylation. Global steady-state H2B ubiquitination and H3 Lys4 dimethylation levels from whole-cell lysates derived from strains UCC6195 (wild-type *UBP10*), UCC6199 (*ubp10*Δ), UCC6184 (*ubp10*^{C371S}*-6Myc*), UCC6185 (*ubp10*$^{\Delta 94\text{-}250}$*-6Myc*), and UCC6186 (*UBP10-6Myc*) were assayed using anti-FLAG antibodies (FLAG-tagged H2B) or antibodies that specifically recognized H3 Lys4 dimethylation. (B) Loss of silencing does not affect H2B ubiquitination or H3 Lys4 methylation. Global steady-state H2B ubiquitination and H3 Lys4 dimethylation levels were assayed as described in panel A using strains UCC6195 (*UBP10*), UCC6196 (*sir2*Δ), UCC6197 (*sir3*Δ), UCC6198 (*sir4*Δ), and UCC6199 (*ubp10*Δ).

similarly found that H2B ubiquitination completely disappears (Fig. 7A). H2B ubiquitination also disappears in either *ubp10*Δ or *ubp8*Δ cells during diauxie, though not completely as trace amounts of H2B ubiquitination could often be detected in both *ubp10*Δ and *ubp8*Δ cells with longer exposures (Fig. 7A and B). In *ubp10*Δ *ubp8*Δ cells, however, the majority of H2B ubiquitination originally detected in log phase is retained in diauxie (Fig. 7A). Although it is not known whether Rad6p-Bre1p ubiquitination activity is reduced as cells enter diauxie, maintenance of the high steady-state levels of H2B ubiquitination in *ubp10*Δ *ubp8*Δ cells indicates that Ubp10p and Ubp8p are the primary enzymes required for reduction of H2B ubiquitination during this time. The persistence of global H2B ubiquitination in *ubp10*Δ *ubp8*Δ cells during diauxie, but not in *ubp10*Δ or *ubp8*Δ cells, further supports the idea that Ubp10p and Ubp8p overlap in many of the chromatin regions that they modify.

The H2B ubiquitination that is still present in *ubp10*Δ *ubp8*Δ cells during diauxie is eliminated as cells enter stationary phase (Fig. 7A). The loss of H2B ubiquitination in stationary phase is the likely result of two things: Rad6p-Bre1p no longer ubiquitinates H2B and another mechanism eliminates ubiquitinated H2B. In *ubp10*Δ *ubp8*Δ cells we frequently observed an additional modified form of H2B with an increased molecular weight indicative of diubiquitination (Fig. 7B). This correlated with the slow loss of H2B ubiquitination in *ubp10*Δ *ubp8*Δ cells as they transited into stationary phase (Fig. 7A). We speculate that the persistence of monoubiquitin on H2B in *ubp10*Δ *ubp8*Δ cells increases the chance that H2B will become polyubiquitinated and ultimately removed by the proteasome, perhaps by degradation. It is not clear if this mode of H2B ubiquitination removal is normally operative in wild-type cells or if it is only a condition of losing both Ubp10p and Ubp8p function.

We also examined the steady-state levels of H3 Lys4 and Lys79 methylation in diauxic and stationary cells. In contrast to the increased steady-state levels of H2B ubiquitination that disappear in *ubp10*Δ cells during diauxie and stationary phase, the increased steady-state levels of H3 Lys4 and Lys79 methylation remain throughout all phases (Fig. 7A). Thus, the transient increase in H2B ubiquitination levels in *ubp10*Δ cells leads to relatively stable increases in H3 Lys4 and Lys79 methylation.

Ubp10/Dot4p has a role in gene expression beyond telomeric loci. From the synergistic increase in H2B ubiquitination in *ubp10*Δ *ubp8*Δ cells (Fig. 1 and 7), it seemed that Ubp10p and Ubp8p might regulate H2B ubiquitination levels within some of the same chromatin regions. To examine this issue further, we examined gene expression profiles of *ubp10*Δ, *ubp8*Δ, and *ubp10*Δ *ubp8*Δ cells.

As stated above, 90 genes in *ubp10*Δ cells have increased expression of 1.5-fold or greater, with 50 of these located within 20 kbp of the telomeres (Fig. 3 and 8). Forty genes have reduced expression of at least 1.5-fold in *ubp10*Δ cells, with only 7 genes located within 20 kbp of the telomeres (Fig. 3 and 8).

By contrast, 17 genes have increased expression of 1.5-fold or greater in *ubp8*Δ cells, and none are located within 20 kbp of telomeres (Fig. 8), which is consistent with the fact that Ubp8p does not function in telomeric silencing (Fig. 5). Also in *ubp8*Δ cells, 17 genes have reduced expression of at least 1.5-fold, and only 4 of these genes are located within 20 kbp of the telomeres. Of the genes with altered expression in the *ubp8*Δ transcript profile, the majority (22 of a total of 34) have SAGA-dominated gene expression (38), as expected from Ubp8p function in SAGA-mediated transcription (18, 33, 80). It is worth noting that none of the 17 genes with increased expression in *ubp8*Δ cells overlaps with those affected in *ubp10*Δ cells, while just 3 genes with decreased expression in *ubp8*Δ cells are shared with *ubp10*Δ cells (Fig. 8A).

As expected, the majority of genes affected in *ubp10*Δ and *ubp8*Δ cells are also affected in *ubp10*Δ *ubp8*Δ cells (Fig. 8A). However, over 160 additional genes have increased expression of 1.5-fold or greater in *ubp10*Δ *ubp8*Δ cells compared to cells carrying either *ubp10*Δ or *ubp8*Δ alone. Of these additional genes, only 13 are located within 20 kbp of the telomeres (Fig. 8B; see also Table S1 in the supplemental material). The greater number of nontelomeric genes with increased expression in *ubp10*Δ *ubp8*Δ cells indicates a possible redundancy for Ubp10p and Ubp8p at these additional loci—either ubiquitin protease may be able to compensate in the absence of the

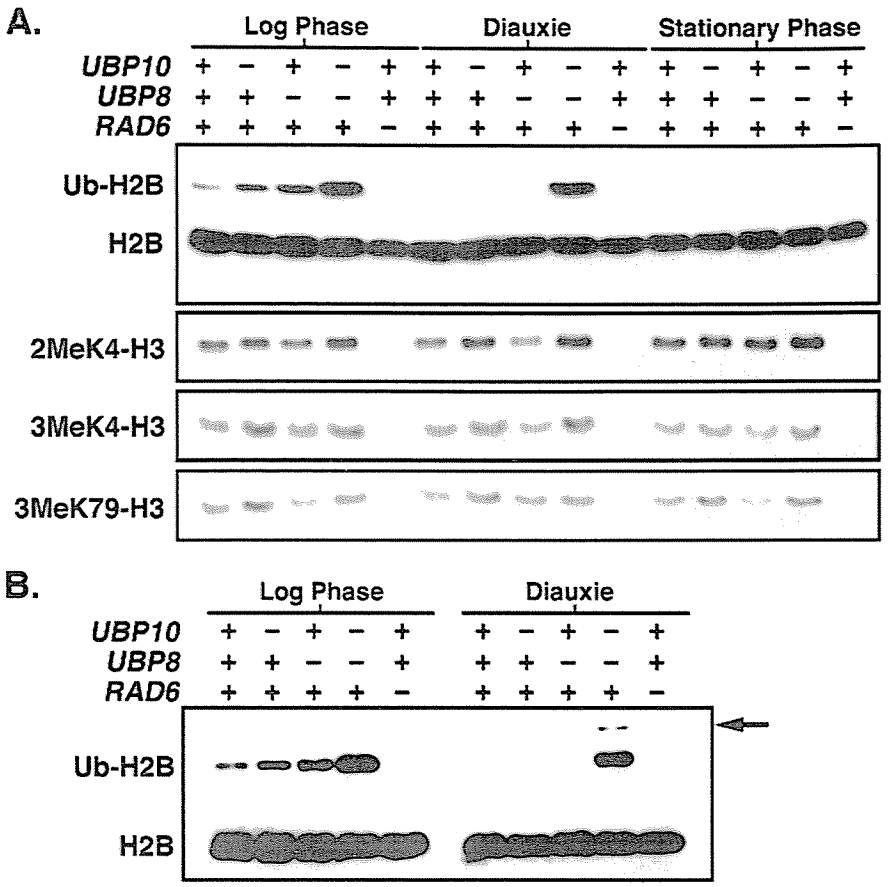

FIG. 7. Ubp10p and Ubp8p overlap in their target chromatin regions. (A) Global steady-state levels of H2B ubiquitination and H3 Lys4 and Lys79 methylation from whole-cell lysates were assayed as described in the legend of Fig. 1. Whole-cell lysates were derived from strains UCC6369 (wild type), UCC6390 (*ubp10*Δ), UCC6392 (*ubp8*Δ), UCC6393 (*ubp10*Δ *ubp8*Δ), and UCC6163 (*rad6*Δ) that were harvested during log-phase growth, diauxie (overnight growth to saturation), and stationary phase (7-day saturation). (B) Some H2B ubiquitination persists in *ubp10*Δ and *ubp8*Δ cells in diauxie. H2B ubiquitination was assayed as described in the legend of Fig. 1. Arrow indicates where diubiquitinated form of H2B would run as expected in *ubp10*Δ *ubp8*Δ cells.

other to maintain lower levels of transcription or repression at these loci. A similar situation was seen for genes that have decreased expression in *ubp10*Δ *ubp8*Δ cells. Over 40 additional genes have reduced expression of at least 1.5-fold in *ubp10*Δ *ubp8*Δ cells compared to cells carrying either *ubp10*Δ or *ubp8*Δ alone (Fig. 8A). Together, these data support the idea that Ubp10p and Ubp8p regulate H2B ubiquitination and gene expression at a shared set of loci in the genome.

DISCUSSION

We previously identified Ubp10/Dot4p as a ubiquitin protease whose enzymatic activity is required for optimal telomeric silencing (43, 85). However, we had not identified any ubiquitinated proteins that are Ubp10p substrates. Here we report that Ubp10p negatively regulates histone H2B ubiquitination.

Ubp10/Dot4p's role in telomeric silencing may be the removal of H2B ubiquitination. Consistent with a role in silencing, we found that Ubp10p is targeted to silent regions by its Sir4p-interaction domain (Fig. 2), and this interaction facilitates telomeric silencing by preventing the accumulation of H3 Lys4 and Lys79 methylation (Fig. 4). Given Ubp10p's ubiquitin protease activity and the requirement of H2B ubiquitination for H3 Lys4 and Lys79 methylation (9, 20, 67, 91), we propose that Sir4p targets Ubp10p to silent chromatin to remove ubiquitin from H2B. This, in turn, would decrease the probability that H3 Lys4 and Lys79 become methylated within silenced regions.

The role for Ubp10p in silencing is best considered in light of the dynamic binding nature of chromatin proteins. Chromatin proteins continually associate and dissociate from chromatin, including the proteins considered to have relatively stable associations in vitro (72, 73). Indeed, Sir protein binding to silent chromatin is dynamic throughout the cell cycle, even in G_1 and M when the genome is not being replicated (14, 51, 56). Temporary dissociation of Sir proteins from silent chromatin could leave these regions briefly accessible to the Rad6p-Bre1p complex and thereby susceptible to H2B ubiquitination. If fortuitous H2B ubiquitination persists for too long, this reversible histone mark could be converted into the more permanent marks of H3 Lys4 and Lys79 methylation, which would prevent the reassociation of Sir proteins and result in the loss of si-

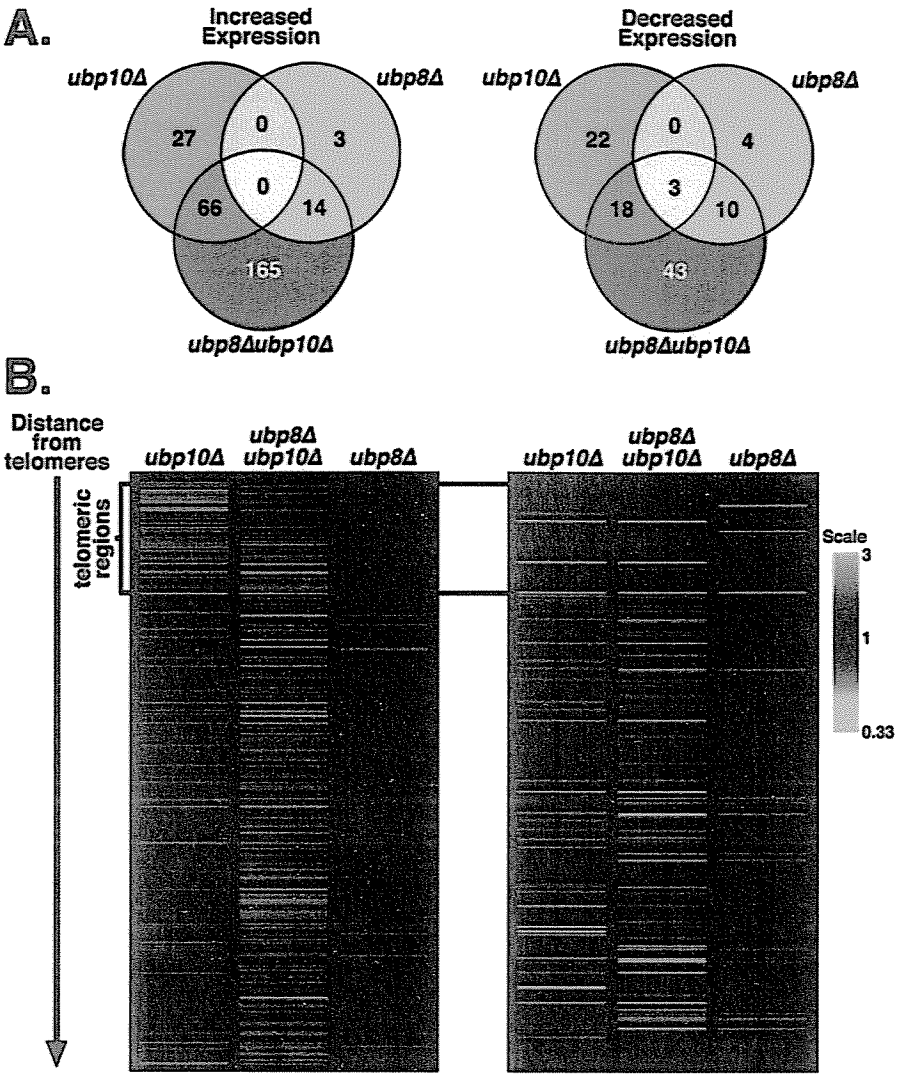

FIG. 8. Loss of *UBP10* and *UBP8* has synergistic transcriptional effects primarily in active chromatin. Transcript array analysis using strains UCC6389 (wild type), UCC6390 (*ubp10*Δ), UCC6392 (*ubp8*Δ), and UCC6393 (*ubp10*Δ *ubp8*Δ) was performed as described in the legend of Fig. 2. (A) Venn diagrams show the degree of overlap in expression changes between *ubp10*Δ, *ubp8*Δ, and *ubp10*Δ *ubp8*Δ cells. (B) Expression changes in *ubp10*Δ *ubp8*Δ cells are primarily in nontelomeric regions. Positional cluster analysis shows expression changes of genes based on distance from telomeres. Only genes that were expressed greater than or less than 1.5-fold in at least one of the strains are shown (total genes shown is 368). Genes located in telomeric regions are marked on the left. See Table S1 in the supplemental material for the entire normalized data set.

lencing. We postulate that Sir4p-dependent enrichment of Ubp10p at silent chromatin concentrates its ubiquitin protease activity to maintain silencing in the face of Sir protein dynamics.

While Ubp10p is localized to the silent mating region *HMR*a in a Sir4p-binding domain-dependent manner (Fig. 2), loss of *UBP10* does not appreciably alter *HM* silencing as measured by silencing reporters placed at either *HM* loci (85), global transcript analysis (see Table S1 in the supplemental material), ChIP assay of H3 Lys4 methylation (Fig. 4), and quantitative mating assays of *ubp10*Δ cells (data not shown). *HM* silencing is inherently more stable than telomeric silencing (31), due to the significant stabilization of Sir protein association with chromatin by the binding of Sir1p to *HM* loci silencer regions (15). If this greater stability occurs by a reduction in Sir protein dissociation, it would readily explain the reduced reliance on Ubp10p action at the silent mating loci and maximal Sir protein binding to *HMR*a in the absence of *UBP10* (Fig. 4).

Ubp10/Dot4p negatively regulates global H2B ubiquitination and H3 Lys4 and Lys79 methylation. We found that loss of silencing, by deletion of any single *SIR* gene or the Sir4p-binding region in Ubp10p, does not result in higher steady-state levels of H2B ubiquitination or H3 Lys4 methylation (Fig. 6), despite the fact that these manipulations result in increases in H3 Lys4 methylation in silent regions (Fig. 4). Yet loss of Ubp10p catalytic activity, by deletion of *UBP10* or mutation of the catalytic Cys residue, does result in higher steady-state levels of H2B ubiquitination and H3 Lys4 and Lys79 methylation (Fig. 6), indicating that Ubp10p activity is not limited to silent chromatin.

From these observations, it is likely that Ubp10p has a similar function elsewhere in the genome as it does in silent

chromatin—to limit or prevent H3 Lys4 and Lys79 methylation by reversing H2B ubiquitination. However, there may be a significant difference in how Ubp10p activity is used. In silent chromatin, it is proposed that all forms of H3 Lys4 and Lys79 methylation will interfere with Sir protein binding (64, 81, 92), so Ubp10p may be recruited to prevent any methylation of H3 Lys4 and Lys79. Elsewhere in the genome, the degree of methylation coincides with different functional states. For example, H3 Lys4 dimethylation and Lys79 methylation are present throughout the genome (5, 63, 64, 66, 82, 92) and help prevent the promiscuous binding of Sir proteins (82, 92). By contrast, H3 Lys4 trimethylation specifically occurs in the 5′ coding portion of active genes and is absent from inactive genes (66, 82). It has been suggested that H3 Lys4 trimethylation facilitates gene transcription and possibly serves as a memory mark for recent transcriptional activity (66, 82). At inactive genes, H2B ubiquitination would have to persist long enough for some methylation of H3 Lys4 and Lys79 to occur but be eliminated before H3 Lys4 trimethylation occurs. Considering how loss of *UBP10* affects the steady-state levels of H3 Lys4 methylation (Fig. 1 and 7), we propose that Ubp10p acts at inactive or repressed genes to facilitate this timely removal of ubiquitin from H2B. Consistent with this idea, the majority of nontelomeric genes with altered expression in *ubp10*Δ and *ubp10*Δ *ubp8*Δ cells have increased transcription (Fig. 3 and 8), indicating that Ubp10p may be involved in maintaining their inactivity or repression. This is not an indirect effect of losing silencing because the altered expression of these genes does not occur in $ubp10^{\Delta 94\text{-}250}$ cells, which are specifically defective in telomeric silencing. Perhaps Ubp10p is targeted to inactive genes by repressive complexes, similar to recruitment by Sir4p to silent regions. If so, Ubp10p binding to repressors would have to be through a different domain than that used for binding to Sir4p. Alternatively, the loss of Ubp10p activity might indirectly affect transcription by alterations in the ubiquitination levels of other proteins in addition to H2B.

Ubp10/Dot4p and Ubp8p have separate and overlapping functions. In addition to its role in silencing, we propose that Ubp10p's regulation of global H2B ubiquitination levels overlaps, in part, with that of Ubp8p. While loss of either *UBP10* or *UBP8* results in higher steady-state levels of H2B ubiquitination and functionally different phenotypic consequences for the cell (Fig. 1 and 5), the absence of both *UBP10* and *UBP8* together results in a synergistic increase in H2B ubiquitination levels and transcription (Fig. 7 and 8). Overlapping roles for Ubp10p and Ubp8p in gene regulation or other chromatin-related functions is further underscored by the persistence of ubiquitinated H2B in *ubp10*Δ *ubp8*Δ cells as they enter diauxie, which contrasts with the virtual disappearance of ubiquitinated H2B in *ubp10*Δ and *ubp8*Δ cells (Fig. 7). Of course, Ubp8p and Ubp10p are separable in some functions: Ubp8p functions in SAGA-mediated transcription (18, 33, 80), whereas Ubp10p functions in silencing (Fig. 5). Also, Ubp10p, but not Ubp8p, regulates steady-state H3 Lys4 and Lys79 methylation levels, even though both regulate steady-state H2B ubiquitination levels (Fig. 1). Despite these separable functions, the synergistic increases in steady-state H2B ubiquitination levels and transcription in *ubp10*Δ *ubp8*Δ cells underscore a potential overlapping role for these ubiquitin proteases.

The $ubp10^{\Delta 94\text{-}250}$ allele demonstrates that Ubp10p regulates H2B ubiquitination outside of its defined role in silencing, but no such separation-of-function alleles that demonstrate a role for Ubp8p outside of the SAGA complex have been isolated. It was recently found that Sgf11p facilitates the interaction of Ubp8p with SAGA (41, 53, 74). Interestingly, while purification of Sgf11p resulted primarily in the copurification of SAGA components, other transcriptional regulators also copurified with Sgf11p (74), indicating that Sgf11p may link Ubp8p to other chromatin-related processes in addition to SAGA-mediated transcription. Taking this and our findings into consideration, we believe Ubp8p functions in other aspects of H2B deubiquitination in addition to its defined role in SAGA-mediated transcription.

Although it is not clear at this point how Ubp10p and Ubp8p regulate H2B ubiquitination at common loci, such an effect could be the result of nonspecific chromatin binding that is independent of their targeted recruitment by Sir complexes and SAGA, respectively. As is the case for a number of histone acetylases and deacetylases (44, 47, 75, 94), Ubp10p and Ubp8p may be able to remove H2B ubiquitination from chromatin throughout the genome without a high-affinity interaction. Some loci may be more susceptible to such "hit-and-run" activities, and alterations in H2B ubiquitination and gene expression are only revealed when both Ubp10p and Ubp8p are absent.

Multiple reasons for removal of ubiquitin from H2B. The cell may modulate H2B ubiquitination levels by these ubiquitin proteases for a variety of reasons. Removal of ubiquitin from H2B may be used during gene repression to prevent H3 Lys4 and Lys79 methylation, similar to Ubp10p's role in silencing (43, 85). Deubiquitination of H2B may also facilitate transcription, as is the case for Ubp8p's role in SAGA-mediated transcription (18, 33, 80). There is evidence that deubiquitination of H2B may also occur during mitosis to allow chromatin compaction (12, 57, 61). Removal of ubiquitin from H2B may be important in halting transcription of mitotic genes as cells exit the cell cycle and may be the reason for deubiquitination of H2B as yeast cells transit into stationary phase (Fig. 7). Lastly, removal of the single ubiquitin moiety from ubiquitinated H2B may be required to prevent multiubiquitination and subsequent degradation of modified H2B by chromatin-associated proteasomes (29, 30, 60). These and other yet to be discovered outcomes of removing H2B ubiquitination likely contribute to the dynamic and flexible nature of chromatin.

Ubp10/Dot4p may have other roles beyond regulating H2B ubiquitination. It is important to note that Ubp10p may target other ubiquitinated proteins in addition to histone H2B. For instance, Ubp10p also appears to regulate the steady-state levels of the general amino acid permease Gap1p (42). Because plasma membrane permeases are subject to regulated ubiquitination and endocytosis (34), Ubp10p may indirectly affect transcription of some genes as a result of altered nutrient transport. In fact, *ubp10*Δ cells have a slow-growth phenotype that is exacerbated in synthetic medium and by the presence of multiple amino acid and nucleotide auxotrophies (43). Thus, in the absence of de novo biosynthetic capabilities, *ubp10*Δ cells may be starved for essential nutrients due to impaired transport. Previous transcript analyses of *ubp10*Δ cells grown in minimal medium found a large number of stress response genes with increased expression, coincident with an increase in

cellular oxidative damage (70). Nutrient starvation often results in a significant transcriptional stress response (28), which is similar to that observed in *ubp10*Δ cells grown in minimal medium (70). Furthermore, protracted amino acid starvation induces production of reactive oxygen species and increases apoptosis in wild-type cells (21), similar to what is observed in *ubp10*Δ cells (70). The increased expression of stress response genes is likely a secondary response to nutrient starvation in *ubp10*Δ cells. Deletion of any *SIR* gene can partially compensate for the slow-growth phenotype and the transcriptional stress response in *ubp10*Δ cells (43, 70). Because a number of subtelomeric genes encoding cell wall stress proteins are regulated by modulation of silencing (1), *sir*Δ suppression is also likely to be a secondary effect resulting from the increased expression of these proteins that allows sufficient cell wall structural changes to facilitate nutrient transport and partially alleviate the starvation of *ubp10*Δ cells.

Understanding the complete nature of Ubp10p action in the cell will require efforts aimed at identifying all of its substrates and target chromatin regions. Construction and analysis of separation-of-function alleles, as done here with $ubp10^{\Delta 94\text{-}250}$, will help delineate Ubp10p action in active chromatin from that in silent chromatin. Because histone deubiquitination may be operative in many different species as a regulatory mode (12, 32, 58, 59, 61), we believe further understanding of the role of Ubp10p in modulating histone H2B ubiquitination will yield greater insight into this common axis of chromatin regulation.

ACKNOWLEDGMENTS

We thank M. A. Osley for the FLAG-tagged H2B plasmids and J. Delrow for statistical analysis of the transcript microarray data. We thank H. Eisen and the members of the Gottschling lab for insightful discussions and critical reading of the manuscript.

R.G.G. is a Bristol Myers Squibb fellow of the Life Sciences Research Foundation. This work was supported by National Institutes of Health grant GM43893 to D.E.G.

REFERENCES

1. **Ai, W., P. G. Bertram, C. K. Tsang, T. F. Chan, and X. F. Zheng.** 2002. Regulation of subtelomeric silencing during stress response. Mol. Cell **10:** 1295–1305.
2. **Amerik, A. Y., S. J. Li, and M. Hochstrasser.** 2000. Analysis of the deubiquitinating enzymes of the yeast Saccharomyces cerevisiae. Biol. Chem. **381:** 981–992.
3. **Baldi, P., and A. D. Long.** 2001. A Bayesian framework for the analysis of microarray expression data: regularized t-test and statistical inferences of gene changes. Bioinformatics **17:**509–519.
4. **Benjamini, Y., and Y. Hochberg.** 1995. Controlling the false discovery rate: A practical and powerful approach to multiple testing. J. R. Stat. Soc. Ser. B **57:**289–300.
5. **Bernstein, B. E., E. L. Humphrey, R. L. Erlich, R. Schneider, P. Bouman, J. S. Liu, T. Kouzarides, and S. L. Schreiber.** 2002. Methylation of histone H3 Lys 4 in coding regions of active genes. Proc. Natl. Acad. Sci. USA **99:**8695–8700.
6. **Braunstein, M., A. B. Rose, S. G. Holmes, C. D. Allis, and J. R. Broach.** 1993. Transcriptional silencing in yeast is associated with reduced nucleosome acetylation. Genes Dev. **7:**592–604.
7. **Braunstein, M., R. E. Sobel, C. D. Allis, B. M. Turner, and J. R. Broach.** 1996. Efficient transcriptional silencing in *Saccharomyces cerevisiae* requires a heterochromatin histone acetylation pattern. Mol. Cell. Biol. **16:**4349–4356.
8. **Briggs, S. D., M. Bryk, B. D. Strahl, W. L. Cheung, J. K. Davie, S. Y. Dent, F. Winston, and C. D. Allis.** 2001. Histone H3 lysine 4 methylation is mediated by Set1 and required for cell growth and rDNA silencing in *Saccharomyces cerevisiae*. Genes Dev. **15:**3286–3295.
9. **Briggs, S. D., T. Xiao, Z. W. Sun, J. A. Caldwell, J. Shabanowitz, D. F. Hunt, C. D. Allis, and B. D. Strahl.** 2002. Gene silencing: trans-histone regulatory pathway in chromatin. Nature **418:**498.
10. **Brown, T. A., and B. L. Trumpower.** 1995. Strain-dependent variation in carbon source regulation of nucleus-encoded mitochondrial proteins of *Saccharomyces cerevisiae*. J. Bacteriol. **177:**1380–1382.
11. **Buck, S. W., and D. Shore.** 1995. Action of a RAP1 carboxy-terminal silencing domain reveals an underlying competition between HMR and telomeres in yeast. Genes Dev. **9:**370–384.
12. **Cai, S. Y., R. W. Babbitt, and V. T. Marchesi.** 1999. A mutant deubiquitinating enzyme (Ubp-M) associates with mitotic chromosomes and blocks cell division. Proc. Natl. Acad. Sci. USA **96:**2828–2833.
13. **Carmen, A. A., L. Milne, and M. Grunstein.** 2002. Acetylation of the yeast histone H4 N terminus regulates its binding to heterochromatin protein SIR3. J. Biol. Chem. **277:**4778–4781.
14. **Cheng, T. H., and M. R. Gartenberg.** 2000. Yeast heterochromatin is a dynamic structure that requires silencers continuously. Genes Dev. **14:**452–463.
15. **Chien, C. T., S. Buck, R. Sternglanz, and D. Shore.** 1993. Targeting of SIR1 protein establishes transcriptional silencing at HM loci and telomeres in yeast. Cell **75:**531–541.
16. **Chiu, Y. H., Q. Yu, J. J. Sandmeier, and X. Bi.** 2003. A targeted histone acetyltransferase can create a sizable region of hyperacetylated chromatin and counteract the propagation of transcriptionally silent chromatin. Genetics **165:**115–125.
17. **Cullen, P. J., W. Sabbagh, Jr., E. Graham, M. M. Irick, E. K. van Olden, C. Neal, J. Delrow, L. Bardwell, and G. F. Sprague, Jr.** 2004. A signaling mucin at the head of the Cdc42- and MAPK-dependent filamentous growth pathway in yeast. Genes Dev. **18:**1695–1708.
18. **Daniel, J. A., M. S. Torok, Z. W. Sun, D. Schieltz, C. D. Allis, J. R. Yates III, and P. A. Grant.** 2004. Deubiquitination of histone H2B by a yeast acetyltransferase complex regulates transcription. J. Biol. Chem. **279:**1867–1871.
19. **Dong, L., and C. W. Xu.** 2004. Carbohydrates induce mono-ubiquitination of H2B in yeast. J. Biol. Chem. **279:**1577–1580.
20. **Dover, J., J. Schneider, M. A. Tawiah-Boateng, A. Wood, K. Dean, M. Johnston, and A. Shilatifard.** 2002. Methylation of histone H3 by COMPASS requires ubiquitination of histone H2B by Rad6. J. Biol. Chem. **277:** 28368–28371.
21. **Eisler, H., K. U. Frohlich, and E. Heidenreich.** 2004. Starvation for an essential amino acid induces apoptosis and oxidative stress in yeast. Exp. Cell. Res. **300:**345–353.
22. **Ezhkova, E., and W. P. Tansey.** 2004. Proteasomal ATPases link ubiquitylation of histone H2B to methylation of histone H3. Mol. Cell **13:**435–442.
23. **Fazzio, T. G., C. Kooperberg, J. P. Goldmark, C. Neal, R. Basom, J. Delrow, and T. Tsukiyama.** 2001. Widespread collaboration of Isw2 and Sin3-Rpd3 chromatin remodeling complexes in transcriptional repression. Mol. Cell. Biol. **21:**6450–6460.
24. **Feng, Q., H. Wang, H. H. Ng, H. Erdjument-Bromage, P. Tempst, K. Struhl, and Y. Zhang.** 2002. Methylation of H3-lysine 79 is mediated by a new family of HMTases without a SET domain. Curr. Biol. **12:**1052–1058.
25. **Frolova, E., M. Johnston, and J. Majors.** 1999. Binding of the glucose-dependent Mig1p repressor to the GAL1 and GAL4 promoters in vivo: regulation by glucose and chromatin structure. Nucleic Acids Res. **27:**1350–1358.
26. **Gardner, R. G., and R. Y. Hampton.** 1999. A "distributed degron" allows regulated entry into the ER degradation pathway. EMBO J. **18:**5994–6004.
27. **Gardner, R. G., Z. W. Nelson, and D. E. Gottschling.** 2005. Degradation-mediated protein quality control in the nucleus. Cell **120:**803–815.
28. **Gasch, A. P., P. T. Spellman, C. M. Kao, O. Carmel-Harel, M. B. Eisen, G. Storz, D. Botstein, and P. O. Brown.** 2000. Genomic expression programs in the response of yeast cells to environmental changes. Mol. Biol. Cell **11:** 4241–4257.
29. **Gillette, T. G., F. Gonzalez, A. Delahodde, S. A. Johnston, and T. Kodadek.** 2004. Physical and functional association of RNA polymerase II and the proteasome. Proc. Natl. Acad. Sci. USA **101:**5904–5909.
30. **Gonzalez, F., A. Delahodde, T. Kodadek, and S. A. Johnston.** 2002. Recruitment of a 19S proteasome subcomplex to an activated promoter. Science **296:**548–550.
31. **Gottschling, D. E., O. M. Aparicio, B. L. Billington, and V. A. Zakian.** 1990. Position effect at *S. cerevisiae* telomeres: reversible repression of Pol II transcription. Cell **63:**751–762.
32. **Henchoz, S., F. De Rubertis, D. Pauli, and P. Spierer.** 1996. The dose of a putative ubiquitin-specific protease affects position-effect variegation in *Drosophila melanogaster*. Mol. Cell. Biol. **16:**5717–5725.
33. **Henry, K. W., A. Wyce, W. S. Lo, L. J. Duggan, N. C. Emre, C. F. Kao, L. Pillus, A. Shilatifard, M. A. Osley, and S. L. Berger.** 2003. Transcriptional activation via sequential histone H2B ubiquitylation and deubiquitylation, mediated by SAGA-associated Ubp8. Genes Dev. **17:**2648–2663.
34. **Hicke, L., and R. Dunn.** 2003. Regulation of membrane protein transport by ubiquitin and ubiquitin-binding proteins. Annu. Rev. Cell Dev. Biol. **19:**141–172.
35. **Hirschhorn, J. N., A. L. Bortvin, S. L. Ricupero-Hovasse, and F. Winston.** 1995. A new class of histone H2A mutations in *Saccharomyces cerevisiae* causes specific transcriptional defects in vivo. Mol. Cell. Biol. **15:**1999–2009.

36. **Hochstrasser, M.** 1996. Ubiquitin-dependent protein degradation. Annu. Rev. Genet. **30:**405–439.
37. **Huang, H., A. Kahana, D. E. Gottschling, L. Prakash, and S. W. Liebman.** 1997. The ubiquitin-conjugating enzyme Rad6 (Ubc2) is required for silencing in *Saccharomyces cerevisiae*. Mol. Cell. Biol. **17:**6693–6699.
38. **Huisinga, K. L., and B. F. Pugh.** 2004. A genome-wide housekeeping role for TFIID and a highly regulated stress-related role for SAGA in *Saccharomyces cerevisiae*. Mol. Cell **13:**573–585.
39. **Hwang, W. W., S. Venkatasubrahmanyam, A. G. Ianculescu, A. Tong, C. Boone, and H. D. Madhani.** 2003. A conserved RING finger protein required for histone H2B monoubiquitination and cell size control. Mol. Cell **11:**261–266.
40. **Imai, S., C. M. Armstrong, M. Kaeberlein, and L. Guarente.** 2000. Transcriptional silencing and longevity protein Sir2 is an NAD-dependent histone deacetylase. Nature **403:**795–800.
41. **Ingvarsdottir, K., N. J. Krogan, N. C. Emre, A. Wyce, N. J. Thompson, A. Emili, T. R. Hughes, J. F. Greenblatt, and S. L. Berger.** 2005. H2B ubiquitin protease Ubp8 and Sgf11 constitute a discrete functional module within the *Saccharomyces cerevisiae* SAGA complex. Mol. Cell. Biol. **25:**1162–1172.
42. **Kahana, A.** 2001. The deubiquitinating enzyme Dot4p is involved in regulating nutrient uptake. Biochem. Biophys. Res. Commun. **282:**916–920.
43. **Kahana, A., and D. E. Gottschling.** 1999. *DOT4* links silencing and cell growth in *Saccharomyces cerevisiae*. Mol. Cell. Biol. **19:**6608–6620.
44. **Katan-Khaykovich, Y., and K. Struhl.** 2002. Dynamics of global histone acetylation and deacetylation in vivo: rapid restoration of normal histone acetylation status upon removal of activators and repressors. Genes Dev. **16:**743–752.
45. **Krogan, N. J., J. Dover, S. Khorrami, J. F. Greenblatt, J. Schneider, M. Johnston, and A. Shilatifard.** 2002. COMPASS, a histone H3 (lysine 4) methyltransferase required for telomeric silencing of gene expression. J. Biol. Chem. **277:**10753–10755.
46. **Krogan, N. J., J. Dover, A. Wood, J. Schneider, J. Heidt, M. A. Boateng, K. Dean, O. W. Ryan, A. Golshani, M. Johnston, J. F. Greenblatt, and A. Shilatifard.** 2003. The Paf1 complex is required for histone H3 methylation by COMPASS and Dot1p: linking transcriptional elongation to histone methylation. Mol. Cell **11:**721–729.
47. **Kuo, M. H., E. vom Baur, K. Struhl, and C. D. Allis.** 2000. Gcn4 activator targets Gcn5 histone acetyltransferase to specific promoters independently of transcription. Mol. Cell **6:**1309–1320.
48. **Kurdistani, S. K., D. Robyr, S. Tavazoie, and M. Grunstein.** 2002. Genome-wide binding map of the histone deacetylase Rpd3 in yeast. Nat. Genet. **31:**248–254.
49. **Lacoste, N., R. T. Utley, J. M. Hunter, G. G. Poirier, and J. Cote.** 2002. Disruptor of telomeric silencing-1 is a chromatin-specific histone H3 methyltransferase. J. Biol. Chem. **277:**30421–30424.
50. **Landry, J., A. Sutton, S. T. Tafrov, R. C. Heller, J. Stebbins, L. Pillus, and R. Sternglanz.** 2000. The silencing protein SIR2 and its homologs are NAD-dependent protein deacetylases. Proc. Natl. Acad. Sci. USA **97:**5807–5811.
51. **Lau, A., H. Blitzblau, and S. P. Bell.** 2002. Cell-cycle control of the establishment of mating-type silencing in *S. cerevisiae*. Genes Dev. **16:**2935–2945.
52. **Laurenson, P., and J. Rine.** 1992. Silencers, silencing, and heritable transcriptional states. Microbiol. Rev. **56:**543–560.
53. **Lee, K. K., L. Florens, S. K. Swanson, M. P. Washburn, and J. L. Workman.** 2005. The deubiquitylation activity of Ubp8 is dependent upon Sgf11 and its association with the SAGA complex. Mol. Cell. Biol. **25:**1173–1182.
54. **Levinger, L., and A. Varshavsky.** 1982. Selective arrangement of ubiquitinated and D1 protein-containing nucleosomes within the *Drosophila* genome. Cell **28:**375–385.
55. **Lieb, J. D., X. Liu, D. Botstein, and P. O. Brown.** 2001. Promoter-specific binding of Rap1 revealed by genome-wide maps of protein-DNA association. Nat. Genet. **28:**327–334.
56. **Martins-Taylor, K., M. L. Dula, and S. G. Holmes.** 2004. Heterochromatin spreading at yeast telomeres occurs in M phase. Genetics **168:**65–75.
57. **Matsui, S. I., B. K. Seon, and A. A. Sandberg.** 1979. Disappearance of a structural chromatin protein A24 in mitosis: implications for molecular basis of chromatin condensation. Proc. Natl. Acad. Sci. USA **76:**6386–6390.
58. **Mimnaugh, E. G., H. Y. Chen, J. R. Davie, J. E. Celis, and L. Neckers.** 1997. Rapid deubiquitination of nucleosomal histones in human tumor cells caused by proteasome inhibitors and stress response inducers: effects on replication, transcription, translation, and the cellular stress response. Biochemistry **36:**14418–14429.
59. **Mimnaugh, E. G., G. Kayastha, N. B. McGovern, S. G. Hwang, M. G. Marcu, J. Trepel, S. Y. Cai, V. T. Marchesi, and L. Neckers.** 2001. Caspase-dependent deubiquitination of monoubiquitinated nucleosomal histone H2A induced by diverse apoptogenic stimuli. Cell Death Differ. **8:**1182–1196.
60. **Morris, M. C., P. Kaiser, S. Rudyak, C. Baskerville, M. H. Watson, and S. I. Reed.** 2003. Cks1-dependent proteasome recruitment and activation of CDC20 transcription in budding yeast. Nature **423:**1009–1013.
61. **Mueller, R. D., H. Yasuda, C. L. Hatch, W. M. Bonner, and E. M. Bradbury.** 1985. Identification of ubiquitinated histones 2A and 2B in *Physarum polycephalum*. Disappearance of these proteins at metaphase and reappearance at anaphase. J. Biol. Chem. **260:**5147–5153.
62. **Nagy, P. L., J. Griesenbeck, R. D. Kornberg, and M. L. Cleary.** 2002. A trithorax-group complex purified from *Saccharomyces cerevisiae* is required for methylation of histone H3. Proc. Natl. Acad. Sci. USA **99:**90–94.
63. **Ng, H. H., D. N. Ciccone, K. B. Morshead, M. A. Oettinger, and K. Struhl.** 2003. Lysine-79 of histone H3 is hypomethylated at silenced loci in yeast and mammalian cells: a potential mechanism for position-effect variegation. Proc. Natl. Acad. Sci. USA **100:**1820–1825.
64. **Ng, H. H., S. Dole, and K. Struhl.** 2003. The Rtf1 component of the Paf1 transcriptional elongation complex is required for ubiquitination of histone H2B. J. Biol. Chem. **278:**33625–33628.
65. **Ng, H. H., Q. Feng, H. Wang, H. Erdjument-Bromage, P. Tempst, Y. Zhang, and K. Struhl.** 2002. Lysine methylation within the globular domain of histone H3 by Dot1 is important for telomeric silencing and Sir protein association. Genes Dev. **16:**1518–1527.
66. **Ng, H. H., F. Robert, R. A. Young, and K. Struhl.** 2003. Targeted recruitment of Set1 histone methylase by elongating Pol II provides a localized mark and memory of recent transcriptional activity. Mol. Cell **11:**709–719.
67. **Ng, H. H., R. M. Xu, Y. Zhang, and K. Struhl.** 2002. Ubiquitination of histone H2B by Rad6 is required for efficient Dot1-mediated methylation of histone H3 lysine 79. J. Biol. Chem. **277:**34655–34657.
68. **Nickel, B. E., C. D. Allis, and J. R. Davie.** 1989. Ubiquitinated histone H2B is preferentially located in transcriptionally active chromatin. Biochemistry **28:**958–963.
69. **Noma, K., and S. I. Grewal.** 2002. Histone H3 lysine 4 methylation is mediated by Set1 and promotes maintenance of active chromatin states in fission yeast. Proc. Natl. Acad. Sci. USA **99**(Suppl. 4)**:**16438–16445.
70. **Orlandi, I., M. Bettiga, L. Alberghina, and M. Vai.** 2004. Transcriptional profiling of *ubp10* null mutant reveals altered subtelomeric gene expression and insurgence of oxidative stress response. J. Biol. Chem. **279:**6414–6425.
71. **Peterson, C. L., and M. A. Laniel.** 2004. Histones and histone modifications. Curr. Biol. **14:**R546–R551.
72. **Phair, R. D., and T. Misteli.** 2000. High mobility of proteins in the mammalian cell nucleus. Nature **404:**604–609.
73. **Phair, R. D., P. Scaffidi, C. Elbi, J. Vecerova, A. Dey, K. Ozato, D. T. Brown, G. Hager, M. Bustin, and T. Misteli.** 2004. Global nature of dynamic protein-chromatin interactions in vivo: three-dimensional genome scanning and dynamic interaction networks of chromatin proteins. Mol. Cell. Biol. **24:**6393–6402.
74. **Powell, D. W., C. M. Weaver, J. L. Jennings, K. J. McAfee, Y. He, P. A. Weil, and A. J. Link.** 2004. Cluster analysis of mass spectrometry data reveals a novel component of SAGA. Mol. Cell. Biol. **24:**7249–7259.
75. **Reid, J. L., V. R. Iyer, P. O. Brown, and K. Struhl.** 2000. Coordinate regulation of yeast ribosomal protein genes is associated with targeted recruitment of Esa1 histone acetylase. Mol. Cell **6:**1297–1307.
76. **Robzyk, K., J. Recht, and M. A. Osley.** 2000. Rad6-dependent ubiquitination of histone H2B in yeast. Science **287:**501–504.
77. **Roguev, A., D. Schaft, A. Shevchenko, W. W. Pijnappel, M. Wilm, R. Aasland, and A. F. Stewart.** 2001. The *Saccharomyces cerevisiae* Set1 complex includes an Ash2 homologue and methylates histone 3 lysine 4. EMBO J. **20:**7137–7148.
78. **Rusche, L. N., A. L. Kirchmaier, and J. Rine.** 2003. The establishment, inheritance, and function of silenced chromatin in *Saccharomyces cerevisiae*. Annu. Rev. Biochem. **72:**481–516.
79. **Rusche, L. N., A. L. Kirchmaier, and J. Rine.** 2002. Ordered nucleation and spreading of silenced chromatin in *Saccharomyces cerevisiae*. Mol. Biol. Cell **13:**2207–2222.
80. **Sanders, S. L., J. Jennings, A. Canutescu, A. J. Link, and P. A. Weil.** 2002. Proteomics of the eukaryotic transcription machinery: identification of proteins associated with components of yeast TFIID by multidimensional mass spectrometry. Mol. Cell. Biol. **22:**4723–4738.
81. **Santos-Rosa, H., A. J. Bannister, P. M. Dehe, V. Geli, and T. Kouzarides.** 2004. Methylation of H3 lysine 4 at euchromatin promotes Sir3p association with heterochromatin. J. Biol. Chem. **279:**47506–47512.
82. **Santos-Rosa, H., R. Schneider, A. J. Bannister, J. Sherriff, B. E. Bernstein, N. C. Emre, S. L. Schreiber, J. Mellor, and T. Kouzarides.** 2002. Active genes are tri-methylated at K4 of histone H3. Nature **419:**407–411.
83. **Shi, Y., F. Lan, C. Matson, P. Mulligan, J. R. Whetstine, P. A. Cole, and R. A. Casero.** 2004. Histone demethylation mediated by the nuclear amine oxidase homolog LSD1. Cell **119:**941–953.
84. **Sikorski, R. S., and P. Hieter.** 1989. A system of shuttle vectors and yeast host strains designed for efficient manipulation of DNA in *Saccharomyces cerevisiae*. Genetics **122:**19–27.
85. **Singer, M. S., A. Kahana, A. J. Wolf, L. L. Meisinger, S. E. Peterson, C. Goggin, M. Mahowald, and D. E. Gottschling.** 1998. Identification of high-copy disruptors of telomeric silencing in *Saccharomyces cerevisiae*. Genetics **150:**613–632.
86. **Smith, J. S., C. B. Brachmann, I. Celic, M. A. Kenna, S. Muhammad, V. J. Starai, J. L. Avalos, J. C. Escalante-Semerena, C. Grubmeyer, C. Wolberger, and J. D. Boeke.** 2000. A phylogenetically conserved NAD^+-dependent protein deacetylase activity in the Sir2 protein family. Proc. Natl. Acad. Sci. USA **97:**6658–6663.
87. **Smith, J. S., C. B. Brachmann, L. Pillus, and J. D. Boeke.** 1998. Distribution

of a limited Sir2 protein pool regulates the strength of yeast rDNA silencing and is modulated by Sir4p. Genetics **149:**1205–1219.

88. **Strahl, B. D., R. Ohba, R. G. Cook, and C. D. Allis.** 1999. Methylation of histone H3 at lysine 4 is highly conserved and correlates with transcriptionally active nuclei in *Tetrahymena*. Proc. Natl. Acad. Sci. USA **96:**14967–14972.
89. **Strahl-Bolsinger, S., A. Hecht, K. Luo, and M. Grunstein.** 1997. SIR2 and SIR4 interactions differ in core and extended telomeric heterochromatin in yeast. Genes Dev. **11:**83–93.
90. **Suka, N., Y. Suka, A. A. Carmen, J. Wu, and M. Grunstein.** 2001. Highly specific antibodies determine histone acetylation site usage in yeast heterochromatin and euchromatin. Mol. Cell **8:**473–479.
91. **Sun, Z. W., and C. D. Allis.** 2002. Ubiquitination of histone H2B regulates H3 methylation and gene silencing in yeast. Nature **418:**104–108.
92. **van Leeuwen, F., P. R. Gafken, and D. E. Gottschling.** 2002. Dot1p modulates silencing in yeast by methylation of the nucleosome core. Cell **109:**745–756.
93. **van Leeuwen, F., and D. E. Gottschling.** 2002. Genome-wide histone modifications: gaining specificity by preventing promiscuity. Curr. Opin. Cell Biol. **14:**756–762.
94. **Vogelauer, M., J. Wu, N. Suka, and M. Grunstein.** 2000. Global histone acetylation and deacetylation in yeast. Nature **408:**495–498.
95. **Wood, A., N. J. Krogan, J. Dover, J. Schneider, J. Heidt, M. A. Boateng, K. Dean, A. Golshani, Y. Zhang, J. F. Greenblatt, M. Johnston, and A. Shilatifard.** 2003. Bre1, an E3 ubiquitin ligase required for recruitment and substrate selection of Rad6 at a promoter. Mol. Cell **11:**267–274.
96. **Wood, A., J. Schneider, J. Dover, M. Johnston, and A. Shilatifard.** 2003. The Paf1 complex is essential for histone monoubiquitination by the Rad6-Bre1 complex, which signals for histone methylation by COMPASS and Dot1p. J. Biol. Chem. **278:**34739–34742.